UNIVERSITY OF TURKU

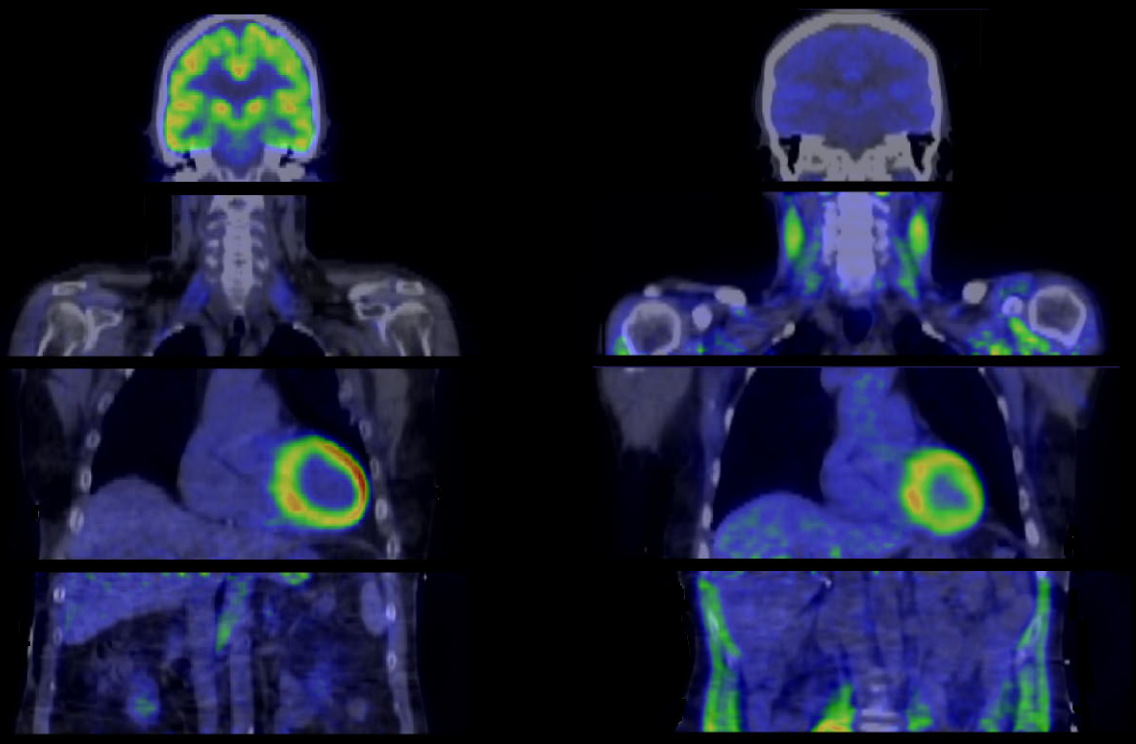

REGULATORS OF CENTRAL AND PERIPHERAL INSULIN SENSITIVITY IN HUMANS

Aino Latva-Rasku

TURUN YLIOPISTON JULKAISUJA – ANNALES UNIVERSITATIS TURKUENSIS
SARJA - SER. D OSA - TOM. 1495 | MEDICA - ODONTOLOGICA | TURKU 2020

UNIVERSITY OF TURKU

REGULATORS OF CENTRAL AND PERIPHERAL INSULIN SENSITIVITY IN HUMANS

Aino Latva-Rasku

TURUN YLIOPISTON JULKAISUJA – ANNALES UNIVERSITATIS TURKUENSIS
SARJA - SER. D OSA – TOM. 1495 | MEDICA – ODONTOLOGICA | TURKU 2020

University of Turku

Faculty of Medicine
Department of Internal Medicine
Doctoral Programme in Clinical Research
Turku PET Centre
Turku University Hospital

Supervised by

Professor Pirjo Nuutila, MD, PhD
Turku PET Centre,
University of Turku and
Department of Endocrinology,
Turku University Hospital
Turku, Finland

Professor Markku Laakso, MD, PhD
Internal Medicine,
Institute of Clinical Medicine,
University of Eastern Finland and
Kuopio University Hospital
Kuopio, Finland

Reviewed by

Professor Tommy G. Olsson, MD, PhD
Institute of Public Health and Clinical Medicine,
Umeå University
Umeå, Sweden

Adj. Professor Kirsi L. Timonen, MD, PhD
Department of Clinical Physiology and Nuclear Medicine,
Central Finland Health Care District,
Jyväskylä, Finland

Opponent

Professor Jan W. Eriksson, MD, PhD
Clinical Diabetology and Metabolism,
Department of Medical Sciences,
Uppsala University
Uppsala, Sweden

The originality of this publication has been checked in accordance with the University of Turku quality assurance system using the Turnitin OriginalityCheck service.

Cover Image: Aino Latva-Rasku

ISBN 978-951-29-8111-3 (PRINT)
ISBN 978-951-29-8112-0 (PDF)
ISSN 0355-9483 (Print)
ISSN 2343-3213 (Online)
Painosalama, Turku, Finland 2020

To Eerika

UNIVERSITY OF TURKU
Faculty of Medicine
Department of Internal Medicine
Turku PET Centre
AINO LATVA-RASKU: Regulators of Central and Peripheral Insulin Sensitivity in Humans
Doctoral Dissertation, 132 pp.
Doctoral Programme in Clinical Research (DPCR)
July 2020

ABSTRACT

Insulin, secreted by pancreatic β-cells, has a preeminent role in regulating metabolism in virtually all tissues. Highly conserved through evolution, intracellular insulin signaling pathways are tightly regulated, but have been recently challenged by drastic changes in our lifestyles. The following impairment in insulin response, termed insulin resistance, is an important feature of type 2 diabetes, a condition that has reached the proportions of a worldwide epidemic.

It is therefore important to gain a better understanding of how insulin resistance develops, what the interplay is between different tissues, and whether pharmacologically enhancing insulin sensitivity is possible. This thesis focuses on gathering novel information about how an inherited failure in insulin signaling (Study I), brain insulin signaling (Study II), and antidiabetic medicine dapagliflozin (Study III) can alter whole-body and tissue-specific insulin sensitivity.

The studies were performed by using positron emission tomography (PET) scans with a glucose analogue tracer ([^{18}F]-FDG) together with systemic (Studies I and III) and central hyperinsulinemia (Study II) to assess changes in tissue insulin-stimulated glucose uptake (GU).

The results from Study I revealed that inherited impairment in skeletal muscle insulin sensitivity resulted in insulin resistance in all key metabolic organs even before the onset of T2D, while also establishing the role of [^{18}F]-FDG-PET in determining the phenotype associated with a rare genetic variant. In Study II, it was demonstrated that brain insulin signaling induced by intranasal insulin does not have a significant effect on GU in peripheral tissues, but results in lower brain GU under mild systemic hyperinsulinemia. While dapagliflozin did not improve insulin sensitivity either (Study III), 8 weeks of treatment reduced liver fat content, as well as subcutaneous and visceral adipose tissue mass, in overweight T2D subjects.

In conclusion, these studies elucidate how a genetic variant primarily impairing skeletal muscle insulin sensitivity, central response to hyperinsulinemia, and treatment with dapagliflozin can affect tissue-specific insulin sensitivity.

KEYWORDS: Insulin sensitivity, glucose uptake, PET, intranasal insulin, dapagliflozin

TURUN YLIOPISTO
Lääketieteellinen tiedekunta
Sisätautioppi
Valtakunnallinen PET-keskus, Turku
AINO LATVA-RASKU: Sentraalisen ja perifeerisen insuliiniherkkyyden säätelytekijät ihmisillä
Väitöskirja, 132 s.
Turun kliininen tohtoriohjelma (TKT)
heinäkuu 2020

TIIVISTELMÄ

Haiman β-solujen erittämällä insuliinilla on merkittävä rooli aineenvaihdunnan säätelijänä lähes kaikissa kudoksissa. Solunsisäinen insuliinisignalointi on kehittynyt evoluutiossa varhain ja on tiukasti säädeltyä, eikä ole vielä onnistunut vastaamaan erittäin nopeaan muutokseen elämäntyylissämme. Tästä seuraava kudosten heikentynyt kyky reagoida insuliiniin, eli insuliiniresistenssi, voi johtaa tyypin 2 diabeteksen puhkeamiseen.

Sen vuoksi on tärkeää ymmärtää paremmin miten insuliiniresistenssi syntyy, miten eri kudokset vaikuttavat siihen, ja voidaanko tilannetta parantaa lääkkeellisesti. Tämän väitöskirjan tavoitteena on tutkia miten perinnöllinen vika erityisesti lihaksen insuliinisignaloinnissa (osatyö I), keskushermoston säätely (osatyö II) ja diabeteslääke dapagliflotsiini (osatyö III) voivat vaikuttaa kudosten insuliiniherkkyyteen.

Tutkimuksissa käytettiin positroniemissiotomorafia (PET) –kuvauksia yhdessä glukoosimerkkiaineen ([^{18}F]-FDG) kanssa. Insuliiniherkkyyden mittaamiseksi kuvausten aikana tutkittaville annettiin insuliinia verenkiertoon (osatyöt I ja III) tai nenäsumutteena (osatyö II).

Osatyössä I todettiin ensisijaisesti lihaksen insuliiniherkkyyttä alentavan geenivariantin aiheuttavan insuliiniresistenssiä laajasti myös muissa kudoksissa. Lisäksi tutkimuksella vahvistettiin [^{18}F]-FDG-PET:n roolia harvinaisten geenivarianttien vaikutusten tutkimisessa. Osatyössä II todettiin, ettei nenäsumutteena annettu insuliini saanut aikaan merkittävää muutosta muiden kudosten glukoosiaineenvaihdunnassa, mutta aivojen glukoosinotto väheni merkittävästi sumutteen jälkeen. Myöskään dapagliflotsiini ei vaikuttanut merkitsevästi kudosten insuliiniherkkyyteen (osatyö III), mutta 8 viikon hoito vähensi maksan ja vartalon rasvan määrää ylipainoisilla tyypin 2 diabetesta sairastavilla tutkittavilla.

Yhdessä nämä tutkimukset tuovat uutta tietoa siitä, miten lihaksen insuliiniresistenssiä aiheuttava geenivariantti, aivojen vaste korkeaan insuliiniannokseen, sekä hoito dapagliflotsiinilla voivat vaikuttaa kudosten insuliiniherkkyyteen.

AVAINSANAT: Insuliiniherkkyys, glukoosin soluunotto, PET, insuliininenäsumute, dapagliflotsiini

Table of Contents

Abbreviations

[^{18}F]-FDG	2-deoxy-2-[^{18}F]fluoro-D-glucose
Ac-CoA	Acetyl coenzyme A
Agrp/NPY	Agouti-related protein/neuropeptide Y neurons
AKT1, -2, -3	V-AKT murine thymoma viral oncogene homolog 1,2 and 3 (also PKBα, -β, -γ)
ALT	Alanine aminotransferase
AST	Aspartate transaminase
AT	Adipose tissue
ATP	Adenosine triphosphate
BAT	Brown adipose tissue
BBB	Blood-brain barrier
CCK	Cholecystokinin
CNS	Central nervous system
CT	Computed tomography
DAG	Diacylglycerol
DPP-4 inhibitor	Dipeptidyl peptidase 4 inhibitor
EGP	Endogenous glucose production
FFA	Free fatty acid
FGF21	Fibroblast growth factor 21
FOXO	Transcriptional factor forkhead box O
FUR	Fractional uptake rate
G6P	Glucose-6-phosphate
GIP	Glucose-dependent insulinotropic peptide
GIR	Glucose infusion rate
GLP-1	Glucagon-like peptide-1
GLUT1, -2, -3, -4	Glucose transporter 1, 2, 3 and 4
GSK3	Glycogen synthase kinase-3
GU	Glucose uptake
HDL	High-density lipoprotein
HOMA-IR	Homeostatic model assessment for insulin resistance
HU	Hounsfield unit

IL-6	Interleukin-6
INI	Intranasal insulin
IR	Insulin receptor
IRS	Insulin receptor substrate
i.c.v.	Intracerebroventricular
i.v.	Intravenous
LC	Lumped constant
LDL	Low-density lipoprotein
MBq	Megabecquerel
MCR	Metabolic clearance rate
MRI	Magnetic resonance imaging
mTORC1, -2	Mammalian target of rapamycin complex 1 and 2
NAFLD	Non-alcoholic fatty liver disease
NT-proBNP	N-terminal prohormone of brain natriuretic peptide
OGTT	Oral glucose tolerance test
PDC	Pyruvate dehydrogenase complex
PDFF%	Proton density fat fraction
PET	Positron emission tomography
PGC-1α	Peroxisome proliferator-activated receptor γ coactivator 1α
PI3K	Phosphatidylinositol 3-kinase
PKBα, -β, -γ	Protein kinase B α, β and γ (also AKT1, -2, -3)
PKC	Protein kinase C
POMC/CART	Pro-opiomelanocortin/cocaine- and amphetamine-regulated transcript neurons
Rd	Rate of disappearance
SGLT2	Sodim-glucose cotransporter 2
SNS	Sympathetic nervous system
T2D	Type 2 diabetes
TAG	Triacylglycerol
TNFα	Tumor necrosis factor α
WAT	White adipose tissue
VLDL	Very low -density lipoprotein
VOI	Volume of interest

List of Original Publications

This dissertation is based on the following original publications, which are referred to in the text by their Roman numerals:

I Latva-Rasku A., Honka M. J., Stančáková A., Koistinen H. A. , Kuusisto J. , Guan L., Manning A. K. , Stringham H., Gloyn A. L. , Lindgren C. M., T2D-GENES Consortium, Collins F. S., Mohlke K. L., Scott L. J., Karjalainen T., Nummenmaa L., Boehnke M., Nuutila P., Laakso M. A Partial Loss-of-Function Variant in AKT2 is Associated With Reduced Insulin-Mediated Glucose Uptake in Multiple Insulin-Sensitive Tissues: A Genotype-Based Callback Positron Emission Tomography Study. *Diabetes.* 2018 Feb;67(2):334-342.

II Latva-Rasku A., Laurila S., Karjalainen T., Klén R., Löyttyniemi E., Eskola O., Nummenmaa L., Nuutila P. Intranasal Insulin Does Not Affect Peripheral Tissue Glucose Uptake, but Decreases Brain Glucose Uptake in Lean, Healthy Men: A Positron Emission Tomography Study. *Manuscript.*

III Latva-Rasku A., Honka M. J., Kullberg J., Mononen N., Lehtimäki T., Saltevo J., Kirjavainen A. K., Saunavaara V., Iozzo P., Johansson L., Oscarsson J., Hannukainen J. C., Nuutila P. The SGLT2 Inhibitor Dapagliflozin Reduces Liver Fat but Does Not Affect Tissue Insulin Sensitivity: A Randomized, Double-Blind, Placebo-Controlled Study With 8-Week Treatment in Type 2 Diabetes Patients. *Diabetes Care*. 2019 May;42(5):931-937.

1 Introduction

Insulin, produced by pancreatic β-cells in humans, plays a distinct role in promoting anabolic processes in the postprandial state and in regulating cell survival and growth in virtually all tissues. Insulin, insulin receptors (IRs), and the downstream pathways are highly conserved across species demonstrating early development during evolution (Saltiel & Kahn, 2001). This system has been challenged by the relatively recent changes in our lifestyles: constant availability of high-calorie and highly palatable foods, low physical activity, and the associated obesity all contribute to the impairment of insulin response in tissues, termed insulin resistance.

The major effects of increased insulin secretion after a meal are enhanced glucose uptake (GU) and storing in skeletal muscle, promoted storing of excess glucose as glycogen and triacylglycerols (TAGs) in the liver while inhibiting hepatic endogenous glucose production (EGP), and improved storing and restricted release of fatty acids in adipose tissue (AT). These peripheral tissues, as well as the brain, all contribute to maintaining normal metabolic homeostasis, whereas, adversely, impaired insulin sensitivity in one tissue will eventually result in a deteriorated response to insulin in the whole body (Roden & Shulman, 2019).

As insulin resistance is the major characteristic of type 2 diabetes (T2D)—a disease currently affecting over 400 million adults worldwide—and with the number of affected individuals rising steeply (International Diabetes Federation, 2019), it is of high priority to improve our understanding of the development of insulin resistance, tissue cross-talk in mediating insulin's effects, and the possibilities for improving insulin sensitivity.

This thesis targets these aspects by (I) describing the changes in tissue-specific insulin-stimulated GU caused by a rare genetic variant that predominantly affects skeletal muscle GU and glycogen synthesis; (II) investigating whether brain insulin exposure affects peripheral tissue GU under mild systemic hyperinsulinemia in healthy subjects; and (III) determining whether insulin resistance is alleviated in response to treatment with an antidiabetic medicine, sodium-glucose cotransporter 2 (SGLT2) inhibitor dapagliflozin, with the aid of positron emission tomography (PET) and a labeled glucose analogue tracer 2-deoxy-2-[^{18}F]fluoro-D-glucose ([^{18}F]-FDG).

2 Review of the Literature

2.1 Role of insulin in glucose and lipid metabolism

Human cells use mainly glucose and fatty acids to fulfill their energy needs. Both glycolysis and the degradation of fatty acids via β-oxidation produce acetyl coenzyme A (Ac-CoA), which serves as a substrate to the tricarboxylic acid cycle. After entering the cycle, Ac-CoA is further oxidized to generate adenosine triphosphate (ATP), which in turn is required for cellular survival and functions. The preferred substrate varies in different tissues and changes according to, for example, nutritional status and physical activity (Goodpaster & Sparks, 2017). While changes in the levels of circulating nutrients after a meal can alter tissue metabolism *per se*, the most important regulator of whole-body metabolism in the postprandial state is the hormone insulin, which is secreted by the pancreas (Samuel & Shulman, 2016).

2.1.1 Insulin structure and secretion

Insulin is a peptide hormone secreted in response to nutrient availability in the circulation by pancreatic β-cells in islets of Langerhans, which constitute 1% to 2% of the pancreas volume. Insulin is first synthesized as preproinsulin in the rough endoplasmic reticulum (RER) and then transformed into proinsulin after a signal sequence is removed. Proinsulin is folded, transported to the trans-Golgi network, and packed into immature secretory granules. During granule maturation, proinsulin is divided into insulin and C-peptide, and finally, the ready granules are stored either in readily releasable pools responsible for the first phase of insulin secretion or in the reserved pool responsible for delayed second-phase secretion (Hou et al., 2009) (Figure 1).

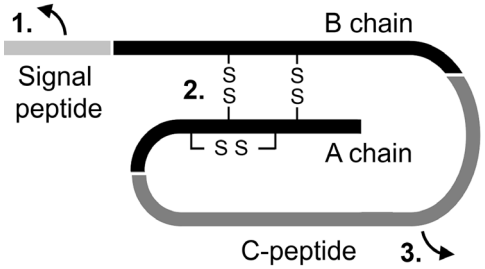

Figure 1. Production of insulin. First, a signal peptide is removed from preproinsulin to form proinsulin. This is followed by the formation of three disulfide bonds. Finally, by cleavage of C-peptide, proinsulin is converted to mature insulin, which consists of an A and B chain that are joined together.

Glucose is the most important regulator of insulin secretion, with even slight increase in blood glucose triggering changes in the release of the hormone within minutes. In addition to glucose, other nutrients, such as fatty acids and amino acids, can stimulate insulin secretion, while incretin hormones secreted by the gut after digestion (glucagon-like peptide-1 [GLP-1], glucose-dependent insulinotropic peptide [GIP], cholecystokinin [CCK], and peptide YY [PYY]) can add to the secretion-promoting effect of glucose. Glucagon, secreted by pancreatic α-cells in response to a lowering of blood glucose; somatostatin, excreted postprandially; and adrenaline and noradrenaline (epinephrine and norepinephrine), excreted during stress and exercise, are known to inhibit the release of insulin (Rutter et al., 2015). In addition, leptin, which is secreted by adipocytes, inhibits insulin secretion, possibly to reduce nutrient storing (Kieffer et al., 1997).

2.1.2 Insulin signaling

An insulin signaling cascade starts from insulin's binding to the IR, or in lesser affinity, to the homologous insulin-like growth factor-1 receptor (IGF1R), on the plasma membrane. There are two isoforms of the receptor: IR-A and IR-B. The latter has a more central role in adult metabolism, and the former likely plays a role in cell survival and mitosis, with a disproportionate increase in expression of IR-A over IR-B associated with insulin resistance, aging, and neoplastic cell proliferation (Belfiore et al., 2017).

An IR is a tyrosine kinase receptor and consists of four parts: two extracellular α-units and two transmembrane β-units. The binding of insulin to the α-subunits activates the β-subunits, which further activate intracellular substrates, such as the insulin receptor substrate (IRS) proteins. Activation of the IRS results in the recruitment of phosphoinositide 3-kinase (PI3K), which further phosphorylates phosphatidylinositol 4,5-bisphosphate (PIP_2) into phosphatidylinositol (3,4,5)-triphosphate (PIP_3), both of which are phospholipids bound to plasma membrane. This results in a translocation of phosphoinositide-dependent kinase-1 (PDK-1) to the membrane (Boucher et al., 2014).

Serine/threonine kinase protein kinase B (PKB or AKT) is consequently transported to the membrane and is phosphorylated by PDK-1; however, it also requires phosphorylation by mammalian target of rapamycin complex 2 (mTORC2) to reach full activation (Sarbassov et al., 2005). There are three isoforms of AKT kinases, which, despite their highly homologous structure, are coded by different genes and seem to have different roles in cell metabolism and survival. AKT1 (or PKBα) is the main isoform in all tissues, while AKT2 (or PKBβ) is mostly active in insulin-sensitive tissues (skeletal muscle, liver, and AT) and is considered to be crucial for insulin-mediated glucose and fatty acid metabolism (Gonzalez &

McGraw, 2009), although a more significant role of ATK1 in skeletal muscle lipid metabolism has also been reported (Bouzakri et al., 2006). AKT3 (PKBγ) is enriched in the brain and is required for normal brain development (Gonzalez & McGraw, 2009). Furthermore, phosphorylated AKT has several substrates, and in addition to tissue metabolism, it plays an important role in cell survival, growth, tissue development, and angiogenesis.

Concerning metabolism, the following are the most important reactions following the binding of insulin to the IR and the activation of the PI3K/AKT pathway (Figure 2):

1. *Increase in insulin-stimulated GU* by inactivation of TBC1D1 and TBC1D4 (AS160), resulting in transportation and fusion of glucose transporter 4 (GLUT4) vesicles to the plasma membrane (Leto & Saltiel, 2012).
2. *Increase in glycogen synthesis* by inactivation of glycogen synthase kinase-3 (GSK3) (Sutherland et al., 1993) or via another pathway (Wan et al., 2013).
3. *Suppression of EGP* in the liver and kidneys by inhibiting the function and interaction of transcriptional factor forkhead box O (FOXO) and transcriptional cofactor peroxisome proliferator-activated receptor γ coactivator 1α (PGC-1α), resulting in decreased expression of gluconeogenic genes (Puigserver et al., 2003).
4. *Increase in lipid synthesis* in the liver either by activating mammalian target of rapamycin complex 1 (mTORC1), which induces activation of sterol regulatory element-binding protein 1 (SREBP-1) (Yecies et al., 2011), or indirectly by inhibition of FOXO, which enables activation of pyruvate dehydrogenase complex (PDC), resulting in enhanced glycolysis and production of precursors for lipogenesis (Jeong et al., 2012).
5. *Stimulation of glycolysis* by activating glucokinase in the liver (Foretz et al., 1999) and hexokinase II in skeletal muscle (Vogt et al., 2000), which convert glucose into glucose-6-phosphate (G6P).
6. *Suppression of lipolysis and promotion of lipogenesis in AT* (Roden & Shulman, 2019).
7. *Decreased fatty acid oxidation* in the liver via inhibition of PGC-1α (Li et al., 2007).

Other than the pathways downstream from AKT, PDK-1 also activates atypical protein kinase C (aPKC), which is required for insulin-stimulated hepatic lipid synthesis and GLUT4 translocation (Farese & Sajan, 2010).

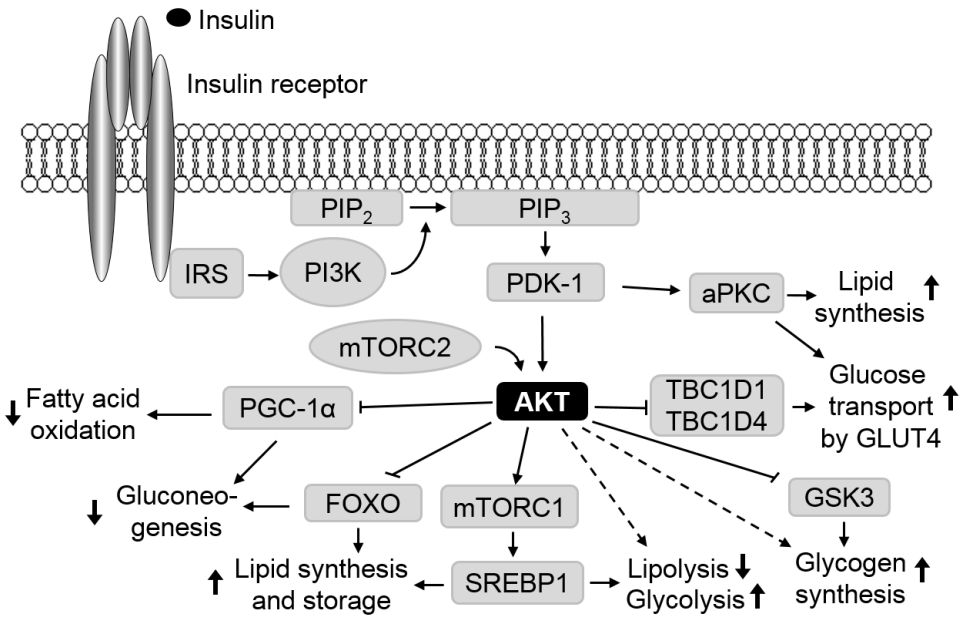

Figure 2. Effects of activation of insulin signaling cascade on cellular glucose and lipid metabolism. Adapted from Boucher et al. (2014) with a permission from publisher, © Cold Spring Harbor Laboratory Press.

2.1.3 Effects of insulin on tissue metabolism in normal physiology

Increased substrate storing in the liver

The liver consists mostly (~80%) of hepatocytes, which use fatty acid oxidation as their main energy source during fasting, but switch to using glucose for fuel in the postprandial state when circulating carbohydrate levels increase. Glucose is primarily transported to hepatocytes via insulin-independent glucose transporter 2 (GLUT2). This transporter has a high capacity but a low affinity to binding glucose, allowing it to carry glucose efficiently using facilitative diffusion, and it enables bidirectional transportation over the membrane (Rui, 2014).

The liver plays a distinct role in handling different substrates derived either from the intestines via the portal vein in the postprandial state or from other tissues during fasting and physical strain (Figure 3). During fasting, the liver takes up fatty acids secreted by white adipose tissue (WAT) and transforms them to glucose (gluconeogenesis). Thereafter, glucose from gluconeogenesis or from hepatic glycogen storages can be released into circulation (the process of EGP) to be used by tissues for which the availability of glucose is essential, most importantly in the

brain. The liver also takes up fatty acids that have been packed in chylomicrons by intestinal enterocytes or that are derived from lipolysis in AT, and it is able to store fatty acids as TAGs or pack and secrete them in very-low-density lipoproteins (VLDLs) to be consumed by or stored in peripheral tissues (Rui, 2014).

In the postprandial state, the increased glucose level results in increased GU in the liver, while insulin has no major direct effect on glucose transportation. However, as insulin promotes the expression of glucokinase, glucose is rapidly converted into G6P, which in turn increases GU into hepatocytes. In addition to the direct effects of insulin, an abundance of G6P also supports postprandial glycogen formation (Roach et al., 2012).

Considering postprandial whole-body glucose homeostasis, insulin's ability to inhibit hepatic endogenous glucose production (EGP) is more important than the effects on liver GU. While G6P again works as an allosteric regulator and inhibits the breakdown of glycogen, insulin is also a potent suppressor of glycogenolysis and EGP either via direct effects or by suppressing WAT lipolysis and subsequent hepatic gluconeogenesis (Perry et al., 2015; Titchenell et al., 2015).

Both insulin and the rise in carbohydrate availability after a meal drive the process of converting excess glucose into fatty acids (*de novo* lipogenesis), which are stored as TAGs in the liver and can be released during fasting, while insulin limits the release of fatty acids packed in VLDLs in the fed state (Sparks et al., 2012). Insulin also inhibits fatty acid oxidation in the liver, resulting in decreased synthesis of ketone bodies, which are important nutrients during extended fasting (Li et al., 2007).

Shift to glucose oxidation and storing in skeletal muscle

Like the liver, skeletal muscle uses mostly fatty acids for fuel during fasting. However, in the fed state, skeletal muscle accounts for the majority (60–80%) of insulin-stimulated GU, as insulin rapidly mobilizes GLUT4s into the cell membrane, followed by a switch from fatty acid uptake and oxidation to glucose oxidation (Mäki et al., 1998; Cartee, 2015; Goodpaster et al., 2017).

Another important process stimulated by insulin is the increased glycogen synthesis in the postprandial state, as skeletal muscle requires swiftly available glucose to produce energy during physical strain at higher intensities when the energy needs are no longer met solely by circulating fatty acids (Romjin et al., 1993). Furthermore, during exercise, when the mitochondrial capacity of producing energy from pyruvate acquired from glycolysis is exceeded, excess pyruvate is converted to lactate, which can then be used as an energy source by skeletal muscle—or more efficiently by the myocardium and the brain—or converted back into pyruvate in the liver (Brooks, 2018) (Figure 3).

Increased storing and reduced release of fatty acids in white adipose tissue

White adipose tissue (WAT), which serves as the reservoir for excess metabolic fuel by storing fatty acids as TAGs, is also capable of *de novo* lipogenesis and re-releasing fatty acids and glycerol when circulating nutrients are scarce (Bódis & Roden, 2018). Glucose uptake into WAT results via insulin-mediated transport by GLUT4, with WAT accounting for 5–10% of postprandial glucose disposal (Virtanen et al., 2002). The more essential effects of insulin result from activation of the mTORC1-SREBP1-pathway, followed by increased storing of fatty acids as TAGs and suppression of lipolysis, as well as increased *de novo* lipogenesis, although the latter remains at a lower rate in WAT than in the liver in the postprandial state (Bódis & Roden, 2018). Insulin also enhances the uptake of fatty acids into WAT by increasing fatty acid transport protein 1 (FATP1) translocation to the plasma membrane, as well as by increasing the expression and activity of lipoprotein lipase (LPL), an enzyme required for the hydrolysis of TAGs into fatty acids and glycerol, which can be taken up by adipocytes (Czech et al., 2013).

Stimulated glucose uptake into brown adipose tissue

Brown adipose tissue (BAT) is mainly located in supraclavicular and paravertebral depots in adults. While it shares some metabolic functions and structures with WAT, its prominent feature is the expression of uncoupling protein-1 (UCP1), which, by blocking the negative feedback loop of mitochondrial levels of high ATP and low ADP, enables a high rate of fatty acid oxidation, resulting in thermogenesis during cold exposure (Carpentier et al., 2018). While insulin can increase the level of BAT GU up to fivefold (Orava et al., 2011), the rate of cold-induced thermogenesis depleting intracellular TAG storages and circulating fatty acids seems to be independent of insulin effects (Blondin et al., 2015).

Brain glucose metabolism

The brain relies almost exclusively on glucose as fuel, using 20% of the whole-body glucose supply, although it can also use ketone bodies produced by the liver during extended fasting, and it seems to prefer lactate when it is available (Aalling et al., 2018). Glucose is first transported across the blood-brain barrier (BBB) down the concentration gradient via facilitative transport by glucose transporter 1 (GLUT1) (Pardridge et al., 1990). Neurons express mainly GLUT3 transporters, which have a higher affinity and capacity for glucose than GLUT1, whereas astrocytes—the main cell type in the brain—take up glucose mostly via GLUT1 transporters and are also able to store some glucose as glycogen. Likely in addition to direct GU via GLUT3, neurons use lactate provided by astrocytes to fulfill their energy needs in response to

neuronal activity ("astrocyte-neuron-lactate shuttle") (Pellerin & Magistretti, 1994), though some consider the evidence to still be controversial (Mason, 2017).

Although brain glucose metabolism has previously been thought to be insulin-independent, and central insulin has been thought to serve mainly as a signal of satiety, neurons have been shown to express both IRs and GLUT4 and to respond to insulin stimulus by increasing GU (Reno et al., 2017). In contrast, in astrocytes, insulin does not seem to increase GU despite expression of GLUT4, but it does stimulate glycogen synthesis (Heni et al., 2011). While supraphysiological circulating insulin levels do not produce a significant effect on the brain GU compared to fasting in healthy, lean subjects (a ~3% to 4% increase) (Hirvonen et al., 2011), brain GU was 15% lower during hypoinsulinemia compared to fasting insulin levels (Bingham et al., 2002), suggesting that insulin might play at least a minor role in brain glucose metabolism.

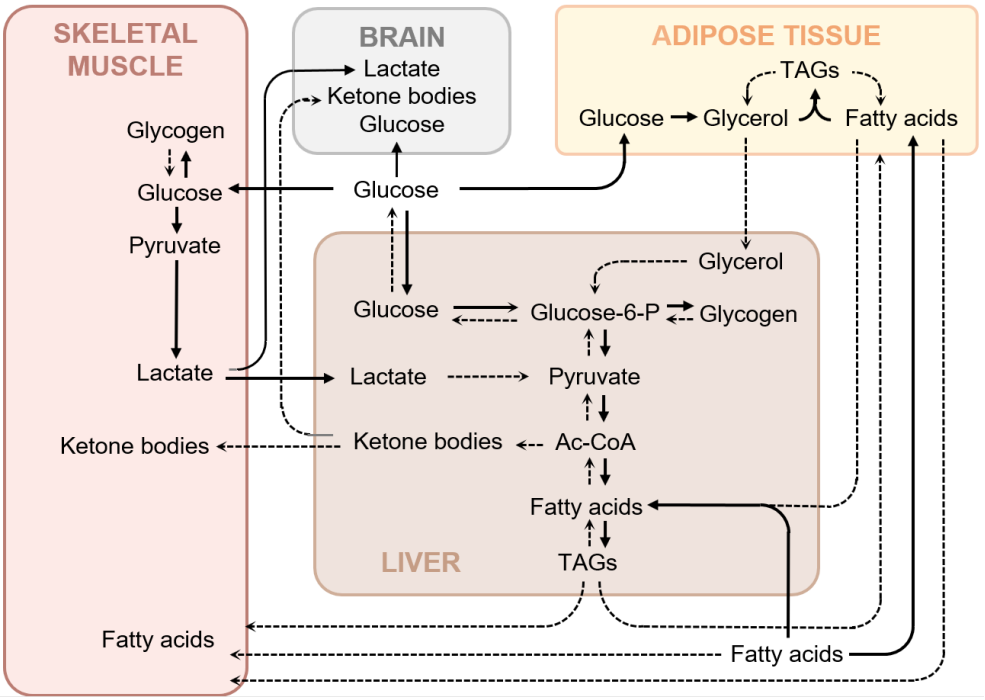

Figure 3. Glucose and lipid fluxes directly or indirectly promoted (black arrows) or inhibited (dashed arrows) by insulin in the postprandial state. In the **liver**, insulin promotes the conversion of glucose into glucose-6-phosphate and glycogen synthesis, which enhances glucose uptake; the conversion of excess carbohydrates into fatty acids (*de novo* lipogenesis); and their storage in the liver as triacylglycerols (TAGs), while inhibiting glycogenolysis and the release of TAGs in very low -density lipoprotein (VLDL) particles. In **skeletal muscle**, insulin stimulates glucose uptake and glycogenesis, consuming carbohydrates as the primary substrate for energy metabolism, and inhibits glycogenolysis. In **white adipose tissue**, insulin increases the uptake of glucose and fatty acids and promotes their storage as TAGs, while inhibiting the reverse processes. Glucose is the primary source of energy for the **brain**, with the uptake rate normally being near constant independently of circulating insulin levels.

2.2 Insulin and the brain in normal physiology

2.2.1 Metabolic inputs from the periphery to the brain

A large body of evidence has recognized the brain as playing a central role in regulating feeding behavior and energy homeostasis, with the brain collecting information about substrate availability in the circulation, as well as about nutritional status via endocrinal and neural pathways from peripheral tissues (Schwartz et al., 2000; Kim et al., 2018).

Research has mostly focused on the role of the hypothalamus in sensing and regulating brain responses to metabolic cues, with the arcuate nucleus (ARC) serving as the first-response area to a variety of signals. The hypothalamic ARC consists of agouti-related protein/neuropeptide Y neurons (Agrp/NPY), inhibited by insulin and leptin (Hahn et al., 1998), and pro-opiomelanocortin/cocaine- and amphetamine-regulated transcript neurons (POMC/CART), which are activated by signals of satiety and adiposity (Elias et al. 1998). These neurons transmit the afferent signals to further locations across the CNS, most the notably paraventricular nucleus, ventromedial nucleus, and dorsomedial nucleus (Schwartz et al. 2000). The nucleus of the solitary tract (NTS), located in the brain stem, likely plays an important role in a) collecting inputs both from the hypothalamic pathway and from the periphery and b) coordinating the response resulting in altered eating behavior (Schwartz et al., 2000) (Figure 4).

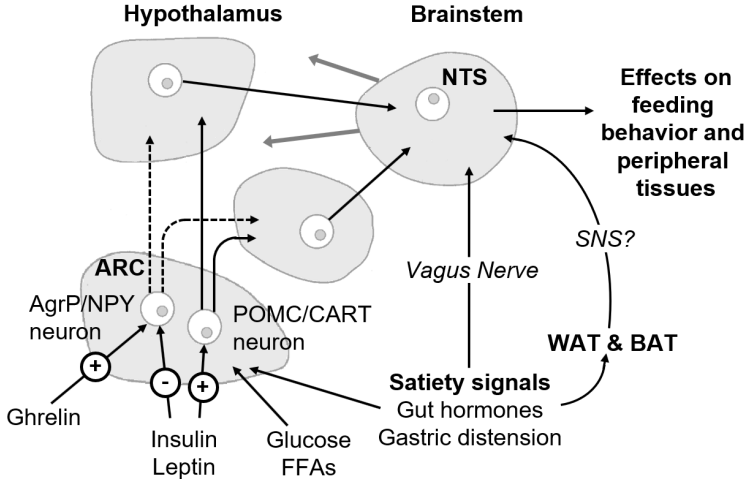

Figure 4. Cues of satiety, hunger, feeding, and body adiposity can be transmitted to the hypothalamus via direct receptor binding, with the activation of POMC/CART neurons and the inhibition of AgrP/NPY neurons resulting in anorexigenic responses. The signals are communicated to the brainstem via second-order neurons in different hypothalamic nuclei. Another route is reverse signaling from the brainstem to the hypothalamus and cortical regions, stimulated by afferent neuronal routes or receptor activation in the hindbrain. ARC: arcuate nucleus, NTS: nucleus of the solitary tract, SNS: sympathetic nervous system, BAT: brown adipose tissue, FFAs: free fatty acids. Based on Porte et al. (2002) and Schwartz et al. (2000).

Insulin levels are affected both acutely, by eating, and continuously, by body adiposity (or, more precisely, the associated insulin sensitivity [Schwartz et al., 1997]), and its central effects on reducing food intake and body mass have long been recognized (Woods et al., 1979). The role of central insulin signaling in energy homeostasis is summarized in the next chapter.

Leptin is secreted by the AT, with the circulating concentrations increasing in line with an increase in body fat mass (Considine et al., 1996) and AT insulin-stimulated GU (Mueller et al., 1998). Soon after its discovery, leptin's lowering effect on body weight and food intake and its stimulating effect on energy expenditure (Halaas et al., 1995) were attributed to its central effects (Campfield et al., 1995), and it has an established role in communicating with the brain about long-term energy balance (Schwartz et al., 2000). WAT has also been proposed to signal the brain via paracrine, endocrine, and neuronal pathways (Guilherme et al., 2019).

In the postprandial state, the secretion of GLP-1, CCK, and PYY from the small intestine increases, while the secretion of ghrelin is inhibited. All of these hormones have been associated with the central regulation of eating behavior, with the aforementioned changes inducing satiety. In addition to a purely endocrinological approach (the secreted hormones reaching the brain via circulation), a variety of routes combining endocrinological and neuronal signaling (mainly via afferent vagal nerve ends) have been suggested (Steinert et al., 2017).

Suprascapular BAT depots are also considered to participate in regulating feeding behavior via afferent signals to the brain (Glick, 1982; Cannon & Nedergaard, 2004). Consuming carbohydrates has been shown to stimulate BAT thermogenesis and activate the sympathetic nervous system (SNS) (Welle et al., 1981), with the hypothesis of a functional BAT-brain axis being further supported by the existence of both an afferent and efferent SNS neural loop between the tissues (Ryu et al., 2015). Interestingly, gut hormone secretin is also able to stimulate BAT directly, as well as induce satiety and reduce food intake (Li et al., 2018). It has even been suggested that diurnal changes in BAT activity orchestrate the daily feeding-fasting cycle (Blessing et al., 2013), but this view is not supported by all (Cannon & Nedergaard, 2004).

While an increased availability of glucose and long-chain FFAs does not seem to affect brain metabolism or body weight, hypothalamic sensing of these nutrients has been reported to participate in regulating hepatic EGP (Grayson et al., 2013).

2.2.2 Transportation of insulin to central insulin receptors

Despite that the central nervous system (CNS) is likely able to produce some insulin, its effect on central and peripheral metabolism remains vague (Lacroix et al., 2008; Mazucanti et al., 2019), and the majority of insulin in cerebrospinal fluid (CSF) is

widely considered to originate from circulation (Margolis et al., 1967; Banks, 2004). Insulin is first transported across the BBB by receptor-mediated endocytosis (King & Johnson, 1985), albeit that receptor knock-out models have shown that there is likely another route as well (Rhea et al., 2018). The transportation is characterized by fast saturability as the increase in CSF insulin concentration plateaus already before a significant lowering of plasma glucose levels can be seen (Baura et al., 1993; Banks et al., 1997). Interestingly, the rate of insulin transportation varies between different brain regions in mouse models, with the olfactory bulb showing remarkably higher rates (Banks et al., 1999), followed by the pons, medulla, and hypothalamus (Banks & Kastin, 1998), while little or no transport occurs in the occipital cortex (Banks & Kastin, 1998). Furthermore, the expression of IRs as well as IRS demonstrates a similar distribution across the brain, with higher concentrations present in areas with enhanced insulin transportation capacity (Havrankova et al., 1978; Kleinridders et al., 2014).

2.2.3 Assessing the effects of central insulin signaling in clinical studies

In experimental settings, insulin's impact on brain metabolism and function has been studied in animal models by administering insulin intracerebroventricularly or into the carotid arteries to isolate the central effects from confounding peripheral effects. Due to the invasiveness of these techniques, studies on humans have been performed by administering insulin intranasally. In rodents, intranasal insulin (INI) reaches the brain via olfactory nerve tracts while avoiding the tightly regulated transportation across the BBB, and this is considered to occur in humans as well (Renner et al., 2012). This hypothesis is supported by a report showing a more rapid and strong increase in CSF insulin concentration after intranasal administration than what should ensue if insulin passed via circulation first (Born et al., 2002). The approach has since been applied by several research groups, and it has proven to be applicable in reproducing results similar to those seen in animal models (Benedict et al., 2011; Heni et al., 2012; Dash et al., 2015).

Another, more indirect way in which to investigate the effects of brain insulin signaling is via pharmacological activation (by diazoxide) or blockage (by sulphonylureas) of central K_{ATP} channels. In the pancreas, activation of these channels mediates insulin secretion, whereas in the brain, their activation in glucoregulatory neurons by insulin is essential for producing peripheral effects (Spanswick et al., 2000; Obici et al., 2002; Pocai et al., 2005).

2.2.4 Brain insulin signaling as a regulator of central and peripheral metabolism

After initial recognition of insulin as a regulator of satiety, a multitude of effects independent of or enhancing insulin's direct actions on peripheral tissues have been described (Figure 5).

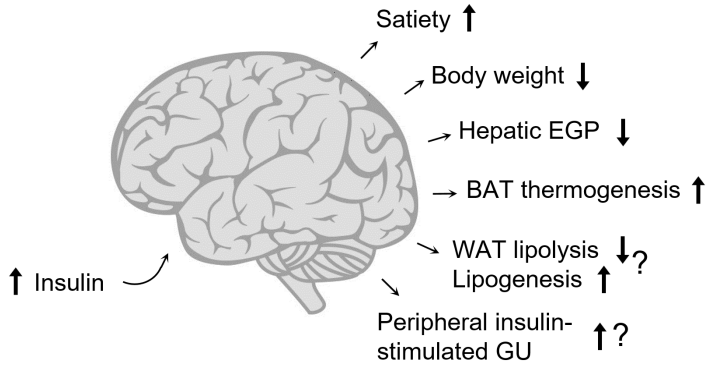

Figure 5. Central insulin sensing produces responses in several tissues and on the whole-body level. EGP: endogenous glucose production, BAT: brown adipose tissue, WAT: white adipose tissue, GU: glucose uptake (Kleinridders et al., 2014; Heni et al., 2015a).

Induction of satiety and weight loss

Insulin has the ability to directly affect the hypothalamus, reduce food intake, and promote satiety and weight loss. These effects were the first metabolic responses to be reported (Debons et al., 1970; Woods et al., 1979), and they have also been reproduced in humans (Hallschmid et al., 2004; Benedict et al., 2008; Jauch-Chara et al., 2012). Interestingly, direct insulin delivery to the brain via intracerebroventricular (i.c.v.) administration in mice or intranasally in humans seems to affect males more strongly, whereas female subjects exhibit a lesser or no effect on feeding behavior or body weight (Clegg et al., 2003; Hallscmid et al,. 2004; Benedict et al., 2008).

The mechanisms underlying the anorexigenic response are still incompletely understood. For one, insulin seems to reduce the appeal of food by decreasing olfactory capacity (Ketterer et al., 2011; Brünner et al., 2013) and suppressing the reaction induced by visual food cues (Guthoff et al., 2010). Enhanced brain metabolism after INI, measured as ATP concentration, has also been suggested to serve as a signal to reduce food intake (Jauch-Chara et al., 2012).

Inhibitory effect on endogenous glucose production and controversial results on hepatic lipid metabolism

The role of central insulin signaling in the suppression of hepatic glucose production (EGP) has been reported in several animal and human studies. In rodents, this effect has been attributed especially to insulin's ability to activate the K_{ATP} channels of the mediobasal hypothalamus or dorsal vagus complex, resulting in the suppression of gluconeogenic gene transcription or the inhibition of EGP (Obici et al., 2002; Pocai et al., 2005; Könner et al., 2007; Filippi et al., 2012). The centrally regulated suppression of hepatic EGP has been shown to be associated with the activation of hepatic interleukin-6 (IL-6), and to follow the activation of signal transducer and activator of transcription-3 (STAT3) (Inoue et al., 2006; Koch et al., 2008).

In contrast, experiments performed in dogs under pancreatic clamp conditions, implying the more physiological 3:1 ratio of hepatic and CSF insulin concentrations, revealed no change in EGP after i.c.v. insulin administration despite an increase in STAT3 phosphorylation. However, in these studies, hepatic glycogen synthesis was augmented as a result of the inhibition of GSK gene transcription and protein expression (Ramnanan et al., 2011, 2013). The same group of researchers later stressed that despite these modest findings, insulin's direct effect on hepatic metabolism prevails over the central regulation (Edgerton et al., 2006; Ramnanan et al., 2012).

Results from human studies, performed almost exclusively on males, have demonstrated that both INI and activation of central K_{ATP} channels with diazoxide enhance insulin's inhibitory effect on EGP during systemic hyperinsulinemia (Dash et al., 2015; Heni et al., 2017; Kishore et al., 2012). Under fasting conditions, INI has no effect on EGP (Gancheva et al., 2015; Plomgaard et al., 2019), whereas one study, using diazoxide with somatostatin to suppress endogenous insulin production and applying intravenous (i.v.) insulin comparable to fasting levels, showed a reduction in EGP (Esterson et al., 2016). These findings support the notion of an additive, rather than an essential role of central insulin signaling on regulating EGP. This view is also confirmed by the almost unaltered postprandial glucose metabolism in subjects lacking a direct neuronal contact between the brain and the liver due to liver transplantation (Perseghin et al., 1997a).

Studies regarding INI's effects on hepatic lipid metabolism have produced more controversial results. In experiments performed under fasting conditions, a single dose of INI has been reported to increase hepatic TAG content (Gancheva et al., 2015) and also inhibit triglyceride-rich lipoprotein secretion (Xiao et al., 2017), while four weeks of daily dosing resulted in no effect on hepatic lipid content (Scherer et al., 2017). The results from mouse studies do not form a clear conclusion either. On the one hand, one report found that i.c.v. insulin acutely stimulates hepatic TAG excretion, resulting in reduced hepatic TAGs when administered chronically

(Scherer et al., 2016). On the other hand, insulin has been shown to suppress NPY-expressing neurons (Qiu et al., 2014), which should act against the initiation of VLDL secretion by these hypothalamic neurons (Stafford et al., 2008).

Promotion of brown adipose tissue activity and white adipose tissue lipogenesis

Thermogenesis in BAT in the postprandial state has been reported in animal models as well as in humans, and it likely contributes to the afferent signals of hunger and satiety, while also being upregulated by central stimuli induced by insulin and other hormones (Cannon & Nedergaard, 2004). In a mouse model, i.c.v. insulin administration has been shown to increase BAT activity via SNS activation (Rahmouni et al., 2004). Accordingly, in male human subjects, INI has been found to increase mean postprandial thermogenesis, an indicator of BAT activity (Benedict et al., 2011).

In the same study by Benedict et al. (2011), INI decreased postprandial levels of circulating free fatty acids (FFAs), suggesting the central regulation of postprandial lipolysis. Indeed, in mouse models, acute and chronic administration of insulin to the brain has been shown to promote lipogenesis and reduce lipolysis in subcutaneous and visceral AT during fasting and hyperinsulinemic-euglycemic clamp conditions (Koch et al., 2008; Scherer et al., 2011; Coomans et al., 2011a), possibly via SNS activation (Scherer & Buettner, 2011). However, the studies in humans that have accounted for the confounding increase in circulating insulin levels after INI have not detected any effects on systemic lipolysis measured as changes in FFA or triglyceride levels during fasting or hyperinsulinemia (Gancheva et al., 2015; Dash et al., 2015; Heni et al., 2015b; Xiao et al., 2017).

Effects on peripheral glucose uptake

The effects of brain insulin signaling on peripheral glucose metabolism are more controversial. Two studies in mice have suggested that central insulin stimulus increases whole-body insulin-stimulated glucose utilization, measured as the glucose infusion rate (GIR) required to sustain normoglycemia during hyperinsulinemia. However, the authors have attributed this to a decrease in EGP and not to enhanced peripheral GU (Coomans et al., 2011b; Filippi et al., 2012), and one study reported no change in the glucose rate of disappearance (Rd) (Obici et al., 2002). However, there have also been reports of a) a remarkable 59% decrease in insulin-stimulated skeletal muscle GU following the inhibition of hypothalamic insulin signaling by blocking central K_{ATP} channels (Coomans et al., 2011b) and b) increased skeletal

muscle glycogenesis and whole-body glucose turnover following i.c.v. insulin infusion (Perrin et al., 2004).

Furthermore, in humans, applying INI has been reported to increase whole-body insulin sensitivity, determined as the homeostatic model assessment for insulin resistance (HOMA-IR) (Heni et al., 2012), or insulin-stimulated glucose consumption represented by GIR as well (Heni et al., 2014). Although in a later study by the same group, only a trend toward a higher GIR remained after taking into account the confounding effects of spillover from INI to circulation (Heni et al., 2017). The rate of glucose disappearance has not been altered by INI (Dash et al., 2015; Heni et al., 2017) or diazoxide (Kishore et al., 2012) in the presence of systemic hyperinsulinemia and normoglycemia.

2.3 Insulin resistance

Insulin resistance is usually referred to as the failure of an insulin stimulus to induce primarily metabolic changes in specific tissues or on the whole-body level, and it was first recognized in the 1930s, when a subgroup of hyperglycemic patients was reported not to respond to insulin treatment (Himsworth, 1936). The condition has since been recognized as the major feature of T2D, and the development, manifestations in different tissues, and treatment of insulin resistance continue to be targets of fervent investigations. A multitude of genetic and epigenetic factors, as well as the sedentary lifestyle associated with obesity and nutrient excess, and changes in gut microbiota have been shown to contribute to increasing the risk of insulin resistance.

The primary defect leading to systemic insulin resistance is impaired GU into skeletal muscle in the postprandial state and a subsequent reduction in glycogen synthesis (DeFronzo et al., 2009), supported by studies in the offspring of T2D patients (Perseghin et al., 1997b; Kashyap et al., 2004; Ferrannini et al., 2003; Vaag et al., 1992). As skeletal muscle should be the predominant site of postprandial GU, impaired GU leads to sustained hyperglycemia, which is met by increased insulin secretion by the pancreatic β-cells. The pancreas is usually capable of accounting for hyperglycemia for a long time, with increased insulin levels being the first signs of insulin resistance. A failure in this response results in a progression towards T2D and usually starts to occur years before the diagnostic criteria of the disease are fulfilled (Tabák et al., 2009; Ohn et al., 2016).

Chronic hyperinsulinemia has disadvantageously been shown to adversely cause insulin resistance, mostly attributed to further reduced glycogen synthesis in skeletal muscle (Del Prato et al., 1994; Koopmans et al., 1999; Iozzo et al., 2001). In the liver, sustained hyperinsulinemia does not have a primary effect on EGP (Del Prato et al., 1994; Koopmans et al., 1999), but increases hepatic *de novo* lipogenesis and

circulating FFA levels (Koopmans et al., 1999). Moreover, in the liver and AT, hyperinsulinemia initially promotes TAG storing. Increased WAT mass is, however, susceptible to hypoxia, inflammation, and dysfunctions in lipid-storing capacity, which contribute to aggravating the situation further (Czech et al., 2017). Chronic hyperglycemia (glucotoxicity) (Rossetti et al., 1990; Burén et al., 2003) and hyperlipidemia (lipotoxicity) (DeFronzo, 2010) can also have detrimental effects on insulin sensitivity. Tissue-specific alterations in insulin resistance are reviewed in Figure 6.

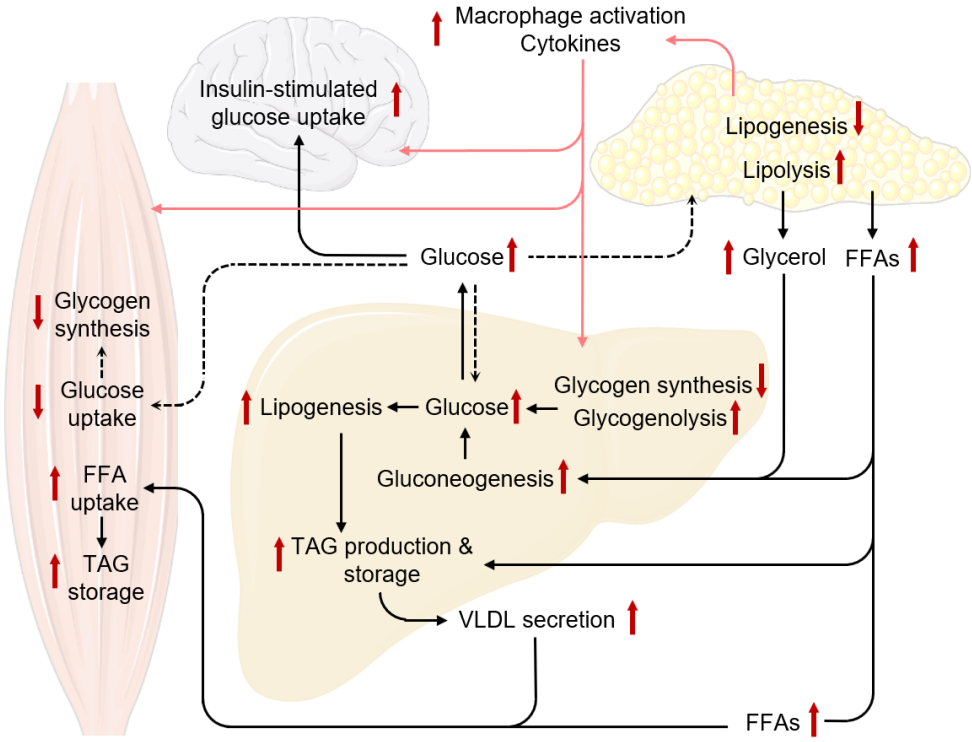

Figure 6. Manifestations of insulin resistance in different tissues and the resulting metabolic crosstalk between tissues. Impaired insulin sensitivity is associated with reduced insulin-stimulated glucose uptake in most peripheral tissues, whereas in the brain, the result seems to be the opposite. In adipose tissue, the key feature is inadequate suppression of lipolysis, resulting in increased levels of circulating glycerol and FFAs. These serve as precursors for gluconeogenesis in the liver, where excess glucose is released back into circulation or directed towards lipogenesis, resulting in an accumulation of ectopic fat. In skeletal muscle, fatty acids are also stored in excess as TAGs, whereas glycogen synthesis is decreased. Inflammatory processes have also been recognized to alter substrate utilization. FFAs: free fatty acids, TAG: triacylglycerol, VLDL: very-low-density lipoprotein. Based on Samuel and Shulman (2016) and Roden and Shulman (2019). Illustrated using SMART (Servier Medical ART; https://smart.servier.com) under the terms of the Creative Commons Attribution 3.0 Unported license (CC BY 3.0).

Genetic predisposition to insulin resistance

Applying genome-wide association studies to large populations has currently led to the recognition of ~403 genetic loci in which a) mutations can be associated with increased risk of T2D (Mahajan et al., 2018) and b) over 80 common genetic variants can be associated with a modest increase in the lifetime risk of T2D (Fuchsberger et al., 2016). In addition to common, small effect variants, low-frequency or rare variants with larger effects, as well as epigenetic factors, contribute to the heritability of T2D. However, part of the known variants are associated with a failure in insulin secretion or an increased prevalence of obesity rather than insulin resistance. Moreover, for many variants, the functional effects are not easy to target, as they are not located in the exome—the area of the gene coding proteins—but in the intron areas regulating protein expression.

Genetic profiling in insulin resistance, possibly later enabling precision medicine and screening for people at higher risk of T2D, would require a better understanding of the functional effects of single variants. Performing genotype-based callback studies on variant carriers could be used to elucidate the significance of a single mutation on tissue metabolism, starting from variants with known effects on insulin sensitivity.

One candidate for further phenotyping is a low-frequency coding variant p.Pro50Thr in the *AKT2* gene, which is present in 1.1% of people with Finnish ancestry, but has not been reported in other populations (Manning et al., 2017). Variant carriers demonstrated hyperinsulinemia and impaired insulin sensitivity during a 2-hour oral glucose tolerance test (OGTT), and they had higher susceptibility to T2D, with further *in vitro* studies confirming a partial loss of phosphorylation of the AKT2 protein, resulting in impaired glycogen synthesis in skeletal muscle (Manning et al., 2017). Previous studies in animal (specifically mice) *AKT2* knock-out models support the functional role of the loss-of-function variant, as these mice presented impaired insulin-stimulated GU and lesser suppression of EGP by insulin (Cho et al., 2001; Wan et al., 2013; Garofalo et al., 2003). While the role of AKT2 in lipid metabolism has been more controversial, its normal function seems to be crucial for lipid handling and for the development and maintenance of AT (Leavens et al., 2009; Garofalo et al., 2003) while having a minor effect on lipolysis (Koren et al., 2015). Furthermore, in one family, a monogenic loss-of-function mutation of *AKT2* (p.Arg274His/*AKT2*) has been shown to result in severe insulin resistance, similarly led by the impaired inhibition of GSK3 by AKT2 (George et al., 2004).

2.3.1 Tissue-specific alterations in insulin resistance

Impaired glucose uptake into skeletal muscle

In skeletal muscle, insulin resistance is usually attributed to a primary defect in insulin signaling (Roden & Shulman, 2019). This results in impaired insulin-stimulated GU, followed by a decrease in glycogen synthesis (Cline et al., 1999).

However, not only faulty insulin signaling, but also increased availability of fatty acids, either from nutrition or resulting from disturbances in AT and hepatic lipid metabolism, complicates skeletal muscle insulin resistance. Fatty acids have been shown to compete with glucose when available, and during insulin stimulation, they inhibit GU (Ferrannini et al., 1983; Yki-Järvinen et al., 1991; Kelley et al., 1993) and insulin signaling possibly by inactivating PI-3K and IRS-1 (Dresner et al., 1999; Griffin et al., 1999). Furthermore, the excess fatty acid availability and associated mitochondrial dysfunction lead to an accumulation of ectopic fat, which further impairs insulin sensitivity via increased levels of diacylglycerols (DAGs) and protein kinase C (PKC), which inactivates IRS and results in the downregulation of several downstream pathways (Yu et al., 2002).

Reduced lipogenesis in white adipose tissue

The primary indication of insulin resistance in WAT is impaired lipid storage resulting from an inadequate suppression of lipolysis and the stimulation of lipogenesis, which also leads to the unphysiological release of fatty acids and glycerol in the postprandial state (Roden & Shulman, 2019).

Insulin resistance in WAT is usually attributed to an increased amount of WAT and an increased size of adipocytes, which results in tissue hypoxia and inflammation due to insufficient vasculature (Pasarica et al., 2009) and relative mitochondrial hypoxia due to excess fatty acids (Lee et al., 2014). Yet, the distribution of AT and genetic factors seem to participate in determining whether WAT will become insulin resistant (Shungin et al., 2015).

In addition to primary defects in insulin signaling, as seen in skeletal muscle, inflammatory response due to hypoxia is considered another major regulator of adipocyte insulin resistance (Bódis & Roden, 2018). Hypoxia-induced secretion of cytokines and cell death promote the differentiation of monocytes into M1 macrophages, which in turn secrete proinflammatory cytokines such as interleukin-1 and -6 (IL-1, IL-6), and tumor necrosis factor α (TNFα), which can also have detrimental effects on insulin sensitivity in different tissues (Thomas & Apovian, 2017).

Interestingly, adipocytes demonstrate reduced insulin-stimulated GU due to downregulated GLUT4 expression, whereas no similar change is seen in skeletal muscle. Moreover, adipose-tissue-specific GLUT4 knock-out mice demonstrate normal WAT development despite impaired insulin-stimulated GU into the tissue, combined with secondary insulin resistance in skeletal muscle and liver (Abel et al., 2001).

Inadequate suppression of endogenous glucose production in the liver

Hepatic insulin resistance reflects the changes in other tissues, with insulin's weakened ability to downregulate EGP being usually considered the main feature. The background of insulin resistance in the liver lies both in impaired IR binding and activation of downstream kinases in hepatocytes (Caro et al., 1986) and in the direct and indirect effects of fatty acids on hepatic metabolism and insulin signaling.

The high rate of EGP has been shown to originate mostly from an impaired downregulation of lipolysis by insulin, resulting in an excess of lipid precursors for gluconeogenesis in the liver (Perry et al., 2015). Furthermore, lower inhibition of glycogenolysis in insulin-resistant subjects (Basu et al., 2005), further impaired by excess fatty acids (Boden et al. 2002), and decreased glycogen synthesis (Krssak et al., 2004) result in surplus glucose being directed towards *de novo* lipogenesis.

In addition to fatty acids from *de novo* lipogenesis and diet, re-esterification of WAT-derived fatty acids plays a major role in TAG accumulation in the liver (Donnelly et al., 2005). In an insulin-resistant state, the TAGs are not only stored in the liver, but also released in VLDL particles (Choi & Ginsberg, 2011). The associated increase in DAGs and PKC, as also seen in skeletal muscle, aggravate insulin resistance, and together with stimulation by cytokines, contributes to the development of non-alcoholic fatty liver disease (NAFLD) (Shulman, 2014).

Increased insulin-stimulated glucose uptake in the brain

Contrarily to other tissues, brain insulin-stimulated GU is increased in insulin-resistant and obese subjects (Hirvonen et al., 2011; Tuulari et al., 2013; Boersma et al., 2018), while there seems to be no significant difference under fasting conditions (Hirvonen et al., 2011). Some studies have associated this change with brain inflammation, manifesting as hypothalamic astrogliosis in magnetic resonance imaging (MRI) studies (Thaler et al., 2012). This would be supported by the finding that brain [^{18}F]-FDG is mostly taken up by astrocytes rather than neurons (Zimmer et al., 2017); however, this division has also been criticized (Dienel et al., 2018). Another theory is that increased brain GU in insulin resistance is reciprocal to insulin's impaired effects on peripheral tissues, and the increase can be translated to

insulin's failure to prevent the brain from being exposed to hyperglycemia (Iozzo & Guzzardi, 2019).

Brain insulin resistance also seems to be associated with defective central regulation of EGP, as two groups reporting centrally mediated effects failed to demonstrate differences when using the same methods in obese and insulin-resistant subjects (Heni et al., 2017; Xiao et al., 2018). Enhanced hepatic TAG accumulation by INI was also absent in T2D subjects (Gancheva et al., 2015).

In addition to tissue metabolism, brain insulin resistance is also associated with poorer control of feeding behavior, brain connectivity, and impaired cognitive function (Heni et al., 2015; Iozzo & Guzzardi, 2019). It seems that changes in glucose metabolism link insulin resistance to cognitive impairment, as brain GU is increased in mild cognitive impairment, while hypometabolism is associated with progression to Alzheimer's disease (Ashraf et al., 2015), although it remains debatable whether increased GU is the precursor of cognitive decline or a response to failing neuronal function.

2.3.2 Treating insulin resistance

Lifestyle modifications

While genetic predisposition to insulin resistance cannot be amended, diet interventions, increasing physical activity, and weight loss have all been proven successful in preventing the progression from impaired insulin sensitivity to T2D (Pan et al., 1997; Tuomilehto et al., 2001; Knowler et al., 2002).

The favorable effects of weight loss on insulin resistance can be largely attributed to a reduction in ectopic fat depots in skeletal muscle and the liver, resulting in improved insulin signaling in these tissues. The decline in AT volume and the subsequent lower release of fatty acids also results in lower hepatic EGP, which alleviates hyperglycemia (Grams &Garvey, 2015). Furthermore, weight loss achieved by lifestyle changes, medications, or bariatric surgery have all been proven efficient in improving insulin sensitivity (Grams & Garvey, 2015), while bariatric surgery has been suggested to affect insulin sensitivity also via several other pathways independently of weight loss (Batterham & Cummings, 2016).

Exercising has been demonstrated to have several beneficial effects on insulin sensitivity, even without weight loss (Roberts et al., 2013). A single bout of physical activity has been shown to increase skeletal muscle GU for up to 48 hours by increasing GLUT4 translocation independently of insulin and by enhancing insulin signal transduction, both in healthy and insulin-resistant subjects (Hawley et al., 2008). In addition, exercise-induced improved oxidative capacity has been postulated to promote fatty acid oxidation, resulting in reduced TAG accumulation

in skeletal muscle (Hawley et al., 2008), while favorable changes in inflammatory biomarkers by exercise have also been reported (Roberts et al., 2013).

Pharmacological approach

Some antidiabetic drugs have been suggested to improve insulin sensitivity in addition to having glucose-lowering effects:

Thiazolidinediones (glitazones) activate the nuclear peroxisome proliferator-activated receptor gamma γ (PPARγ) receptors, resulting in promoted lipogenesis in subcutaneous AT and, most importantly, a redistribution of hepatic TAGs into subcutaneous WAT (Mayerson et al., 2002). These changes are associated with increased insulin-stimulated GU to skeletal muscle (Hällsten et al., 2002), as well as improved perfusion and consequently improved GU in AT (Viljanen et al., 2005).

Sodium-glucose cotransporter 2 (SGLT2) inhibitors act by inhibiting glucose reabsorption from the renal proximal tubules. Despite the almost exclusive expression of SGLT2 in the kidneys (Wright et al., 2011), previous studies have reported improved whole-body insulin-stimulated glucose Rd with the treatment (Merovci et al., 2014, 2016; Mudaliar et al., 2014; Daniele et al., 2016, Matsuba et al. 2018), suggested to result from improved skeletal muscle GU during hyperinsulinemia (Merovci et al., 2014). The latter hypothesis, however, is only based on the major role of skeletal muscle in insulin-stimulated GU, and not on a direct assessment. SGLT2 inhibitors have also been shown to cause a metabolic shift from glucose to fatty acid oxidation and ketone production in the postprandial state and during pharmacolocigal hyperinsulinemia (Ferrannini et al., 2014; Daniele et al., 2016). Interestingly, increased insulin-stimulated glucose disposal has also been shown to be accompanied by a counteracting increase in EGP (Merovci et al., 2014; Ferrannini et al., 2014).

Due to calorie loss and increased osmotic diuresis, treatment with SGLT2 inhibitors also induces significant weight loss (List et al., 2009; Ferrannini et al., 2013), mostly accounted for by a loss of subcutaneous and visceral AT mass (Bolinder et al., 2012). In addition, loss of WAT has been shown to be associated with a decrease in liver fat content in T2D patients with NAFLD in several studies with different SGLT2 inhibitors (Ito et al., 2017; Shibuya et al., 2018; Eriksson et al., 2018; Kuchay et al., 2018).

GLP1-receptor antagonists lower blood glucose by enhancing β-cell function. They have also been suggested to contribute to the regulation of feeding (Htike et al., 2017), and they improve whole-body insulin sensitivity (Zander et al., 2002) and have beneficial effects on hepatic lipid metabolism (Armstrong et al., 2016). However, whether these effects can be solely attributed to the lowering of body weight and blood glucose is currently unknown (DeFronzo, 2017), as studies

supporting the role of the pleiotropic effects of GLP-1 receptor activation in extrapancreatic tissues show partly conflicting results (Jiang et al., 2018; Gil-Lozano et al., 2010; Winzeler et al., 2019).

Furthermore, while metformin has long been the first-line drug in T2D, its glucose-lowering mechanisms of action are still not fully understood. However, the drug does not seem to directly affect whole-body or skeletal muscle insulin sensitivity (Hällsten et al., 2002), and the preeminent effect is usually considered to be the promoted suppression of EGP through reduced hepatic gluconeogenesis (Hundal et al., 2000).

2.4 Quantifying insulin sensitivity

2.4.1 Measures of whole-body insulin sensitivity

Hyperinsulinemic-euglycemic clamp

The hyperinsulinemic-euglycemic clamp technique (DeFronzo et al., 1979) is a well-established approach to measure whole-body insulin-stimulated GU. The method is based on rapidly increasing circulating insulin concentration to high physiological or supraphysiological levels while maintaining euglycemia (plasma glucose concentration 5.0 mmol/L ± 5%) by an i.v. glucose infusion. In insulin-sensitive subjects, hyperinsulinemia inhibits EGP by the liver and the kidneys, whereas euglycemia should prevent activation of other possibly confounding mechanisms regulating glucose metabolism. After an equilibrium phase, the rate of glucose infusion approximates the whole-body glucose disposal rate (M-value), and the following formula can be used:

$$M = GIR - SC - UC$$

where GIR is the glucose infusion rate, SC is the space correction accounting for changes in glucose levels, and UC is the rate of urinary glucose excretion (all µmol/kg/min).

It is also possible to add a somatostatin infusion to the routine protocol to suppress the release of endogenous insulin ("pancreatic clamp"). Furthermore, while no official threshold exists for insulin resistance, a cutoff point of 28 µmol/min/kg lean body mass has been suggested (Stern et al., 2005), with lower values indicating impaired insulin sensitivity.

Stable isotope techniques

Applying substrates, such as glucose or fatty acids, labeled with radioactive (e.g. tritium, ^{3}H) or non-radioactive (e.g. ^{13}C and ^{2}H) stable isotopes allows for the evaluation of their rate of appearance and disappearance (Steele et al., 1956; Dube et al., 2013). 3-[^{3}H]-glucose is often used together with the hyperinsulinemic-euglycemic clamp to allow for the simultaneous determination of glucose appearance, namely EGP. The use of dual or triple tracer techniques enables an investigation into the transportation and further metabolism of nutrients from meals; however, the challenges and inaccuracies resulting from the postprandial non-steady state need to be considered (Dube et al., 2013).

Other estimates of whole-body insulin sensitivity

As the hyperinsulinemic-euglycemic clamp requires experienced staff, and it can be considered time-consuming and invasive, other indices of insulin sensitivity are regularly applied, especially when studying larger study populations.

Whole-body insulin sensitivity can be estimated from fasting laboratory samples of glucose and insulin, by using either formulas such as HOMA-IR (Matthews et al., 1985) or the quantitative insulin sensitivity check index (QUICKI) (Katz et al., 2000), which mainly reflect hepatic insulin sensitivity. Indices facilitating data from an OGTT (Matsuda-ISI [Matsuda & DeFronzo, 1999], the Stumvoll metabolic clearance rate (MCR) or ISI [Stumvoll et al., 2000], Gutt [Gutt et al., 2000], and OGIS [Mari et al., 2001]) offer additional insight into the postprandial state and peripheral insulin sensitivity, while they may fail to differentiate impaired insulin secretion from insulin resistance. Matsuda-ISI, or the composite index, is calculated by dividing 10,000 by the square root of [fasting glucose x fasting insulin] x [mean glucose x mean insulin during OGTT], and it correlates significantly ($r = 0.73$) with *M*-values (Matsuda & DeFronzo, 1999). As with the hyperinsulinemic clamp, no reference range of normal values has been determined. Based on the original publication and the cutoff point for the *M*-value from Stern et al. (2005), Matsuda-ISI <3 indicates insulin resistance. In another population consisting of non-diabetic offspring of T2D patients, the mean Matsuda-ISI was 3.2 for subjects with insulin resistance and 6.4 for subjects without insulin resistance (Lorenzo et al., 2015). A revised QUICKI that also accounts for fasting non-esterified fatty acids (Perseghin et al., 2001) seems to correlate with *M*-values from the hyperinsulinemic-euglycemic clamp equally well as the OGTT-derived models (Otten et al., 2014).

A minimal model analysis of a frequently sampled i.v. glucose tolerance test (FSIVGTT) (Bergman et al., 1987), with additional i.v. insulin or tolbutamide to improve accuracy, correlates well with the *M*-values (Saad et al., 1997), but requires cannulation and frequent blood collection over 3 to 4 hours. Furthermore, the

FSIVGTT shares some of the limitations of the OGTT and loses reliability in subjects with diabetes (Saad et al., 1994).

Another more invasive method to assess whole-body insulin sensitivity is the insulin suppression test (IST) (Shen et al., 1970). This test includes i.v. infusions of somatostatin, insulin, and glucose at steady rates, and the level of insulin sensitivity is determined by the plasma glucose level 150–180 min after the start of the protocol. Compared to the clamp, the IST is as invasive and as laborious, and it can cause hypoglycemia in insulin-sensitive subjects and stimulate urinary glucose excretion in insulin-resistant subjects.

2.4.2 Biochemical approaches to measuring tissue-specific metabolism *in vivo*

Arteriovenous catheterization was the first technique developed to investigate tissue metabolism (Zierler, 1961). It is based on a simple model of different concentrations of substances in afferent and efferent blood vessels while blood flow is assumed to be steady.

Microdialysis is a more sophisticated technique to measure tissue metabolism (Lönnroth et al., 1987), with the inclusion of tissue blood flow measurements allowing for a more accurate assessment of, for example, AT lipolysis (Jansson et al., 1992), skeletal muscle GU (Peltoniemi et al., 2000), and AT GU (Virtanen et al., 2001).

However, the invasiveness of these methods hinders their use in clinical studies, and they also only yield results from a small area, which can cause issues in heterogeneous tissues unless several catheters are used. While the turnover of small, hydrophilic molecules (such as glucose or glycerol) can be reliably measured with microdialysis, investigating larger, lipophilic molecules (such as insulin and fatty acids) is less feasible due to their membrane adhesion and protein binding.

2.4.3 Positron emission tomography

Positron emission tomography (PET) is an imaging technique that enables quantitative *in vivo* studies of tissue metabolism, blood flow, and receptor binding. Compared to several previously described approaches, it is non-invasive, and it also has the advantage of allowing for a direct investigation of deep tissues.

For those studies, a ligand suitable for the aim of the study (e.g. 2-deoxy-D-glucose for studying glucose metabolism) is labeled with a short-lived positron-emitting radionuclide (e.g. fluorine-18) and administered to the study subject typically intravenously, while oral routes of administration and inhalations are also possible. After a varying period of time required for the distribution and

accumulation of the radiotracer into the target tissues, tissue activity, which represents the behavior of the selected ligand, can be measured by using a PET scanner.

Positron emission and operation of a PET scanner

The most commonly used radionuclides for PET imaging are fluorine-18, carbon-11, oxygen-15, gallium-68, and nitrogen-13. These positron-emitting nuclides are produced by exposing stable, non-radioactive isotopes (such as oxygen-18 to produce fluorine-18) to a high-energy beam of protons created by a cyclotron. In addition to different half-lives, ranging from ~2 min of oxygen-15 to ~110 min of fluorine-18, the chemical properties of the nuclei affect their pairing with different ligands. All the nuclei undergo radioactive decay by emitting a positron (β^+) that shortly, after traveling ~1 mm, collides with an electron (e^-). This collision is called annihilation, and it results in the creation of two photons (i.e. two 511-keV gamma rays) moving approximately 180 degrees to each other (Figure 7).

These gamma rays can be detected by a PET scanner (Figure 8). The scanner usually consists of multiple rings of detectors with scintillation crystals, which can absorb gamma radiation and convert it into photons. In analog PET scanners, photomultiplier tubes convert the photons from crystals into electrical signals (Turkington, 2001), whereas recently developed digital PET scanners record the photons directly, resulting in a better signal-to-noise ratio (Nguyen et al., 2015).

When two detectors identify the two gamma rays produced by annihilation simultaneously (within of 6 to 10 nanoseconds), the signal, called a coincidence, is registered (Figure 7) (Turkington, 2001). The line between these two detectors is called the line of response (LOR), and the source of the annihilation can be localized along it based on the relative time difference between registrations.

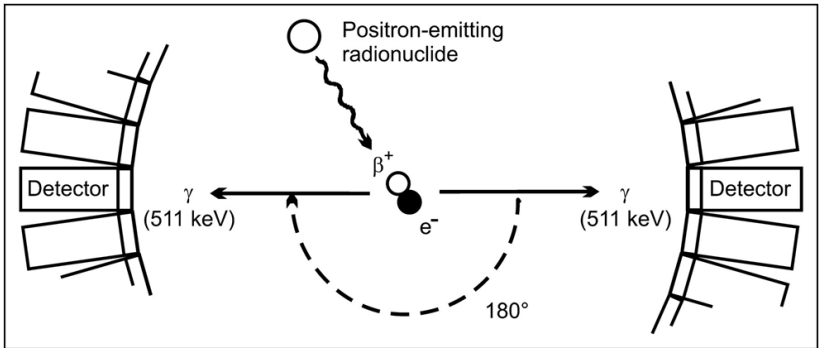

Figure 7. Detection of an annihilation ("coincidence") resulting from the collision of the emitted proton (β^+ particle) and an electron (e^-). Originally published by Verel et al. (2005); reprinted with permission from publisher © SNMMI.

During the PET scan, the number of coincidences between each possible detector pair is counted and then reconstructed into cross-sectional images (Figure 8) (Turkington, 2001). To measure changes in tracer uptake, the PET scan is usually divided into different intervals of time, called frames, ranging from a few seconds to 10 min. Collecting dynamic data in several short, sequential periods from one area allows for the evaluation of tracer fluxes, which is especially useful in the early phase after tracer administration. Later on, tracer concentrations in circulation and tissues change more slowly, and data can be collected using longer, single ("static") scans of 10 min or longer from the area of interest.

Before analysis, the data are typically automatically corrected for dead time (correction for loss of data before another signal can be detected by the scanner), decay (correction accounting for natural decay of the radionuclide after the injection), and photon attenuation (correction for photons that do not reach the detectors but are absorbed in tissues) (Turkington, 2001).

To recognize anatomical regions of interest from PET images, the study is combined with a computed tomography (CT) or magnetic resonance imagin (MRI) scan, or more rarely, a reference image. The CT or MRI data are also required for attenuation correction.

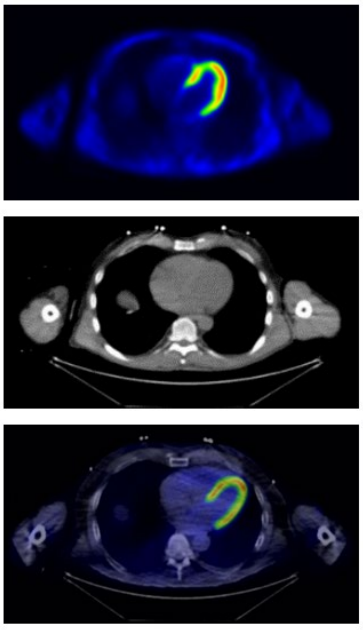

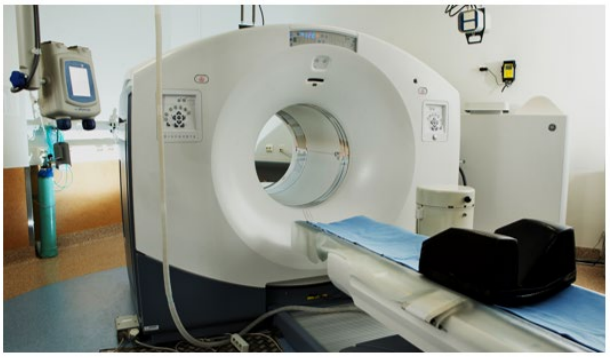

Figure 8. Left: A transverse PET/CT image of the thoracic region from a [^{18}F]-FDG study. A PET image (upper left) and a CT image (middle left) are combined into one (lower left) to aid the localization of [^{18}F]-FDG uptake. The brighter color indicates a higher tracer uptake in the left ventricular myocardial wall in relation to other tissues in the field of vision. Up: Combined PET/CT scanner Discovery 690 (General Electric Medical Systems, Milwaukee, WI) from Turku PET Centre.

2-deoxy-2-[^{18}F]fluoro-D-glucose ([^{18}F]-FDG)

The radiotracer [^{18}F]-FDG is widely used in both diagnostics and research. Its benefits include a relatively long half-life of fluorine-18 (~110 min) and efficient synthesis by nucleophilic fluorination (Hamacher et al., 1986). [^{18}F]-FDG's molecular structure is similar to glucose, with the fluorine-18 having replaced the hydroxyl group in the C-2 position, resulting in comparable transportation into tissues. After transportation, similarly to glucose, [^{18}F]-FDG is phosphorylated by hexokinase into [^{18}F]-FDG-6-phosphate ([^{18}F]-FDG-6-P) (Bessell et al., 1972). However, the absence of the 2-hydroxyl group prevents glycolysis (Bachelard, 1971; Horton et al., 1973) and hinders incorporation into glycogen (Bender et al., 2001; Iozzo et al., 2007), resulting in promoted trapping of the molecule inside the cells until the radioactive fluorine is decayed into stable oxygen-18. This enables quite straightforward modeling of tissue [^{18}F]-FDG uptake during the first 30 to 120 min after injection (Phelps et al., 1979; Huang et al., 1980).

Modeling tissue [^{18}F]-FDG metabolism

Quantitative analysis of tissue [^{18}F]-FDG uptake is performed by comparing the accumulation of the tracer in tissues to tracer availability in circulation during the scan. Tissue activity is determined from PET images, while plasma activity over time ("input function") can be derived from plasma samples collected during the scan, from PET data, or from a combination of the two. The most refined method to measure [^{18}F]-FDG uptake is the graphical analysis, which is based on a compartmental model.

The commonly used three-compartmental model consists of [^{18}F]-FDG in plasma and tissue, the phosphorylated [^{18}F]-FDG-P, and the constant rates between these compartments (Figure 9) (Sokoloff et al., 1977). K_1 and k_2 represent rates of transportation across the cell membrane, while k_3 represents phosphorylation and k_4 dephosphorylation of [^{18}F]-FDG. k_4 is considered insignificant during the early phase of the scan and is further suppressed by insulin stimulation (Iozzo et al., 2017).

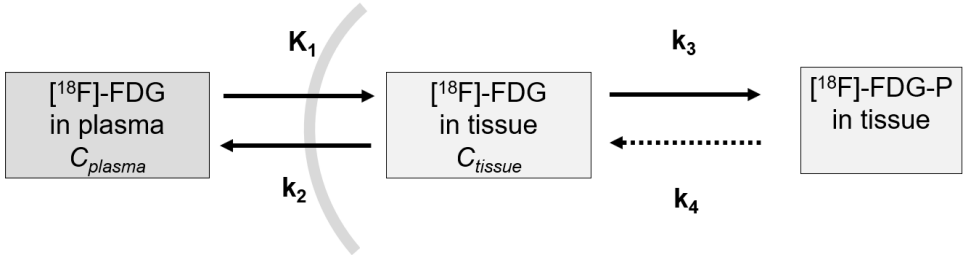

Figure 9. Three-compartmental model of [^{18}F]-FDG kinetics, with Ks representing rates of transportation (K_1 and k_2), phosphorylation (k_3), and dephosphorylation (k_4). Modified from Ratib et al. (1982) with permission from publisher © SNMMI.

In the first ~60 min after [^{18}F]-FDG injection, the dephosphorylation rate (k_4) is assumed to near 0, after which it remains relatively low for another 60 min. During this time, an estimated total rate constant (K_i), representing both transportation and phosphorylation, can be calculated as the product of [^{18}F]-FDG phosphorylation (k_3) and [^{18}F]-FDG distribution volume (Phelps et al., 1979; Ratib et al., 1982):

$$K_i = k_3 \times \frac{K_1}{k_2 + k_3}$$

This model was developed further into graphical analysis (Gjedde, 1982; Patlak et al., 1983). It was later generalized by Patlak and Blasberg, who suggested that as long as there is one irreversible compartment in the target tissue (here the phosphorylated [^{18}F]-FDG-P), and assuming that the tracer concentration in other, reversible compartments is stable and in equilibrium with plasma concentrations, the tracer concentration in tissues divided by plasma concentration represents the overall tissue uptake rate (Patlak & Blasberg, 1985). When a minimum of three measurement points of tissue activity can be fitted linearly, the plot yields a slope (K_i, 1/min) that represents how much of the available tracer has accumulated in the tissue, and this so-called Patlak plot can be described with the following equation:

$$\frac{C_{tissue}(T)}{C_{plasma}(T)} = K_i \times \frac{\int_0^T C_{plasma}(t)dt}{C_{plasma}(T)} + Int$$

where tissue concentration (C_{tissue}) in relation to tracer availability (plasma concentration, C_{plasma}) during a frame is calculated by multiplying K_i (the constant for net tracer influx rate into the tissue) by integral of plasma concentration from injection until the middle of the selected frame, divided by plasma concentration during the frame, and by adding the intercept (Int) of the slope with the y-axis. Calculating K_i is also visualized in Figure 10.

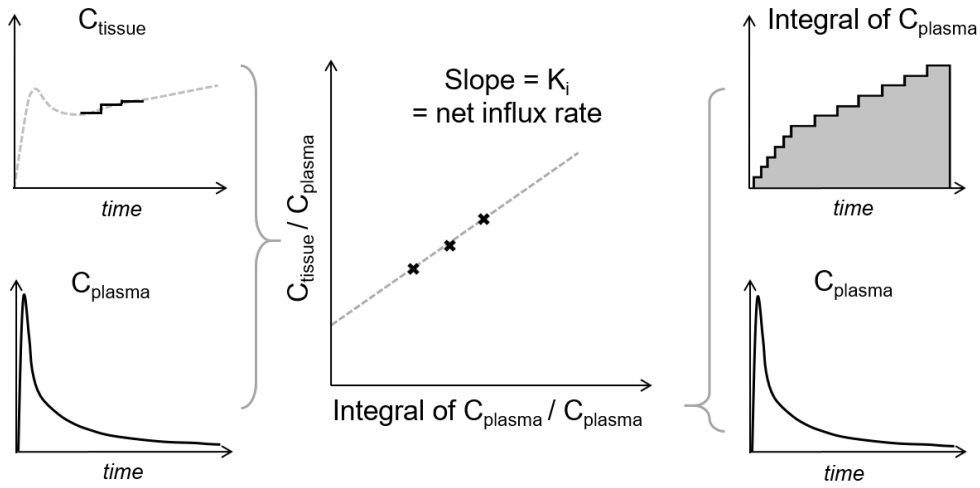

Figure 10. Mean tracer concentration in tissue during three short frames (C_{tissue}, with actual tissue concentration depicted by a dashed line) is divided by plasma tracer concentration (C_{plasma}) to calculate y-axis values. Values for the x-axis come from dividing the integral of C_{plasma} with C_{plasma}. The three measurement points ideally fit linearly and produce a slope representing the tissue net influx rate of the tracer (Based on Oikonen, 2019).

The same plot cannot be applied for static scans, as they only produce one measured value, nor when the assumption of linearly increasing accumulation of activity in the tissue is not fulfilled. For these studies, the [^{18}F]-FDG fractional uptake rate (FUR, 1/min) can be calculated by dividing tissue activity (C_{tissue}) by the integral of plasma activity from injection until the middle of the selected frame (Camici et al., 1986):

$$FUR = \frac{C_{tissue}}{\int_0^T C_{plasma}(t)dt}$$

The formula is an estimate of the Patlak-Gjedde plot, and it is based on the assumption that after a longer period of time since injection, the distribution volume of [^{18}F]-FDG is no longer important (Thie, 1995). Concluding on mathematical simulations, FUR can be considered an adequate estimate, yielding values <5% higher than the true K_i after 70 min from injection, as used in the studies included in this thesis (Oikonen, 2018).

To convert tissue [^{18}F]-FDG uptake into GU, differences in the transportation and phosphorylation rates of glucose and [^{18}F]-FDG, as well as the prevailing blood glucose concentration during the scan, must be taken into account. The method is described in detail in Chapter 4.2.6.

2.4.4 Magnetic resonance spectroscopy

The magnetic resonance spectroscopy (MRS) technique utilizes signals acquired from hydrogen, carbon, nitrogen, and phosphorus, and it offers a possibility to investigate tissue concentrations of, for example, glucose, lactate, and glycogen, as well as tissue lipid content. Compared to PET, it offers the ability to study more rapid changes in metabolite concentrations; however, it is still somewhat limited by a poorer signal-to-noise ratio, especially in tissues with a higher lipid content (Befroy & Shulman, 2011). These issues can be addressed by administering ^{13}C-enriched substrates, such as glucose, lactate, and acetate, when assessing glucose metabolism (Lanz et al., 2013).

3 Aims

This thesis aims to add to the current knowledge on insulin signaling in humans. It details how a genetic variant predominantly affecting skeletal muscle can affect body insulin-stimulated glucose metabolism and whether GU into peripheral tissues can be affected by central insulin stimulation or SGLT2 inhibition facilitating PET.

The specific aims of this thesis are as follows:

- To evaluate a) how a genetic variant known to increase the risk of T2D affects tissue insulin sensitivity before the onset of diabetes and b) whether PET is an appropriate tool to estimate the effects of rare variants on glucose metabolism (Study I).
- To assess whether central hyperinsulinemia can regulate insulin-stimulated glucose metabolism in peripheral tissues (Study II).
- To study the presumed effects of SGLT2 inhibitor dapagliflozin on insulin sensitivity in different tissues in subjects with T2D using PET (Study III).
- To investigate whether SGLT2 inhibitor dapagliflozin can reduce liver and body fat content after 8 weeks of treatment in subjects with T2D facilitating MRI (Study III).

4 Materials and Methods

A total of 86 subjects volunteered for the three sub-studies. All study visits including imaging studies were performed at the Turku PET Centre, Turku University Hospital. The study protocols were approved by the local Ethics Committee of the Hospital District of Southwest Finland (Studies I–III) and the Finnish Medicines Agency Fimea (Studies II–III). All subjects provided their written informed consent before participation, and the studies were conducted according to the Declaration of Helsinki.

4.1 Study designs and subjects

4.1.1 **Study I**: Impact of rare genetic variant p.P50T/*AKT2* on tissue-specific insulin sensitivity

Study design

All the subjects (N = 45) had one study visit to the Turku PET Centre, including a [^{18}F]-FDG PET/CT scan during the hyperinsulinemic-euglycemic clamp. The subjects arrived at Turku the night before the visit, and the clamp commenced in the morning, after an overnight fast of 10–12 hours. The subjects were instructed not to take any medications on the morning before the studies.

Study subjects

Twenty male subjects (19 heterozygous, 1 homozygous) carrying the variant p.P50T/AKT2 and 25 age- and BMI-matched male controls were recruited from the Metabolic Syndrome in Men (METSIM) cohort based in Kuopio (Stančáková et al., 2009; Laakso et al., 2017), and they were pre-screened by the local study team. Inclusion criteria for enrolment were age 50–75 years and BMI 20–40 kg/m2; the characteristics of both study groups are presented in Table 1. Subjects with diabetes (diagnosed previously or in a recent OGTT), as well as subjects with any other chronic disease (e.g. thyroid disorder) or medication affecting glucose metabolism

(e.g. beta blockers, steroids), were excluded from the study. Furthermore, previously unreported data from the METSIM population were used to calculate the sample size, with the mean difference in *M*-values between groups being 25 (SD 18.9) μmol/kg/min, with 95% power at a significance level of 5%.

Table 1. Characteristics of the two study groups. Data are reported as mean ± SD. Modified from Original Publication I (Latva-Rasku et al., 2018).

Variable	Carriers (*N* = 20)	Controls (*N* = 25)	*P* value
Age (years)	62 ± 6.3	64 ± 4.8	0.23
BMI (km/m^2)	28.7 ± 3.4	28.1 ± 3.4	0.60
Waist (cm)	100 ± 9	101 ± 9	0.88
Body fat percentage (%)	28 ± 7	29 ± 7	0.60
Fasting plasma glucose (mmol/L)	6.1 ± 0.3	6.0 ± 0.5	0.28
Fasting plasma insulin (mU/L)	18 ± 10	9 ± 6	0.003

4.1.2 **Study II**: Effects of intranasal insulin on tissue glucose uptake

Study design

The study comprised of three visits: one screening visit and, for the 10 eligible subjects recruited for the complete study, two visits with [^{18}F]-FDG PET/CT scans during the hyperinsulinemic-euglycemic clamp. The screening visit included an inspection of medical history, a physical examination, a measurement of body fat percentage, collection of fasting laboratory samples, and a 2-hour, 75-g OGTT. After eligibility was confirmed by laboratory results, the first scan visit was scheduled 3 to 26 days later, and the second scan visit 2 to 20 days after the first scan. Before the first scan, the subjects were allocated by block randomization to receiving either insulin or placebo nasal sprays first. The study was registered at ClinicalTrials.gov (Identifier: NCT02933645).

Study subjects

Ten lean, healthy male subjects were recruited for the study using personal contacts and advertisements on the university website. The inclusion criteria were age 20–35 years, BMI 18.5–25 kg/m^2, fasting plasma glucose less than 6.1 mmol/L, and 2-hour 75-g OGTT glucose values within reference range. The characteristics of the study

subjects are presented in Table 2. Reasons for exclusion were any chronic disease or medication that could affect glucose metabolism, a history of eating disorders, smoking, taking snuff, the use of narcotics, abusive use of alcohol, and previous participation in a PET study. Three subjects did not meet the inclusion or exclusion criteria and were not included in the following study visits. The sample size was calculated to detect a 21.9% placebo-corrected change in GIR with 95% power at a significance level of 5%, based on then unpublished results by collaborators in Tübingen.

Table 2. Characteristics of the study subjects. Modified from Original Publication II.

Variable	Mean ± SD	Range
Age (years)	24 ± 2.6	20–28
BMI (km/m^2)	23.5 ± 2.0	20.0–25.6
Waist (cm)	82 ± 6	74–92
Hip (cm)	97 ± 5	90–106
Waist-hip ratio	0.84 ± 0.04	0.80–0.91
Body fat percentage (%)	16.5 ± 3.7	9.7–20.3
Fasting plasma glucose (mmol/L)	5.2 ± 0.6	3.7–5.8
Fasting plasma insulin (mU/L)	5 ± 3	1–10
Matsuda-ISI	9.4 ± 6.9	3.5–27.2

4.1.3 **Study III**: Effects of SGLT2 inhibitor dapagliflozin on insulin resistance, liver fat content, and body fat mass after 8 weeks of treatment

Study design

The study flowchart is presented in Figure 11. All volunteers first underwent a screening visit at the Turku PET Centre ($N = 51$) or at a satellite site in Jyväskylä ($N = 4$). Their eligibility for the study was monitored during this visit by investigating their medical history and medications, performing a physical examination, and collecting fasting laboratory samples.

For the 32 eligible subjects, [^{18}F]-FDG PET/CT and MRI scans were performed at Visits 2 and 4 at Turku PET Centre, while treatment follow-up (Visit 3) and telephone follow-up (Visit 5) were organized by the recruiting site. The [^{18}F]-FDG PET/CT scans during the hyperinsulinemic-euglycemic clamp were performed after

an overnight fast of 10–12 hours, and the subjects were instructed not to take metformin, DPP-IV inhibitors, or any concomitant medications known to affect glucose metabolism before the end of the PET scan. On Visits 3 and 4, they were also instructed not to take the study medication on the morning of the visit. The MRI scans were performed after a minimum fast of 4 hours, with no restrictions on taking medications, and at the same time of the day on both visits.

The subjects were randomized on Visit 2 to receive either 10 mg of dapagliflozin (Forxiga®) or the placebo (both provided by AstraZeneca AB, Mölndal, Sweden) in the morning, starting from the day following the scans. Randomization was performed 1:1 in balanced blocks in two strata. One subject in the dapagliflozin group was discontinued from the study on Visit 2 before study drug administration due to elevated liver enzymes. Compliance was evaluated based on the amount of returned study medicine on Visit 4.

The study was registered at ClinicalTrials.gov (Identifier: NCT02426541).

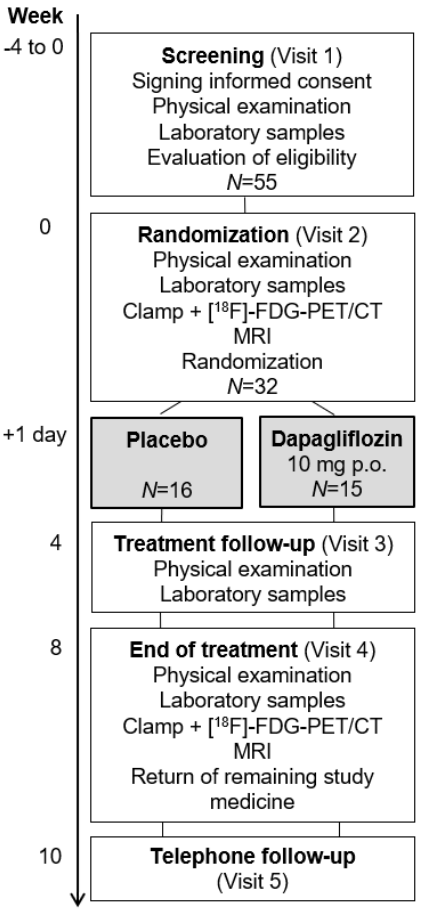

Figure 11. Study flowchart. Modified from Original Publication III (Latva-Rasku et al., 2019).

Study subjects

Fifty-five volunteers, who were initially recruited from outpatient clinics, from patient databases, or by advertisements in newspapers and on the hospital website, were screened. Of them, 32 subjects with previously diagnosed but inadequately controlled (defined as HbA_{1c} 6.5–10.5% or 48–91 mmol/L) T2D were included in the study. The enrolled subjects also fulfilled the following main inclusion criteria: age 35–70 years, BMI less than 40 km/m^2; minimum of 6 months from diagnosis of T2D; and ongoing, stable medication with metformin, dipeptidyl peptidase 4 inhibitor (DPP-4 inhibitor), or a combination of the two. The baseline characteristics of both groups are presented in Table 3. The following exclusion criteria were applied: any other diabetes medication or use of medication possibly affecting glucose metabolism, untreated hypertension at screening visit (>160/100 mmHg),

unstable coronary syndrome, symptomatic cardiac failure, renal impairment (creatinine clearance less than 60 mL/min using the Cockcroft-Gault equation), and significantly increased liver enzyme levels (Alanine aminotransferase [ALT] or aspartate transaminase [AST] >3 times upper limit of normal, or total bilirubin >34.2 μmol/L). The sample size was set to detect a 25% change in skeletal muscle GU, with approximately 90% power at a significance level of 5%.

Table 3. Characteristics of the two treatment arms. Data are reported as mean ± SD. Modified from Original Publication III (Latva-Rasku et al., 2019).

Variable	Dapagliflozin 10 mg (*N* = 15)	Placebo (*N* = 16)	*P* value
Sex (m/f)	13/2	12/4	
Age (years)	60 ± 9.9	61 ± 5.7	0.74
BMI (km/m^2)	32.1 ± 3.9	31.7 ± 5.0	0.81
Waist (cm)	111 ± 9	108 ± 11	0.48
GHbA$_{1c}$ (%)	7.0 ± 0.6	6.9 ± 0.5	0.84
HbA$_{1c}$ (mmol/L)	53 ± 7	51 ± 6	0.38
Fasting plasma glucose (mmol/L)	9.5 ± 1.9	8.8 ± 1.7	0.31
Fasting plasma insulin (mU/L)	20 ± 11	19 ± 12	0.79
Diabetes duration (years)	8.5 ± 2.7	6.4 ± 4.5	0.13

4.2 Methods

4.2.1 Preparing for the PET scans with hyperinsulinemic-euglycemic clamp

In the current studies, the hyperinsulinemic-euglycemic clamp was applied together with PET imaging to measure both whole-body and tissue-specific insulin sensitivity (Nuutila et al., 1992). Two cannulas were initially inserted in opposite forearms: one for the [^{18}F]-FDG injection and infusion of glucose and insulin, and another one for the collection of blood samples. The arm used for sampling was warmed using hot water bottles to acquire arterialized blood. During the clamp in Studies I and III, i.v. fast-acting human insulin (Actrapid, Novo Nordisk A/S, Bagsvaerd, Denmark) was administered at a steady rate of 40 mU/m^2/min (corresponding to 1 mU/kg/min) after 7 min of priming with higher doses. Euglycemia (plasma glucose level 5.0 ± 0.5 mmol/L) was sustained by varying the infusion rate of 20% glucose solution based

on plasma glucose measurements performed every 5–10 min. The clamp was continued until the end of the PET scans.
Plasma insulin was measured at fasting and every 30 min throughout the clamp to ensure adequate insulin levels during the study. Furthermore, serum FFAs were measured at fasting and every 60 min to investigate insulin's effect on lipolysis. Whole-body GU (M-value; DeFronzo et al., 1979) was reported as an average of three to four 20-min periods during steady euglycemia.

Modified low-dose clamp (Study II)

In Study II, the clamp procedure was modified to a lower dose of 0.25 mU/kg/min on both visits. This was done to hinder the strong effect of systemic insulin that could both saturate central IRs and surpass the possible effects of central regulation on peripheral GU, or (Heni et al., 2014; Heni et al., 2017).

Nasal insulin and placebo sprays (Study II)

Nasal sprays containing fast-acting human insulin (Actrapid, Novo Nordisk A/S, Bagsvaerd, Denmark) or a placebo (Insulin Diluting Medium for Novorapid and Levemir, Novo Nordisk A/S, Bagsvaerd, Denmark) were manufactured by the local hospital pharmacy as described by Heni et al. (2014). The sprays were given in a randomized order in a single-blinded fashion.

The nasal insulin sprays were administered 30 (SD 4) min after the start of the clamp, with a total of 160 IU inhaled as eight puffs in each nostril over 4 min. The same spraying protocol was applied with the placebo, beginning at 29 (SD 4) min, with an additional 2.5 mU/kg of i.v. insulin over 15 min started simultaneously to mimic the spillover of nasal insulin into systemic circulation (Plomgaard et al., 2019) (Figure 13B).

Correction for urinary glucose loss (Study III)

The amount of glucose lost to urine during a clamp is usually negligible, but for the subjects on dapagliflozin ($N = 15$), the loss had to be subtracted from the original *M*-value for the calculation to better represent whole-body insulin sensitivity. Rates of urinary loss of glucose and [^{18}F]-FDG were significantly correlated ($r = 0.74$, $p = 0.038$) in eight subjects with both measurements in the dapagliflozin group (Figure 12):

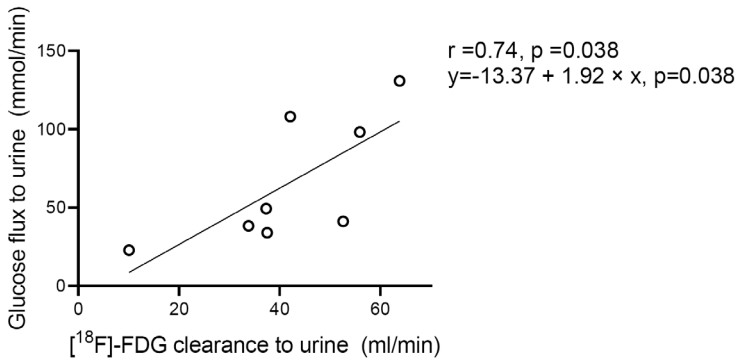

Figure 12. Correlation between clearances of glucose and [^{18}F]-FDG were significantly correlated in the dapagliflozin group after 8 weeks of treatment (*N* = 8). From Original Publication III (Latva-Rasku et al., 2019).

The following linear equation model was hence applied to estimate the rate of glucose excretion into urine in the seven other subjects receiving dapagliflozin:

$$UC_{glucose} = -13.47 + 1.92 \times UC_{FDG}$$

where $UC_{glucose}$ is the rate of urinary glucose loss (µmol/min), and UC_{FDG} is the rate of urinary loss of [^{18}F]-FDG (µmol/min). To combine the rate into the *M*-value calculation, it was divided by subject weight.

4.2.2 Conducting of PET scans during clamp

After reaching steady euglycemia, the subjects were transferred to a PET/CT scanner (Discovery 690, General Electric Medical Systems, Milwaukee, WI) and instructed to lay in supine position. After an initial scout CT to aid in selecting scan locations, the subjects were injected with a single bolus of [^{18}F]-FDG, and the PET scan was started right after (Figure 13A). The mean interval between the start of the clamp and injection was 69 (SD 15) min in Study I and 75 (SD 15) min in Study III, while [^{18}F]-FDG doses were 152 (SD 10) megabecquerel (MBq) and 155 (SD 8) MBq, respectively. In Study II, the tracer administration was fixed to the start of nasal sprays, and the interval was 40 (SD 6) min after insulin sprays and 39 (SD 9) min after placebo sprays (Figure 13B).

All the different areas were scanned sequentially in a single session and included dynamic scans of the thoracic area (for 40 min, 4 x 15 sec, 6 x 20 sec, 2 x 60 sec, 2 x 150 sec, 6 x 300 sec); upper abdomen (15 min, 3 x 300 sec); and thighs (15 min, 3 x 300 sec), followed by static scans of the neck (10 min) and the brain (10 min, only Studies I and II) (Figure 13A). The emission scans were preceded by short low-dose or ultra-low-dose CT scans from the same region. Finally, the plasma samples used to determine blood radioactivity were collected at 5, 10, 20, 30, 40, 47.5, 62.5, 75, and 85 min after injection, and the amount of tracer lost to urine was measured from a urine sample collected at the end of the scan.

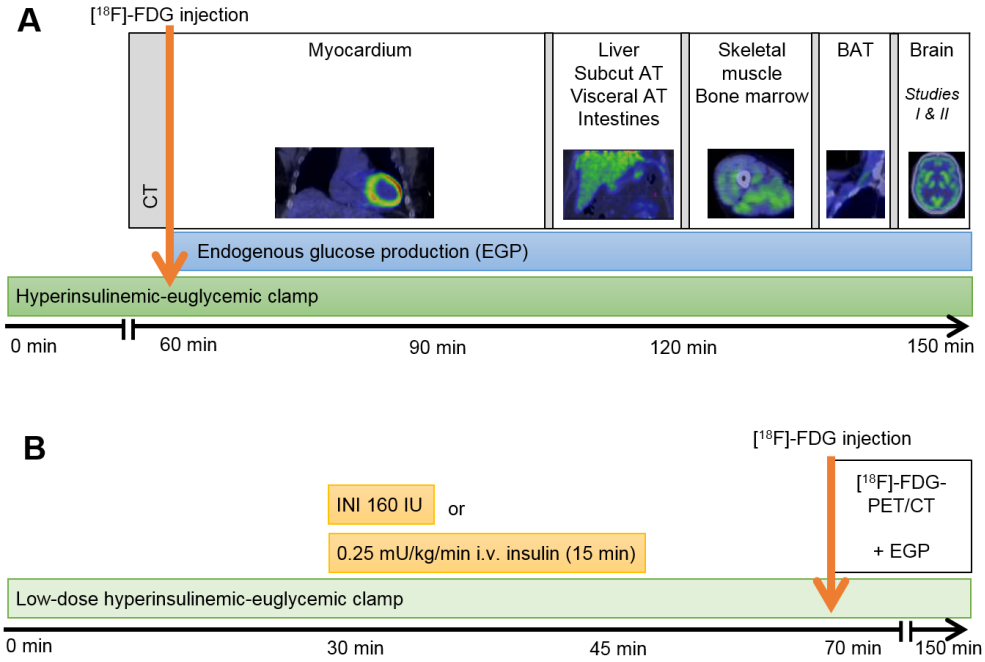

Figure 13. A. Timeline of study procedures for Studies I and III. The PET scan was preceded by a whole-body scout CT and followed by a low-dose or ultra-low-dose CT scan (gray bars) of each area before the PET scan. Brain scans were performed only in Studies I and II. B. Timeline of Study II, in which either a total of 160 IU of intranasal insulin (INI) as eight puffs in each nostril over 4 min or additional i.v. insulin over 15 min was administered before the scan. The scan was performed identically to the one detailed in Figure 13A.

4.2.3 Brown adipose tissue radiodensity

BAT radiodensity measured from CT images as Hounsfield units (HUs) can be used as an indicator of tissue activity, with a lower HU correlating with increased blood flow to the tissue or thermogenesis due to consumed lipid storages (U Din et al., 2017). In Study II, BAT radiodensity was measured by drawing ROIs manually to the supraclavicular depots, excluding voxels that were not within the range of AT density (-250 to -50 HU), as described by U Din et al. (2017).

4.2.4 Magnetic resoncance imaging studies (Study III)

Whole-body MRI was performed in Study III using the 3T MRI part and an integrated body coil of a PET-MR scanner (Philips Ingenuity TF, Philips Healthcare, Cleveland, OH). During the scan, subjects laid in supine position, with arms above the head when feasible, and they were instructed to exhale and hold their breath during imaging of the thoracic area and abdomen. First, a T1-weighted fat-suppressed single-echo sequence was used to measure the liver volume, followed by

an assessment of the liver proton density fat fraction (PDFF%) (Reeder et al., 2012) and whole-body composition by a multi-echo water-fat separation method based on chemical shift (Dixon, 1984).

The analyses of the MRI studies were performed by Antaros Medical AB (Mölndal, Sweden). Liver volume was measured using a semiautomated segmentation tool in SmartPaint software (version 1.0), developed at the Centre for Image Analysis and the Department of Radiology, Oncology and Radiation Sciences, Uppsala University, Uppsala, Sweden) (Malmberg et al., 2017). Furthermore, analysis of the PDFF% was performed on the whole liver, excluding tissue borders, using MATLAB (version 9.1, MathWorks, Natick, MA) as described by Berglund and Kullberg (2012), with minor adjustments, and reported as the median PDFF%. From the whole-body scan, the volumes of subcutaneous and visceral AT were determined from the region between the liver dome and femoral heads, and they were assessed using an automated segmentation algorithm (Kullberg et al., 2009).

4.2.5 Anthropometric measurements

The height and weight of the subjects were measured on-site using the equipment provided, with the weight measured in the morning in light hospital clothing after urinating. Waist circumference was measured from midway between the top of the hip bones and the lowest ribs, and hip circumference was measured around the largest part of the hips with the subjects standing up, exhaling slowly, and relaxing their muscles. In Study II, body fat percentage was measured using bioimpedance (Omron BF400 [MBF-400-E], Omron Healthcare Co Ltd, Kyoto, Japan). Moreover, blood pressure was measured in supine position after a minimum of 2 min rest with the cuff placed around the right upper arm.

4.2.6 PET data analysis

Measurement of peripheral tissue glucose uptake

All the analyses were performed using Carimas Software (version 2.9, developed in Turku PET Centre). Volumes of interest (VOIs) were drawn manually to cover the quadriceps' femoris muscles in both legs and the right lobe of the liver, avoiding large vessels, waistline subcutaneous AT, intraperitoneal visceral AT, supraclavicular depots of brown AT, femoral bone marrow, and several segments of the small intestine. Myocardial GU was measured from the walls of the left ventricle with the aid of a segmenting tool. Except for the myocardium and liver, the reported values are averages of several VOIs.

The input, arterial plasma time-activity curve of [^{18}F]-FDG, was determined by combining data from the PET data (first 10 min) and arterialized plasma samples. Tissue GU (GU, μmol/kg/min) was then calculated using the following formula:

$$Tissue\ GU = \frac{K_i \times plasma\ glucose}{tissue\ density \times LC} \times 1000$$

where K_i (or FUR) is the fractional uptake (1/min), plasma glucose is the mean glucose level from injection to the end of the scanned area (mmol/L), tissue density (kg/L; ICRP, 1975), and lumped constant (LC) is a previously validated constant accounting for the differences in transportation and phosphorylation of [^{18}F]-FDG and glucose (1.2 for skeletal muscle, 1.0 for liver and myocardium, 1.14 for AT, and 0.65 for the brain) (Peltoniemi et al., 2000; Iozzo et al., 2007; Bøtker et al., 1997; Virtanen et al., 2001; Orava et al., 2011; Honka et al., 2013; Wu et al., 2003).

Measurement of brain glucose uptake

Insulin-stimulated GU to the brain was assessed in Studies I and II. Preprocessing and analysis of brain PET data was performed using statistical parametric mapping (SPM; SPM 12 software [http://www.fil.ion.ucl.ak.uk/spm/]). PET images were first spatially normalized using linear and non-linear transformations and smoothing with Gaussian kernel (8-mm full width at half maximum) to an in-house [^{18}F]-FDG template, similar to the Montreal Neurological Institute standard brain (MNI International Consortium for Brain Mapping). Then, FUR was calculated for each voxel in the same manner as in other tissues. Both the comparison of FUR in each voxel in the whole brain using nonparametric mapping in the SnPM13 toolbox (http://warwick.ac.uk/snpm) and the comparison of GU in different anatomical brain regions (GU calculated as described in the previous chapter) were performed between groups (Study I) and interventions (Study II).

Measurement of endogenous glucose production

The mean rate of EGP during the PET scan was calculated as described by Iozzo et al. (2006). First, the metabolic clearance rate of [^{18}F]-FDG (MCR_{FDG}, mL/min) was calculated by using the following formula:

$$MCR_{FDG} = \frac{dose_{FDG} - urine_{FDG}}{AUC_{FDG}}$$

where $dose_{FDG}$ is the injected dose (in kBq); $urine_{FDG}$ is the amount of tracer lost to urine during the entire scan (in kBq); and AUC_{FDG} is the area under curve from injection to infinity, estimated from the blood tracer time-concentration curve of [^{18}F]-FDG used in tissue GU analyses (kBq/mL*min).

Then, the rate of glucose disappearance (Rd, µmol/min/kg) was calculated as follows:

$$Rd = \frac{MCR_{FDG} \times plasma\ glucose}{weight}$$

where MCR_{FDG} (mL/min) is the metabolic clearance rate, plasma glucose is the average level during the entire scan (mmol/L), and weight is the subject's weight (kg).

Finally, EGP (µmol/min/kg) was computed with the following formula:

$$EGP = Rd + V_{glucose} \times \frac{\Delta_{glucose}}{\Delta_{time}} - GIR + urine_{glucose}$$

where Rd is the rate of glucose disappearance (µmol/min/kg), $V_{glucose}$ is an estimated constant for glucose distribution volume (0.19 L/kg), $\Delta_{glucose}$ is the change in glucose level from injection to the last collected sample (mmol/L), Δ_{time} is the interval between injection and the last sample (min), and GIR is the total amount of infused glucose during the scan (mg/kg). Moreover, $Urine_{glucose}$ is the excretion rate of glucose into urine (µmol/min/kg), which was only applied for subjects on dapagliflozin treatment in Study III, as the amount usually equates to 0.

4.2.7 Biochemical analyses

During the clamp and scans, plasma glucose was analyzed in duplicates using the glucose oxidase method (Analox GM9; Analox Instruments, London, UK). Furthermore, plasma and urine activity were analyzed using an automatic gamma counter (Wizard1480 3; Wallac, Turku, Finland) at the local PET Centre laboratory.

In Studies I and III, plasma insulin at fasting and during clamp was measured with automated electrochemiluminescence immunoassay, ECLIA (Cobas 8000, Roche Diagnostics, Mannheim, Germany) at the Turku University Hospital laboratory. In Study II, samples for serum insulin and C-peptide levels during clamp were first frozen at -70 ^{0}C and later sent to be analyzed by collaborators in Eberhard Karls University Tübingen (Tübingen, Germany) with chemiluminescence assays (ADVIA Centaur, Siemens, Erlangen, Germany).

Fasting plasma glucose and urinary glucose (Study III) were assessed by enzymatic hexokinase method (Cobas 8000, Roche Diagnostics, Mannheim, Germany); blood HbA1c with immunoturbidimetry (Cobas 6000, Roche Diagnostics, Mannheim, Germany); and plasma ALT, AST, ALP, and total bilirubin with photometric methods (Cobas 8000, Roche Diagnostics, Mannheim, Germany) at the Turku University Hospital laboratory on the day of collecting samples. Other samples were separated and stored at -70 ^{0}C at the Turku PET Centre and analyzed

in larger batches. Serum FFAs were analyzed with enzymatic colorimetric method assay (NEFA-HR2, ACS-ACOD; Wako Chemicals, Neuss, Germany; Cobas 8000 c502 Analyzer, Roche Diagnostics), and plasma N-terminal prohormone of brain natriuretic peptide (NT-proBNP) and troponine T (TnT) with ECLIA (Cobas 8000, Roche Diagnostics, Mannheim, Germany) at the Turku University Hospital laboratory. Serum IL-6, MCP-1, and TNF-alpha were assessed with immunoassay (Milliplex® MAP Human Cytokine/ Chemokine Magnetic Bead Panel, cat.no. HCYTOMAG-60K, EMD Millipore, Billerica, MA, USA) by collaborators at the University of Tampere, (Tampere, Finland).

Before sample collection, tubes for glucagon and active GLP-1 samples were prepared by adding KIE/ml of trypsin inhibitor aprotinin (Bayer AG, Leverkusen, Germany) and 0.1 mmol/l of DPP-IV-inhibitor Diprotin A (Sigma Aldrich, St Louis, MO, USA) to chilled EDTA tubes. Glucagon was analyzed with radioimmunoassay (RIA; GL-32K, EMD Millipore, Billerica, MA, USA), active GLP-1 with enzyme-linked immunosorbent assay (ELISA; EGLP-35K, EMD Millipore, Billerica, MA, USA), and FGF-21 with ELISA (Quantikine® Human FGF-21 Immunoassay, R&D Systems, Inc., MN, USA) at the Lund University Diabetes Centre (Lund, Sweden).

4.2.8 Statistical methods

Study I

Statistics were performed with IBM SPSS Statistics for Windows software (version 21.0, IBM Corp, Armonk NY). After correcting data with skewed distributions using logarithmic transformation, differences between groups were studied using an independent samples *t* test. Correlations between GUs in different tissues were tested using Spearman's rank correlation and the comparison of correlation coefficients between the groups was performed using Fisher's *Z*-transformation. The effect of outside temperature in the previous 7, 14, and 30 days on BAT GU was tested using linear regression.

Study II

Analyses for peripheral tissue GU and BAT radiodensity were performed using a mixed model for repeated measurements with fixed effects of intervention and sequence using SAS software (version 9.4, SAS Institute, Cary, NC). Brain GU was analyzed using a paired *t*-test in SPM12, with $p < 0.05$ as the cluster-defining threshold. Only statistically significant ($p < 0.05$) clusters after FWE-correction are reported. Statistical analyses for serum metabolites were conducted with Rstudio (RStudio Inc., Boston MA), with the values first being normalized to the moment of

spray application, and then compared between interventions at 60 min and 90 min later using the paired Wilcoxon signed rank test.

Study III

Statistics were performed by a statistician assigned by AstraZeneca AB (Mölndal, Sweden), and all analyses were performed with SAS software (version 9.4, SAS Institute Inc., Cary, NC). Changes in anthropometric measurements and laboratory results at baseline, Week 4, and at the end of study were analyzed using a mixed model for repeated measurements, with the fixed categorical effects of treatment, week, treatment-by-week interaction, the randomization strata of sex, and the sex-by-week interaction, and with fixed covariates of baseline values and baseline measurement-by-week interaction. Changes in *M*-value, tissue GU, liver fat content, and body adiposity were analyzed by two-way ANCOVA, set to detect a change at a 5% level of significance and applying fixed effects of treatment, sex, and baseline value. The baseline NT-proBNP values of subjects with or without hypertension or cardiovascular disease were compared using the Wilcoxon sign rank sum test, and correlations were tested using Spearman's rank correlation.

5 Results

5.1 Impact of rare genetic variant p.P50T/*AKT2* on tissue-specific insulin sensitivity (Study I)

5.1.1 Carriers of p.P50T/*AKT2* show impaired insulin sensitivity in most peripheral tissues

There were no differences in mean plasma glucose levels during the clamp between the groups (5.0±0.4 mmol/L in p.P50T/*AKT2* carriers vs. 5.0±0.2 mmol/L in non-carriers, $p = 0.53$). While fasting levels of serum FFAs did not differ between the groups (0.43±0.16 vs. 0.39±0.16 mmol/L, $p = 0.36$), lipolysis was less suppressed after 60 min (65±15% vs. 76±12%, $p = 0.01$), but not after 120 min (80±12% vs. 84±19 %, $p = 0.10$) of clamp.

Whole-body GU assessed as both the clamp-based *M*-value and [^{18}F]-FDG-derived Rd was significantly lower in the carriers of p.P50T/*AKT2* versus controls. Endogenous glucose production (EGP) also remained at a higher rate in the carriers (Figure 14A).

Glucose uptake (GU) into skeletal muscle was lower in carriers compared to non-carriers and correlated highly with the *M*-values ($r \geq 0.90$ in both groups). Insulin-stimulated GU was also lower in the liver of the carriers. Furthermore, there were no significant differences in the subcutaneous AT or visceral AT of the carriers vs. non-carriers, but GU was lower in both the brown AT and femoral bone marrow of the p.P50T/*AKT2* carriers (Figure 14B). Finally, no differences were observed in the GU into myocardium (34.2±16.8 vs. 35.0±12.6 µmol/100 g/min, $p = 0.87$), duodenum (31.9±7.0 vs. 31.7±7.1 µmol/kg/min, $p = 0.93$), or jejunum (33.2±7.0 vs. 32.4±7.2 µmol/kg/min, $p = 0.71$).

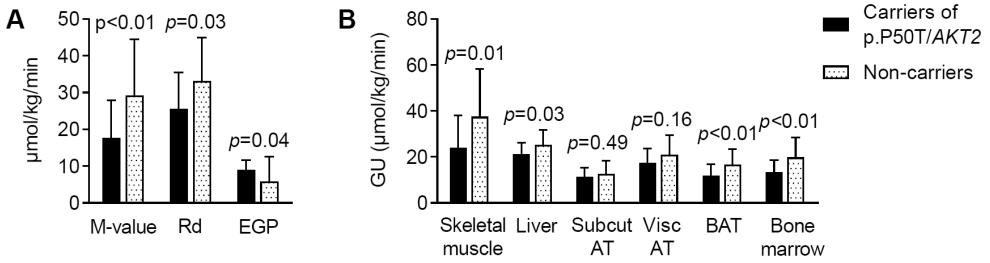

Figure 14. A. Whole-body insulin sensitivity, measured as *M*-value or glucose rate of disappearance (Rd), was significantly lower in variant carriers, and EGP remained at a higher rate during hyperinsulinemia. B. Peripheral insulin-stimulated glucose uptake was significantly lower in key metabolic tissues of p.P50T/*AKT2* carriers compared to matched controls. Bar height represents group mean and whiskers SD. Modified from Original Publication I (Latva-Rasku et al., 2018).

5.1.2 Increased brain glucose uptake and lost association between glucose uptake and endogenous glucose production in p.P50T/*AKT2* carriers

Insulin-stimulated GU was globally higher in the brain of p.P50T/*AKT2* carriers (p = 0.001 in all seven anatomical regions: temporal, parietal, occipital, and frontal lobes; midbrain; limbic system; and cerebellum) (Figure 15A). The correlation between *M*-value and mean brain GU was similar in carriers versus non-carriers (ρ = -0.56 vs. ρ = -0.66); however, while GU correlated significantly with EGP in the non-carriers' brains, there was no correlation between the two in p.P50T/*AKT2* carriers (p = 0.016 for the difference between groups) (Figure 15B and C).

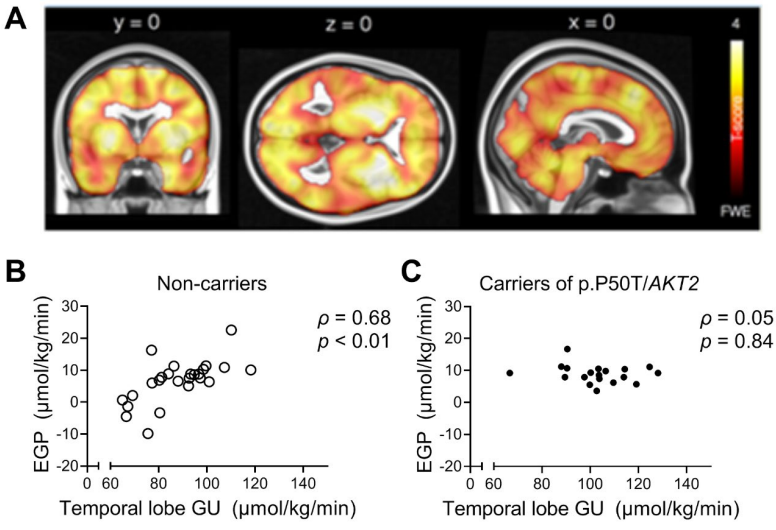

Figure 15. A. Insulin-stimulated brain GU was globally higher across the whole brain in variant carriers. The colors refer to T-scores, with brighter areas showing statistically more significant changes. B. and C. Brain GU correlated with EGP only in the control group. Modified from Original Publication I (Latva-Rasku et al., 2018).

5.2 Effects of intranasal insulin on tissue glucose uptake (Study II)

5.2.1 No change in whole-body insulin sensitivity despite higher circulating insulin levels after intranasal insulin

Plasma glucose and serum fatty acid levels did not differ significantly between the interventions (Figure 16A&B). Despite additional infusion of i.v. insulin after placebo sprays, serum insulin levels were significantly higher after INI, starting from 25 min after spray application until the end of study, with the insulin levels being higher than fasting values but significantly lower than maximal values during the OGTT (Figure 16C). The required GIR seemed to be higher after INI, but the difference did not reach statistical significance (maximal effect at 120 min: mean difference 0.85 mg/kg/min, 95% CI -0.16, 1.9, $p = 0.07$) (Figure 16D).

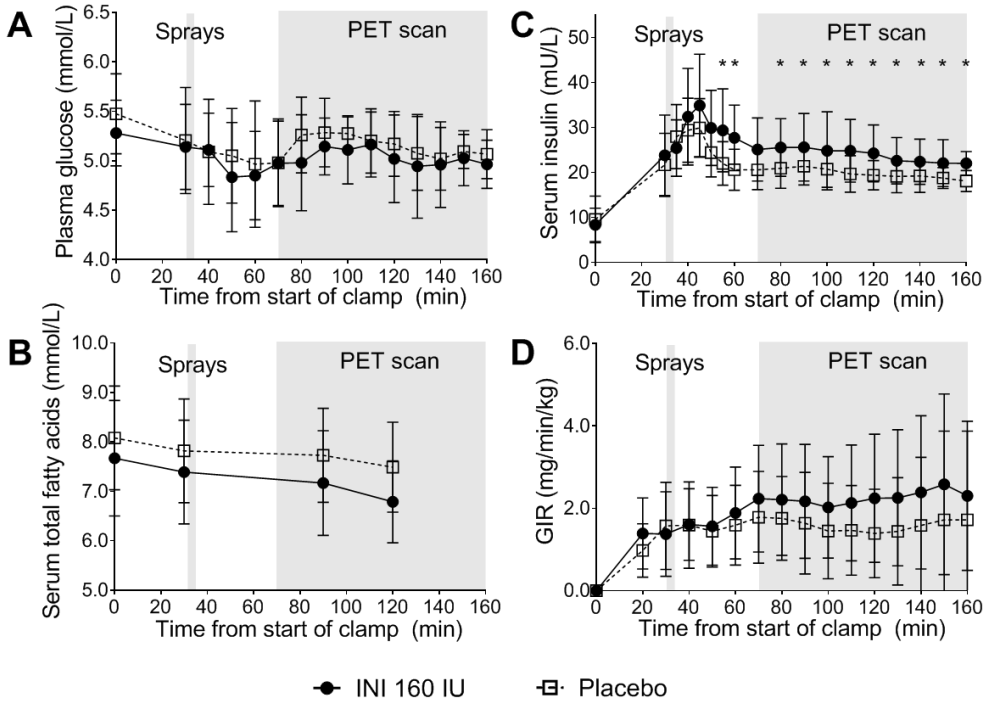

Figure 16. A. Plasma glucose levels were similar and within euglycemia in both interventions. B. Serum total fatty acid levels did not differ between interventions when values were corrected for lower initial level on INI visits. C. Serum insulin levels remained significantly elevated after INI. D. Difference between glucose infusion rates (GIRs) did not reach statistical significance within the period studied. Data are presented as means and SDs, *p<0.05. The gray backgrounds represent the 4-min period of spray application at 30 min and the duration of the PET scan.

5.2.2 Decreased global brain glucose uptake after intranasal insulin

Cluster-level analysis revealed significantly lower GU after INI in large regions in the brain when using a threshold of $p < 0.05$ (Figure 17), and essentially in the whole brain when using a threshold of $p < 0.10$.

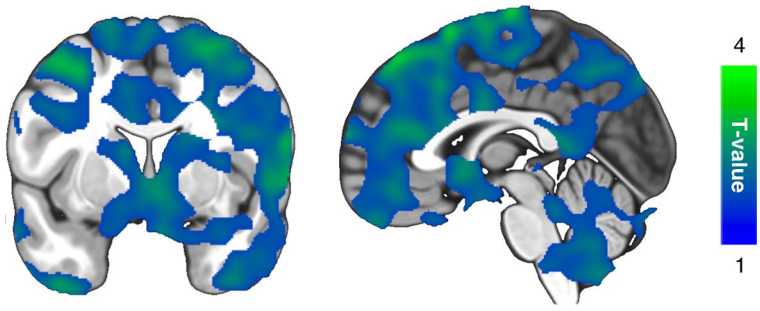

Figure 17. A. Brain glucose uptake was significantly lower after INI. The FWE-corrected SPM data have a threshold at level $p < 0.05$ and were colored according to voxelwise T-scores, with the green shade representing a statistically more significant effect.

5.2.3 Intranasal insulin shows no effect on peripheral tissue glucose uptake or brown adipose tissue radiodensity

Glucose uptake under mild systemic hyperinsulinemia was not altered by INI in skeletal muscle ($p = 0.78$), the liver ($p = 0.56$), or waist subcutaneous AT ($p = 0.81$) when including differences in the serum insulin levels at the moment of injection in the statistical model (Figure 18). The mean rate of EGP from injection was slightly more suppressed after INI, but not to a statistically significant degree ($p = 0.15$) (Figure 18).

Moreover, BAT GU ($p = 0.78$, Figure 18B) and radiodensity (-1.1 HU, 95% CI -2.7, 0.4, $p = 0.13$) were not significantly affected by INI. One subject was excluded from all BAT analyses due to abnormally high GU on the placebo visit, although including him had no effect on the interpretation of the result.

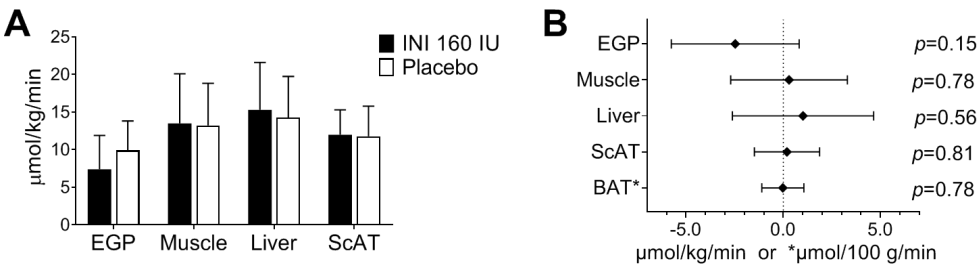

Figure 18. A. and B. INI had no significant effect on GU in skeletal muscle, liver, subcutaneous adipose tissue (ScAT), or brown adipose tissue (BAT), and the minor lowering of EGP did not reach statistical significance. A. Bar heights represent group mean and whiskers SD. B. Placebo-corrected mean changes with 95% CI of changes.

5.2.4 Unaffected serum markers of lipid metabolism

Levels of serum total fatty acids, glycerol, apolipoprotein AI or B, and total triglycerides or triglycerides in VLDL, low-density lipoprotein (LDL), and high-density lipoprotein (HDL) normalized to the moment of spray application were not affected by INI (Figure 19).

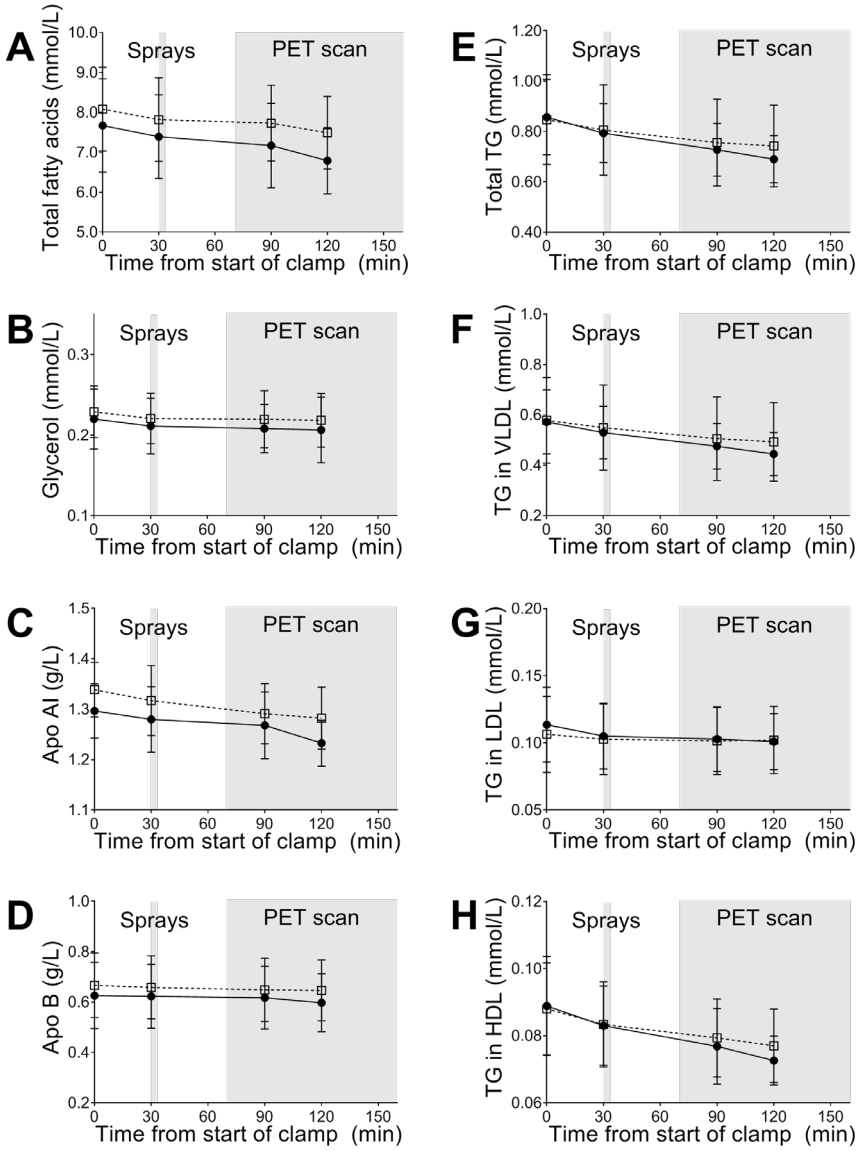

Figure 19. Serum concentrations of lipid metabolism markers were not affected by INI (black dots and lines) compared to placebo (white squares, dashed lines). Total fatty acids (A), glycerol (B), apolipoproteins AI (C) and B (D), total triglycerides (TG) (E), and triglycerides in very low -dendity lipoproteins (VLDL) (F), low-density lipoproteins (LDL) (G), and high-density lipoproteins (HDL) (H). Data are presented as means and SDs.

5.3 Effects of SGLT2 inhibitor dapagliflozin on insulin resistance, liver fat content and body fat mass after 8 weeks of treatment (Study III)

5.3.1 Improved glycemic control and weight loss by dapagliflozin and effects on biomarkers

Dapagliflozin treatment reduced subjects' weight and improved their fasting plasma glucose and HbA1c values. No changes in fasting plasma insulin, serum FFAs, or β-hydroxybutyrate were observed. Furthermore, mean glucose values were similar in both groups and did not differ between visits. Suppression of lipolysis during hyperinsulinemia was not affected by dapagliflozin at 60 or 120 min from the start of clamp (Table 4).

Fibroblast growth factor 21 (FGF21) tended to lower (-111 pg/mL, 95% CI -232, 9.4, $p = 0.07$), with the change in liver PDFF% showing a statistically significant effect on the decrease ($p = 0.01$). In addition, levels of IL-6 were decreased by dapagliflozin by 1.9 pg/mL (95% CI -3.6, -0.14, $p = 0.04$). The change correlated with the decrease in subcutaneous AT volume ($\rho = -0.62$, $p = 0.02$), with the treatment effect remaining close to significant despite including the change in subcutaneous AT volume in the model. Finally, TNFα levels were not affected by dapagliflozin.

Table 4. Baseline and post-treatment values are reported as mean ± SD. P-*v*alues are placebo-corrected adjusted mean changes from baseline for the dapagliflozin group. FPG: fasting plasma glucose, FFA: free fatty acids, GCG: glucagon, β-OHBut: β-hydroxybutyrate, ALT: alanine aminotransferase, AST: aspartate aminotransferase, FGF21: fibroblast growth factor 21, TNFα: tumor necrosis factor α (pg/mL), and EGP: endogenous glucose production during clamp. Mean glucose is the mean value during clamp steady state, and ΔFFAs represent percentage change from fasting after 60 or 120 min of clamp. Modified from Original Publication III (Latva-Rasku et al., 2019).

VARIABLE	DAPAGLIFLOZIN 10 MG (*N* = 15)		PLACEBO (*N* = 16)		*P* VALUE
	Baseline	At 8 weeks	Baseline	At 8 weeks	
BMI (kg/m^2)	32.1 ± 3.9	31.3 ± 3.7	31.7 ± 5.0	31.8 ± 4.8	<0.0001
FPG (mmol/L)	9.5 ± 1.9	7.8 ± 0.9	8.7 ± 1.7	9.0 ± 1.5	<0.01
GHbA$_{1c}$ (%)	7.0 ± 0.6	6.6 ± 0.6	6.8 ± 0.5	6.8 ± 0.4	<0.01
HbA$_{1c}$ (mmol/L)	53 ± 7	49 ± 7	51 ± 6	51 ± 5	
Fasting insulin (mU/L)	20 ± 11	17 ± 8	19 ± 12	17 ± 8	0.52
Fasting FFA (mmol/L)	0.64 ± 0.15	0.67 ± 0.14	0.69 ± 0.18	0.66 ± 0.21	0.62
Fasting GCG (pg/mL)	104.9 ± 15.4	105.8 ± 20.4	111.3 ± 27.6	108.2 ± 26.4	0.68

β-OHBut (mmol/L)	0.09 ± 0.05	0.17 ± 0.18	0.12 ± 0.11	0.12 ± 0.09	0.33
ALT (U/l)	50 ± 21	45 ± 16	38 ± 14	39 ± 15	0.47
AST (U/l)	30 ± 10	30 ± 10	32 ± 12	31 ± 10	0.92
FGF21 (pg/mL)	388 ± 315	334 ± 198	293 ± 194	362 ± 272	0.07
Interleukin-6 (pg/mL)	6.6 ± 8.2	5.8 ± 8.9	3.5 ± 2.4	4.0 ± 4.4	0.04
TNFα (pg/mL)	4.6 ± 1.4	4.7 ± 1.5	3.6 ± 2.3	3.7 ± 2.2	0.38
***M*-value (μmol/m^2/min)**	6.2 ± 3.3	7.7 ± 3.6	7.8 ± 5.2	8.3 ± 5.1	0.50
EGP (μmol/kg/min)	7.6 ± 4.4	7.0 ± 4.2	9.4 ± 3.9	7.8 ± 4.0	1.0
Mean glucose (mmol/L)	5.4 ± 0.4	5.1 ± 0.2	5.5 ± 0.6	5.3 ± 0.6	0.18
ΔFFA 0 to 60 min (%)	-58 ± 13	-59 ± 15	-60 ± 14	-61 ± 14	0.71
ΔFFA 0 to 120 min (%)	-71 ± 10	-75 ± 11	-71 ± 13	-70 ± 15	0.35

5.3.2 Glucose uptake not improved by dapagliflozin

The baseline *M*-value was low in both groups (Table 4) and was not improved by dapagliflozin compared to the placebo ($p = 0.90$) (Figure 20). The rate of EGP during clamp was similar in both groups (Table 4) and was not changed by dapagliflozin ($p = 1.0$) (Figure 20).

Furthermore, dapagliflozin had no effect on tissue-specific insulin-stimulated GU in skeletal muscle ($p = 1.0$); the liver ($p = 0.53$); visceral adipose tissue, subcutaneous adipose tissue, or BAT ($p = 0.71$; $p = 0.19$; $p = 0.65$, respectively), nor on left ventricular myocardial GU ($p = 0.46$) (Figure 20). However, the small changes in the *M*-value and skeletal muscle GU correlated in the dapagliflozin group ($\rho = 0.64$, $p = 0.01$)

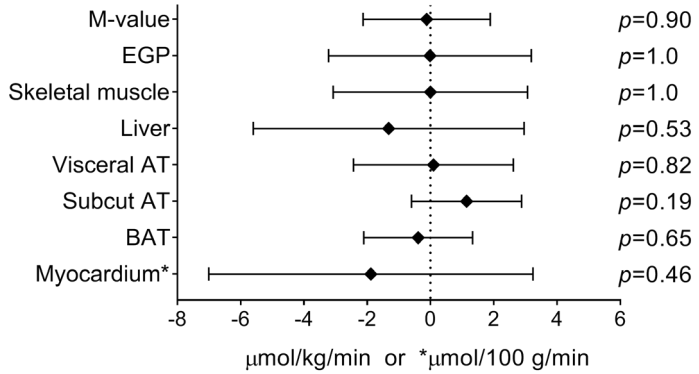

Figure 20. Dapagliflozin had no significant effect on whole-body insulin sensitivity, reported as *M*-value, on EGP, or on tissue-specific insulin-stimulated glucose uptake. Data are presented as placebo-corrected mean changes with 95% CI. Modified from Original Publication III (Latva-Rasku et al., 2019).

5.3.3 Reduced liver steatosis and body fat mass by dapagliflozin

The baseline liver fat content (PDFF%) was similar between groups: 22% (SD 11) in the dapagliflozin group and 21% (SD 9.3) in the placebo group. At the end of treatment, there was a significant decrease in both liver PDFF% (placebo-corrected mean change -3.7%, 95% CI -6.18, -1.30, $p < 0.01$) and liver volume (-0.10 L, 95% CI -0.19, -0.003, $p = 0.04$) (Figure 21A). Post-hoc analyses revealed that introducing changes in BMI or visceral AT volume in the model had a significant effect on the reduction of liver fat ($p = 0.02$ and $p = 0.01$, respectively).

Volumes of visceral AT and abdominal subcutaneous AT were significantly reduced by dapagliflozin (placebo-corrected mean changes -0.35 L, 95% CI -0.59, -0.12, $p < 0.01$; and -0.28 L, 95% CI -0.52, -0.05, $p = 0.02$, respectively) (Figure 21B). Finally, there was no significant change in lean body mass (-1.2 L, 95% CI -2.8, 0.41, $p = 0.14$).

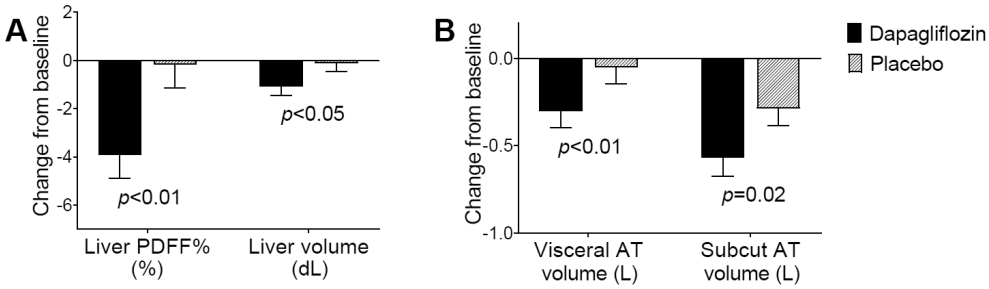

Figure 21. A. Change in liver proton density fat fraction (PDFF%) and volume was significant in the dapagliflozin group. B. Changes in volumes of visceral and subcutaneous adipose tissue (AT) were significantly reduced by 8 weeks of dapagliflozin treatment. Bar height represents mean change in each group and whiskers SD. Modified from Original Publication III (Latva-Rasku et al., 2019).

6 Discussion

6.1 A partial loss-of-function variant in *AKT2* is associated with insulin resistance in several insulin-sensitive tissues (Study I)

The results from this study demonstrate that a low-frequency partial loss-of-function variant p.P50T/*AKT2* is associated with insulin resistance in several key metabolic organs in middle-aged and elderly male subjects without T2D. This is in line with previous studies showing that variant carriers presented hyperinsulinemia, suggesting impaired insulin sensitivity (Manning et al., 2017). To the authors' knowledge, this is the first time a rare variant has been demonstrated to widely affect tissue glucose metabolism *in vivo*. In addition to key insulin-sensitive tissues, skeletal muscle, and liver, the results revealed surprising alterations in several other tissues as well.

Lower whole-body glucose disposal in variant carriers can be explained, at least in part, by a) the 36% lower skeletal muscle GU, supported by the central role of AKT2 in skeletal muscle glucose GU and glycogen synthesis (Bouzakri et al., 2006) and b) the enrichment of the specific isoform in skeletal muscle (Manning et al., 2017). In addition to the primary defect in insulin signaling, the possible lifetime effects of hyperinsulinemia and other manifestations of insulin resistance could have further aggravated the situation.

Manning et al. (2017) also showed, in their *in vitro* experiments on human hepatocytes, that p.P50T/*AKT2* is associated with impairment in liver insulin signaling, similarly to skeletal muscle. In accordance with this previous report, EGP was less suppressed during hyperinsulinemia in variant carriers, indicating hepatic insulin resistance. The decrease in liver GU compared to controls can also result from lower rates of glycogen synthesis and the associated inefficient glucose handling and accumulation of G6P. Both the impaired insulin-stimulated GU and the inadequate suppression of EGP by insulin, resulting from impaired AKT2 function, have also been displayed in mouse knock-out models (Cho et al., 2001; Garofalo et al., 2003; Wan et al., 2013).

Although insulin-stimulated GU into AT occurs via the AKT2-regulated translocation of GLUT4 (George et al., 2004), and while the rates of GU in

subcutaneous and visceral WAT were slightly lower in variant carriers compared to non-carriers, the difference was not statistically significant. However, a change in FFA levels from fasting to 60 min of hyperinsulinemia was more limited in p.P50T/*AKT2* carriers, suggesting an impaired inhibition of lipolysis. A previous report in AKT2 knock-out mice found no effect on lipolysis measured as changes in FFA and glycerol levels (Koren et al., 2015), supported by findings that in adipocytes, GLUT4 translocation is mediated solely by AKT2 and lipolysis via both AKT1 and AKT2 acting on FOXO1 (Gonzalez & McGraw, 2011). Therefore, it is possible that in our subjects, the effect was secondary and not a direct result of impaired AKT2 function.

Supraclavicular BAT depots have previously been shown to increase GU in response to insulin stimulus more efficiently than WAT (Orava et al., 2011), which might explain why we saw a significantly lower GU in the BAT of variant carriers. As the used method only allows for an estimation of BAT based on anatomical region and radiodensity, it is also possible that the lower GU p.P50T/*AKT2* carriers had a smaller amount of active BAT, which has previously been shown to be associated with obesity and insulin resistance (Orava et al., 2013). Furthermore, in other research, mice lacking adipocyte *AKT1* and *AKT2* had no discernible BAT and developed WAT lipodystrophy (Shearin et al., 2016). However, our subjects displayed a BMI and fat distribution similar to the controls, opposing several defects in AT development by p.P50T/*AKT2*.

Adult femoral bone marrow consists mostly of adipocytes, which seem to share characteristics of both white and brown adipocytes. In insulin-resistant mice, marrow AT demonstrates a decreased expression of genes participating in insulin-mediated responses in BAT, but not WAT (Krings et al., 2012), which could explain the similar significantly lower GU in femoral bone marrow as seen in BAT. Furthermore, femoral marrow GU and BAT GU correlated positively in both groups ($r \geq 0.53$, $p < 0.01$ in both groups, using log-transformed values). The concept of femoral bone marrow AT as insulin-sensitive tissue is also supported by the correlation between tissue GU and *M*-value seen in the current study ($r \geq 0.79$, $p < 0.01$ in both groups, using log-transformed values) and in a previous report in elderly female subjects (Huovinen et al., 2016).

These two PET studies provide interesting new insights into the role of insulin in bone marrow AT metabolism, as research in this regard has been scarce. Insulin seems to play an important role in marrow adipocyte expansion, but not development (Qiang et al., 2016), and several studies have previously demonstrated that insulin resistance, possibly because of sustained hyperinsulinemia, is associated with increased marrow AT content (Yu et al., 2016; Ermetici et al., 2018). It can be postulated that as insulin resistance is associated with less browning of AT (Bartelt & Heeren, 2014), the marrow adipocytes of p.P50T/*AKT2* have started to resemble

more white than brown adipocytes, resulting in higher intracellular lipid content and less stimulation of GU by insulin. Further studies combining *in vivo* assessments of tissue metabolism and the amount of marrow AT, as well as the characterization of adipocytes, would be required to draw more detailed conclusions. Nevertheless, the amount of yellow bone marrow (~8% of body fat mass in adults; Tencerova et al. 2019) would not be significant enough to have a large effect on whole-body insulin-stimulated glucose disposal.

Contrarily to peripheral tissues, insulin-stimulated brain GU was higher in p.P50T/*AKT2* carriers. This is in line with previous studies showing that higher brain GU during hyperinsulinemic-euglycemic clamps has previously been reported in insulin-resistant and morbidly obese subjects, with the rate correlating negatively with whole-body insulin sensitivity (Hirvonen et al., 2011; Tuulari et al., 2013; Boersma et al., 2018). Determining whether the increase in insulin-stimulated GU results from altered central insulin signaling, central inflammation, blood brain barrier dysfunction, or some other reason would require further studies directly aimed at answering this question. Interestingly, brain GU correlated with EGP only in non-carriers. In subjects with impaired insulin sensitivity due to morbid obesity, the two values do, however, correlate (Rebelos et al., 2019). This might indicate that AKT2 has a distinct role in the function of brain-liver axis, possibly by participating in hypothalamic insulin signaling (Obici et al., 2002).

6.2 Intranasal insulin does not promote peripheral glucose uptake, but might reduce brain glucose uptake acutely (Study II)

Based on our results, contrarily to the initial hypothesis, INI does not alter peripheral tissue GU or serum markers of lipid metabolism under mild systemic hyperinsulinemia in normal-weight, healthy males. However, intriguingly, INI was associated with a significant decrease in brain GU when the [^{18}F]-FDG-PET scan was started 40 min after spray application. The applied method was planned to detect whether the brain, after insulin stimulus, would be able to alter peripheral tissue metabolism. While the high dose of insulin administered rapidly straight to CNS does not reflect normal physiology, seeing no significant effect in the periphery under these pharmacological conditions suggests that brain insulin signaling does not orchestrate whole-body metabolism normally either.

A globally lower cerebral GU after INI in humans has not been reported earlier. Interestingly, a recent report using a mouse model found a similar effect when the interval between spray application and [^{18}F]-FDG-PET scan was 30 min (Sanguinetti et al., 2019). The authors hypothesized that the unphysiologically high CNS insulin exposure could result in an inhibition of local insulin action and a lower brain GU,

and this can indeed be explained by the downregulation of IR activity by insulin itself (Boucher et al., 2014).

Alternatively, further downstream on the insulin signaling pathway, it can also be that the strong insulin stimulus results in increased intracellular G6P, which hinders insulin-independent GU regulated by the concentration gradient across cell membrane (Whitesell et al., 1995) at the time when [^{18}F]-FDG was administered. This would be a possible result from an initial increase in GLUT4-mediated neuronal GU (Benomar et al., 2006; Reno et al., 2017) and later saturation of glycogen stores in astrocytes (Heni et al., 2011), resulting in excess G6P as the glucose demand in the resting state would be low. Furthermore, the conflict between the brain receiving no signals of hyperinsulinemia from the periphery and sensing no adjacent decrease in glycaemia could also contribute to the finding. As peripheral glucose disposal did not increase, the effect should not result from increased glucose disposal in other tissues.

It remains debatable whether the decrease in brain GU could result from limited glucose delivery to the brain. This is because while some studies have shown lower cerebral blood flow in the hypothalamus and prefrontal cortex after INI in lean subjects during fasting (Kullmann et al., 2015, 2017), others have reported no change in major cerebral arteries in young, healthy subjects (Akintola et al., 2017).

At the moment, increased skeletal muscle GU by central insulin stimulus has only been demonstrated by one study in mice (Coomans et al., 2011b), while other studies have report no effect (Scherer et al., 2011). A significant increase in GIR as a sign of improved tissue GU has currently been reported in one human study (Heni et al., 2014), but the effect was diminished when the same group accounted for the increase in serum insulin levels after INI on the placebo visit (Heni et al., 2017). Furthermore, INI has not been shown to affect the whole-body glucose disposal rate (Dash et al., 2015; Heni et al., 2017). Two studies attributed the increase in GIR to a decrease in EGP (Coomans et al., 2011b; Filippi et al., 2012); therefore, as we did not observe changes in EGP, it seems reasonable that the small change in GIR remained insignificant.

Not seeing an effect on EGP is not, however, contradictory to previous reports. The method used in our study only enables the estimation of mean EGP from [^{18}F]-FDG administration until the end of scan (app. 40 to 120 min post sprays), and the previous reports have shown the decrease to occur 100 to 120 min (Heni et al., 2017) or 3 to 6 hours after spray administration (Dash et al., 2015), or even more delayed, as demonstrated in studies activating central K_{ATP} channels with diazoxide (Kishore et al., 2011, Esterson et al., 2016). Moreover, the systemic insulin levels on both interventions might have been high enough to suppress up to 50% of EGP (Rizza et al., 1981), leaving the possible additional effect of INI too small to detect in this small sample. This would, however, further emphasize the additive, rather than

essential role of central regulation in EGP (Perseghin et al., 1997, Edgerton et al., 2006, Plomgaard et al., 2019).

The effects of central insulin signaling in inducing BAT thermogenesis via SNS activation has also currently been shown only in mice, and under fasting conditions (Rahmouni et al., 2014). While Benedict et al. (2011) reported an increase in mean postprandial energy expenditure during the 2.5 hours following INI, the difference in separate 30 min intervals did not reach statistical significance, and the possible spillover of insulin to circulation was not simulated on placebo visits. The different timeframe and methodology can also be the reasons we did not observe changes in BAT activity.

Decreased lipolysis and increased lipogenesis following insulin administration to the brain, more specifically mediobasal hypothalamus, has been demonstrated in mice as a reduced rate of appearance of glycerol during pancreatic clamp (Scherer et al., 2011). The transient lowering of glycerol appearance has also been reported in humans 0–60 min after INI administration during fasting (Iwen et al., 2014), while glycerol levels in circulation and subcutaneous WAT interstitium remained unchanged (Gancheva et al., 2015; Iwen et al., 2014). In the current study, no significant changes were observed in serum glycerol, although it tended to decrease with INI compared to placebo, which is in line with previous studies. Moreover, seeing no change in serum triglycerides, apolipoproteins, or fatty acids is in agreement with previous studies during fasting (Iwen et al., 2014; Gancheva et al., 2015) and pancreatic clamp with a constant fed state (Xiao et al., 2017), although assessing only total fatty acids instead of free fatty acids limits comparing the current results to previous reports.

6.3 SGLT2 inhibitor dapagliflozin does not improve tissue insulin-stimulated glucose uptake, but alleviates hepatic steatosis and reduces body fat content (Study III)

The results from this study show that the previously reported ameliorating of insulin resistance by SGLT2 inhibitors is not a result of perpetual improvement in insulin-stimulated GU in peripheral tissues—to some extent in contradiction to previous studies lacking the ability to quantify tissue metabolism directly. However, in line with several recent reports, dapagliflozin treatment induced a significant decrease in liver steatosis and size, as well as in subcutaneous and visceral AT volumes, without affecting lean body mass.

Surprisingly, the observation of no effect on whole-body and tissue-specific insulin-stimulated GU and EGP differs from previous reports (Merovci et al., 2014, 2016; Mudaliar et al., 2014; Daniele et al., 2016; Matsuba et al., 2018). Comparing

the results from the current study with previous ones is not, however, completely straightforward, as other groups used two- to threefold higher rates of insulin infusion and longer clamp durations (Merovci et al., 2014, 2016; Mudaliar et al., 2014; Daniele et al., 2016; Matsuba et al., 2018). It has been shown that increasing the insulin infusion rate first results in an enhanced suppression of EGP, followed by increased tissue GU (Rizza et al., 1981), while the slow increase in GIR in response to increasing insulin sensitivity often seen in longer hyperinsulinemic clamp studies can be attributed to, for example, prolonged fasting, diurnal changes in insulin sensitivity, and changes in endogenous insulin production (Swinnen et al., 2008). As a consequence, EGP seems to have been less completely suppressed in our study. However, this does not affect the fact that we saw no change in tissue-specific GU measured from PET data, as the directly quantified results are independent of EGP.

The improvement in whole-body insulin sensitivity has been considered as a proof-of-concept for glucotoxicity—hyperglycemia *per se* deteriorating insulin sensitivity—as SGLT2 inhibition should not have direct effects on major insulin-sensitive tissues (Merovci et al., 2014; Mudaliar et al., 2014). Others argue that the insulin-sensitizing effect of SGLT2 inhibitors results from significantly promoted fatty acid oxidation and alleviated lipotoxicity caused by a reduced amount of ectopic fat (Ferrannini et al., 2014, 2016; Daniele et al. 2016).

Indeed, four studies (Ferrannini et al., 2014, 2016; Mudaliar et al., 2014; Daniele et al., 2016) have shown a substrate shift from the oxidation of glucose to fatty acids. Only Daniele et al. (2016) have currently reported an increase in net glucose disposal because of a significant increase in skeletal muscle glycogen synthesis, whereas Ferrannini et al. (2016a) demonstrated a decrease in total postprandial glucose disposal, possibly resulting from increased lipolysis.

The paradoxical increase in EGP reported by Merovci et al. (2014) and Ferrannini et al. (2014) — but not by Mudaliar et al. (2014) and Daniele et al. (2016) — was hypothesized to result from the body trying to account for the glucose lost to urine by increasing the secretion of glucagon. Indeed, in these two studies administration of SGLT2 inhibitor, decrease in plasma glucose and responsive increases in glucagon and EGP seemed to have a temporal relationship. The lack of an effect on EGP in the current study might therefore be associated with no change in fasting glucagon levels or in the glucagon/insulin ratio. This can be because, as opposed to earlier reports, the study drug in the current study was not administered on the day of the measurements, and the increase in glucagon has been shown to result from acute glucose-lowering effects of SGLT2 inhibition (Lundkvist et al., 2019) rather than improved hepatic insulin sensitivity or direct stimulation of α-cells (Bonner et al., 2015). Furthermore, the interval of over 24 hours between the last dose of study medication and the PET studies can also contribute to the observation of no change in glucose disposal or systemic lipolysis, as enhanced lipolysis has also

been suggested to occur to compensate for glucose lost to urine (Daniele et al., 2016). Therefore, the results from the current study support the view that SGLT2 inhibitors might ameliorate insulin resistance via promoting fatty acid mobilization and oxidation acutely, while improved glycaemia alone is not sufficient in increasing tissue insulin sensitivity.

Since the planning of the current study, several reports have demonstrated the beneficial effects of SGLT2 inhibitors on liver volume and lipid accumulation (Ito et al., 2017; Shibuya et al., 2018; Eriksson et al., 2018; Kuchay et al., 2018). Similarly to these previous studies, we also found the association between decreased liver steatosis and fat volumes significant, with the connection being further established by earlier reports (van der Poorten et al., 2008; Musso et al., 2012). The reduction has been attributed to the metabolic shift of tissues favoring fatty acid oxidation over glucose oxidation, further augmented by glucagon-driven glycogenolysis and gluconeogenesis during fasting (Eriksson et al., 2018; Esterline et al., 2018).

The association between the statistical trend towards lower FGF21 by dapagliflozin and the change being strongly associated with the decrease in liver fat is in line with the report by Eriksson et al. (2018), who found a significant lowering of FGF21, and earlier studies showing a correlation between higher FGF21 concentrations and NAFLD (Giannini et al., 2013). Interestingly, FGF21 can also be considered a marker of mitochondrial function and endoplasmic reticulum stress (Jiang et al., 2014) and mitochondrial function and hepatic insulin sensitivity (Koliaki et al., 2015; Chavez et al., 2009) in patients with hepatic steatosis.

Surprisingly, the significant decreases in IL-6 and subcutaneous AT volume were negatively correlated, although the excrement by the tissue has been estimated to account for up to 35% of systemic IL-6 (Mohamed-Ali et al., 1997). IL-6 can also serve as an index of insulin sensitivity (Wang et al., 2013); therefore, it seems that the change was driven by some other beneficial inflammatory or metabolic effect by dapagliflozin.

Favorable effects of SGLT2 inhibitors on myocardium have been reported widely, with consistent results showing reduced LV mass and improved diastolic function (Soga et al, 2018; Verma et al., 2019), while effects on myocardial metabolism have not been previously published. In the non-ischemic myocardium, energy is mostly (50–70%) derived from FA β-oxidation, but also from degradation of glucose, lactate, and ketone bodies, depending on substrate availability (Lopaschuk et al., 2010). In insulin resistance, FFA uptake has been shown to increase, while β-oxidation is impaired, resulting in impaired myocardial function (Lopaschuk et al., 2010). Contrarily, GU is largely unaffected (Paternostro et al., 1996; Utriainen et al., 1998), especially when accounting for changes or differences in circulating FFAs. As lipolysis was not significantly affected by dapagliflozin in

the current study, it seems reasonable that the ratio of fatty acid to GU (known as the Randle cycle) was not altered.

However, it can be speculated that as both attenuated FA oxidation (Lopaschuk et al., 2010) and a shift from fatty acid to ketone utilization (Ferrannini et al., 2016b) could explain the advantageous effects of SGLT2 inhibitors on cardiac health, favoring these substrates over glucose could have resulted in decreased GU in the current study (Lopaschuk et al., 2010). Further studies are required to determine whether the change was not observed because of the interval between dapagliflozin administration and PET scans or because the effect on myocardial metabolism remains minor in comparison to, for example, changes in preload due to decreased blood volume also associated with the treatment.

6.4 Strengths and limitations

The strength of these studies lies in the established method of combining [^{18}F]-FDG-PET with clamp protocols, with much experience with this approach at the Turku PET Centre, resulting in the ability to create hypotheses that can be addressed with the available techniques. The study procedures and analyses performed with the researchers blinded to the genotype of the subjects in Study I and to the treatment arm in Study III, as well as the subjects being blinded to intervention in Studies II and III, increase the reliability of the results. Furthermore, additional analyses performed for the first 24 subjects in Study I revealed a high intra- and interobserver reliability of the results: Pearson correlations for skeletal muscle GU were 0.99 between repeated measurements, 0.98 between original values and those reproduced by another analyzer, and 0.92 between repeated measurements of liver GU.

However, the methods used for insulin stimulation and PET imaging both have their limitations. First, although the hyperinsulinemic-euglycemic clamp is recognized as the golden standard of measuring insulin sensitivity, the sustained high circulating insulin levels and converse proportions of peripheral and portal insulin concentrations do not represent normal physiology (Radziuk, 2000). Second, and similarly, investigating the effects of insulin on brain metabolism and function by applying a large dose of INI produces a pharmacological rather than physiological effect (Edgerton et al., 2015), but still appears to be the least invasive and best option for investigating brain-specific effects in humans *in vivo*, at least to create hypotheses that can be addressed in further studies.

Third, the PET/CT machine used in the studies has a resolution of ~5 mm, which restrains its use in analyzing small VOIs, such as smaller brain regions (e.g. the hypothalamus, intestinal walls, BAT, and subcutaneous, and visceral AT) in slender subjects. Smaller structures are all also sensitive to spillover of activity signals from surrounding tissues and to motion artefacts from breathing. Fourth, while [^{18}F]-FDG

can be considered a reliable measure of glucose transport into the cells for the first 60 to 80 min after injection, the current methodology does not allow for an investigation into intracellular glucose traffic, the possible effects on, for example, glycogen metabolism thus cannot be directly assessed. In the late scans (in the current studies, this applies to the brain data), it is also possible that some release of [^{18}F]-FDG from the cells starts to occur, while the rate and, more importantly, relevance of the phenomenon can be disputed.

Fifth, all PET studies include exposure to ionizing radiation because of the PET tracers, and the additional CT was used for anatomical reference. Despite the technical development of the PET scanners, the adjustment of the CT to ultra-low doses (or using MRI for reference), and the use of insulin infusion in our studies reducing the radiation burden, a [^{18}F]-FDG can only be performed twice for the same subject in order to stay within the limit of 10 mSv set for scientific studies by the Finnish Radiation and Nuclear Safety Authority and EU legislation.

Sixth, given the radiation burden and the price of PET studies, the number of subjects in these studies is usually kept as low as possible. Moreover, attempts to avoid large between-subject variability might result in recruiting very homogenous study groups and poorer generalizability of the results. With regard to female subjects of fertile age, not only is the radiation burden limiting their recruitment, but the possible confounding effects of menstrual cycle (Yeung et al. 2010) and hormonal contraception (Sitruk-Ware & Nath, 2011) on insulin sensitivity must also be considered when using small sample sizes. While including only male subjects in Studies I and II can be justified based on the experimental settings, the results should not be generalized to females without careful consideration.

6.5 Future aspects

To elaborate further on the results from the studies in this thesis and answer the questions that have arisen, a wide range of options using PET are available. For example, the used protocols could be applied to a wider, more diverse population or, after slight modifications, be repeated in similar study groups. In addition, a large variety of PET ligands enable the targeting of different hypotheses directly.

Given the small sample sizes, it was mandatory to try to recruit quite a homogenous group of study subjects for Studies I and II. Therefore, it would be interesting to study the effects seen in these studies on a wider population in the future, as both AKT2 function and INI seem to have diverging effects depending on the gender and insulin sensitivity of the subjects. For one, studying the effects of p.P50T/*AKT2* on female subjects or younger variant carriers with the same validated methods already used in Study I would be interesting. In an AKT2 knock-out mouse model, female mice displayed less dramatic effects on insulin sensitivity than males

(Garofalo et al. 2003), whereas in a family with a loss-of-function mutation of the *AKT2* gene, heterozygous variant carriers demonstrated severe insulin resistance and early-onset T2D in three female subjects but no significant effect on the one male family member (George et al., 2004). Investigating the changes in tissue insulin sensitivity caused by a less dramatic effect (i.e. in female p.P50T/*AKT2* carriers) could shed some more light on the possible gender-specific entities regulating insulin signaling. Moreover, studying younger variant carriers could elucidate the order in which inherited insulin resistance starts to affect different tissues, as data especially on the brain are scarce.

Furthermore, as it might be that impaired signaling via the PI3K-AKT pathway, or even more specifically AKT2, is the link between metabolic syndrome and Alzheimer's disease (Gabbouj et al., 2019a, 2019b), performing studies on variant carriers that would combine the assessment of insulin-stimulated glucose metabolism with [^{18}F]-FDG, scans with PET tracers used specifically for Alzheimer's disease ([^{11}C]Pittsburgh Compound B, [^{18}F]florbetapir [^{18}F]florbetaben or [^{18}F]flutemetamol [Marcus et al., 2014]), and evaluation of cognitive function could establish the association in real patients. In addition, the hypothesis of central inflammation being the reason for increased insulin-stimulated GU could be confirmed by using PET tracers binding to brain inflammatory cells, such as R-[^{11}C]PK11195 or [^{11}C]deuterium-l-deprenyl (Janssen et al., 2016). Moreover, previous studies have found no weight loss or suppression of appetite in females after INI (Hallschmid et al., 2004; Benedict et al., 2008), but a more pronounced beneficial effect on working memory (Benedict et al., 2008); it is thus possible that INI could also have a more distinct role in enhancing brain metabolism in females. Therefore, investigating whether INI affects insulin-stimulated tissue glucose metabolism in female subjects could also be of interest.

Obese subjects have also shown a contrasting response to brain insulin stimulation by INI, with little metabolic effects and supposed faulty brain-liver axis (Heni et al., 2017; Xiao et al., 2018). Previous studies performed at the Turku PET Centre have demonstrated that morbid obesity is associated with increased insulin-stimulated brain GU (Tuulari et al., 2013), but applying INI could elucidate whether this is a direct central insulin effect or a result of faulty peripheral input to the brain.

Concerning Study II, in addition to recruiting a more diverse study population, rescheduling the PET scans could provide more interesting results: Starting the brain PET scan soon after nasal spray application would enable documenting dynamic changes in brain glucose metabolism. Moreover, skeletal muscle and liver GU could be reassessed at a later timepoint (100–120 min from spray application) to detect possible later effects. However, the most crucial action to clarify the results from Study II concerning brain metabolism would be to use a method allowing dynamic measurement of not only GU to the brain, but also the changes in further metabolic

pathways, most notably concentrations of glycogen and lactate. While dynamic scans and changes in the initial uptake rate can be detected with PET, investigating further effects could be more feasible by combining a [^{13}C]-enriched glucose tracer with MRS (Lundqvist et al., 2019). Performing studies on brain metabolism in a more physiological setting, postprandially or by stimulating pancreatic insulin release, could also be of interest, especially when comparing healthy and insulin-resistant subjects.

For the dapagliflozin study, administering the study drug on the day of the PET studies and possibly using a higher rate of insulin infusion, or even a two-step clamp with increased insulin infusion rates and repeated scans, could help to explain the differing results in our studies and provide answers to the hypotheses made by others. In a yet unpublished study, the effects of dapagliflozin on myocardial metabolism in particular were investigated using PET with fatty acid analogue 14(R,S)-[^{18}F]fluoro-6-thia-heptadecanoic acid ([^{18}F]-FTHA) and ketone [1-^{11}C]acetoacetate (Åkerblom et al., 2019), so these results might elucidate whether the hypothesized substrate shift or enhancement of fatty acid oxidation actually occurs. Furthermore, in a previous study, bariatric surgery resulted in normalization of insulin-stimulated brain GU (Tuulari et al., 2013), but the effect of antidiabetic medicines on brain glucose metabolism in T2D subjects has not been reported.

7 Conclusions

This thesis aimed to clarify the effects of a genetic variant causing primarily skeletal muscle insulin resistance (Study I), as well as central insulin stimulation (Study II), on tissue insulin-stimulated GU. It also aimed to determine whether SGLT2 inhibitor dapagliflozin could serve as a treatment for insulin resistance (Study III).

In Study I, it was shown that a rare genetic variant causing a partial loss-of function of the *AKT2* gene not only decreases GU into skeletal muscle, but is also associated with signs of lowered insulin sensitivity in all metabolic key organs. This was the first time tissue-specific effects of a rare variant have been demonstrated in humans *in vivo*. Therefore, the report also establishes the role of PET in investigating possible outcomes of risk-increasing genetic variants in detail.

In Study II, it was concluded that INI does not have a major effect on peripheral insulin-stimulated GU in healthy subjects, with the major glucoregulatory effect of central insulin exposure likely being the suppression of hepatic glucose production, either directly or via inhibition of WAT lipolysis. Surprisingly, INI did cause a significant decrease in brain GU when the PET scan was started 40 min after administration. This can be attributed either to methodological causes or to the unphysiological setting, but solving this is outside of the scope of the current study.

In Study III, it was demonstrated that 8 weeks of treatment with SGLT2 inhibitor dapagliflozin does not induce a sustained improvement in tissue-specific insulin-stimulated GU in subjects with T2D. However, it does have beneficial reducing effects on liver fat content, liver volume, and subcutaneous and visceral fat volumes.

Finally, although [^{18}F]-FDG PET has some limitations as a method, it is currently the best approach to assessing tissue-specific insulin-stimulated GU in several tissues in one setting. The Small Number of subjects in Study II and including only male subjects in Studies I and II can be considered limitations.

In summary, these studies elaborate the roles of impaired peripheral insulin signaling, stimulation of central insulin signaling, and alleviated hyperglycemia and decreased body adiposity by a short intervention with dapagliflozin in regulating whole-body insulin sensitivity.

Acknowledgements

This work was conducted at the Turku PET Centre and within the Finnish Centre of Excellence in Cardiovascular and Metabolic Diseases, supported by Academy of Finland, University of Turku, Turku University Hospital, Åbo Akademi University and University of Eastern Finland during the years 2015-2020.

I owe my deepest gratitude to my supervisors, professor Pirjo Nuutila and professor Markku Laakso. They always seemed to have more faith in me and this project than I did, and I truly admire their long-lasting and contagious enthusiasm towards metabolic research. I would like to address special thanks to Pirjo for always being ready to discuss any problems I have had and managing to lighten up the mood despite setbacks. Although the times have been regrettably few due to geographical reasons, I really appreciate Markku for taking up the time to discuss research with me.

I am very much looking forward to having professor Jan W. Eriksson as my opponent, and I would like to thank him for accepting the invitation.

I would like to thank professor Tommy G. Olsson and adjunct professor Kirsi Timonen for reviewing this thesis and offering their valuable feedback, which really aided me in clarifying why the performed studies were interesting and important. Professor Markus Juonala and professor Jussi Pihlajamäki are acknowledged for participating in my follow-up committee.

My warmest appreciation goes to professor Kirsi Virtanen and docent Jarna Hannukainen for helping me in many practical issues, as well as for their positive and encouraging attitude towards the younger researchers. I would also like to thank Marita Kailajärvi for kindly guiding me in working in clinical trials.

A special thank you goes to my colleagues in Turku PET Centre for a supportive atmosphere and the many good times in the bunker as well as on conference trips. So thank you Miikka Honka, Minna Lahesmaa, Sanna Laurila, Prince Dadson, Sanna Honkala, Eleni Rebelos, Henri Honka, Jukka Koffert, Mueez U Din, Heidi Immonen, Laura Pekkarinen, Henry Karlsson, Priyanka Motiani, Kumail Motiani, Petri Elo and Tiina Saanijoki. Miikka deserves my special gratitude for getting me started with PET data analysis, backing up on statistical issues and always being ready to discuss any topic I have come up with, from hepatic insulin resistance to board games.

Performing the studies, and even enjoying it, would not have been possible without the great team on the second floor, so thank you for the radiographers (Minna, Anne-Mari, Hannele, Marjo, Aliisa, Pirkko, Silja, Sofia, Adi and Jonna), laboratory staff (Sanna, Eija, Heidi, Hanna, Leena, Emilia and Tintti), and physicists Virva Saunavaara and Tuula Tolvanen. Rami Mikkola and Marko Tättäläinen deserve a warm thank you for always being ready to help with computer issues, and Vesa Oikonen for clarifying the questions I have had about modelling. I also owe thank yous to the department of radiochemistry, especially Sarita Forsback, Anna Kirjavainen and Olli Eskola. Juhani Knuuti is acknowledged as the head of Turku PET Centre for providing the exceptional environment for performing the studies.

Mia Koutu, I could not have hoped for a better study nurse to work with. I'll never be able to thank you enough for getting through both the too busy and the boring days with me. Thank you for all your hospitality and friendship.

A heartily thanks goes also to all the collaborators and co-authors. I would especially like to thank Tomi Karjalainen and professor Lauri Nummenmaa for the brain data analyses; Alena Stančakova for her contributions to the AKT2 study; Jan Oscarsson for his positive and tireless attitude while working on the dapagliflozin manuscript; Joel Kullberg and Lars Johansson for working on the MRI data of the dapagliflozin study; Patricia Iozzo for her valuable professional and linguistic aid in the dapagliflozin study; and Riku Klén and Eliisa Löyttyniemi for their statistical work. I would also like to thank professors Martin Heni and Hans-Ulrich Häring for collaborating on the intranasal insulin project.

The 89 subjects participating in the studies, not to forget the many more interested ones to have dropped out at screening visits, are acknowledged for voluntarily taking their time to advance our understanding of insulin sensitivity.

I should also thank my friends from throughout the years. Thank you for reminding me about life outside of work and the endless fun and support, and a special thank you to those of my friends who have survived their thesis and have been able to share this experience with me.

I'd like to thank my mother for her relentless support and love, and my father for sparking an interest towards a life as a researcher. I'd also like to thank my extended family, Markku, Iiris, Liisa, Saara and Otso, for being in my life.

Finally, I need to thank the most important people I have: my husband Eero and daughter Eerika. Thank you for daily reminding me about what's truly important.

This work was financially supported by the Finnish Diabetes Research Foundation and the Finnish Cultural Foundation, Varsinais-Suomi Regional Fund.

Turku, July 2020

Aino Latva-Rasku

References

Aalling, N., Nedergaard, M. & DiNuzzo, M. (2018) Cerebral Metabolic Changes during Sleep. *Current Neurology and Neuroscience Rep* 18:1-17.

Abel, E.D., Peroni, O., Kim, J.K., Kim, Y.B., Boss, O., Hadro, E., Minnemann, T., Shulman, G.I. & Kahn, B.B. (2001) Adipose-Selective Targeting of the GLUT4 Gene Impairs Insulin Action in Muscle and Liver. *Nature* 409:729-733.

Akintola, A.A., van Opstal, A.M., Westendorp, R.G., Postmus, I., Van Der Grond, J., & Van Heemst, D. (2017) Effect of Intranasally Administered Insulin on Cerebral Blood Flow and Perfusion; a Randomized Experiment in Young and Older Adults. *Aging, 9*(3), 790-802

Armstrong, M.J., Hull, D., Guo, K., Barton, D., Hazlehurst, J.M., Gathercole, L.L., Nasiri, M., Yu, J., Gough, S.C., Newsome, P.N. & Tomlinson, J.W. (2016) Glucagon-Like Peptide 1 Decreases Lipotoxicity in Non-Alcoholic Steatohepatitis. *Journal of Hepatology* 64:399-408.

Ashraf, A., Fan, Z., Brooks, D.J. & Edison, P. (2015) Cortical Hypermetabolism in MCI Subjects: A Compensatory Mechanism? *European Journal of Nuclear Medicine and Molecular Imaging* 42:447-458.

Bachelard, H.S. (1971) Specificity and Kinetic Properties of Monosaccharide Uptake into Guinea Pig Cerebral Cortex in Vitro. *Journal of Neurochemistry* 18:213-222.

Banks, W.A., Jaspan, J.B., Huang, W. & Kastin, A.J. (1997) Transport of Insulin across the Blood-Brain Barrier: Saturability at Euglycemic Doses of Insulin. *Peptides* 18:1423-1429.

Banks, W.A. & Kastin, A.J. (1998) Differential Permeability of the Blood–Brain Barrier to Two Pancreatic Peptides: Insulin and Amylin. *Peptides* 19:883-889.

Banks, W.A., Kastin, A.J. & Pan, W. (1999) Uptake and Degradation of Blood-Borne Insulin by the Olfactory Bulb. *Peptides* 20:373-378.

Banks, W.A. (2004) The Source of Cerebral Insulin. *European Journal of Pharmacology* 490:5-12.

Bartelt, A. & Heeren, J. (2014) Adipose Tissue Browning and Metabolic Health. *Nature Reviews Endocrinology* 10:24-36.

Basu, R., Chandramouli, V., Dicke, B., Landau, B. & Rizza, R. (2005) Obesity and Type 2 Diabetes Impair Insulin-Induced Suppression of Glycogenolysis as Well as Gluconeogenesis. Diabetes 54:1942-1948.

Batterham, R.L. & Cummings, D.E. (2016) Mechanisms of Diabetes Improvement Following Bariatric/Metabolic Surgery. *Diabetes Care* 39:893-901.

Baura, G.D., Foster, D.M., Porte, J., D, Kahn, S.E., Bergman, R.N., Cobelli, C. & Schwartz, M.W. (1993) Saturable Transport of Insulin from Plasma into the Central Nervous System of Dogs in Vivo. a Mechanism for Regulated Insulin Delivery to the Brain. *Journal of Clinical Investigation* 92:1824-1830.

Befroy, D.E. & Shulman, G.I. (2011) Magnetic Resonance Spectroscopy Studies of Human Metabolism. *Diabetes* 60:1361-1369.

Belfiore, A., Malaguarnera, R., Vella, V., Lawrence, M.C., Sciacca, L., Frasca, F., Morrione, A. & Vigneri, R. (2017) Insulin Receptor Isoforms in Physiology and Disease: An Updated View. *Endocrine Reviews* 38:379-431.

Bender, D., Munk, O.L., Feng, H.Q. & Keiding, S. (2001) Metabolites of (18)F-FDG and 3-O-(11)C-Methylglucose in Pig Liver. *Journal of Nuclear Medicine* 42:1673.

Benedict, C., Kern, W., Schultes, B., Born, J. & Hallschmid, M. (2008) Differential Sensitivity of Men and Women to Anorexigenic and Memory-Improving Effects of Intranasal Insulin. *Journal of Clinical Endocrinology & Metabolism* 93:1339-1344.

Benedict, C., Brede, S., Schiöth, H.B., Lehnert, H., Schultes, B., Born, J. & Hallschmid, M. (2011) Intranasal Insulin Enhances Postprandial Thermogenesis and Lowers Postprandial Serum Insulin Levels in Healthy Men. *Diabetes* 60:114-118.

Benomar, Y., Naour, N., Aubourg, A., Bailleux, V., Gertler, A., Djiane, J., Guerre-Millo, M. & Taouis, M. (2006) Insulin and Leptin Induce Glut4 Plasma Membrane Translocation and Glucose Uptake in a Human Neuronal Cell Line by a Phosphatidylinositol 3-Kinase- Dependent Mechanism. *Endocrinology* 147:2550-2556.

Berglund, J. & Kullberg, J. (2012) Three-Dimensional Water/Fat Separation and T 2 Estimation Based on Whole-Image Optimization—Application in Breathhold Liver Imaging at 1.5 T. *Magnetic Resonance in Medicine* 67:1684-1693.

Bergman, R.N., Prager, R., Volund, A. & Olefsky, J.M. (1987) Equivalence of the Insulin Sensitivity Index in Man Derived by the Minimal Model Method and the Euglycemic Glucose Clamp. *Journal of Clinical Investigation* 79:790-800.

Bessell, E.M., Foster, A.B. & Westwood, J.H. (1972) The Use of Deoxyfluoro-D-Glucopyranoses and Related Compounds in a Study of Yeast Hexokinase Specificity. *Biochemical Journal* 128:199-204.

Bingham, E.M., Hopkins, D., Smith, D., Pernet, A., Hallett, W., Reed, L., Marsden, P.K. & Amiel, S.A. (2002) The Role of Insulin in Human Brain Glucose Metabolism. *Diabetes* 51:3384.

Blessing, W., Mohammed, M. & Ootsuka, Y. (2013) Brown Adipose Tissue Thermogenesis, the Basic Rest–Activity Cycle, Meal Initiation, and Bodily Homeostasis in Rats. *Physiology and Behavior* 121:61-69.

Blondin, D.P., Labbé, S.M., Noll, C., Kunach, M., Phoenix, S., Guérin, B., Turcotte, ÉE., Haman, F., Richard, D. & Carpentier, A.C. (2015) Selective Impairment of Glucose but Not Fatty Acid or Oxidative Metabolism in Brown Adipose Tissue of Subjects with Type 2 Diabetes. *Diabetes* 64:2388-2397.

Boden, G., Cheung, P., Stein, T.P., Kresge, K. & Mozzoli, M. (2002) FFA Cause Hepatic Insulin Resistance by Inhibiting Insulin Suppression of Glycogenolysis. *American Journal of Physiology - Endocrinology and Metabolism* 283:12-19.

Bódis, K. & Roden, M. (2018) Energy Metabolism of White Adipose Tissue and Insulin Resistance in Humans. *European Journal of Clinical Investigation* 48:E13017-N/A.

Boersma, G.J., Johansson, E., Pereira, M.J., Heurling, K., Skrtic, S., Lau, J., Katsogiannos, P., Panagiotou, G., Lubberink, M., Kullberg, J., Ahlström, H. & Eriksson, J.W. (2018) Altered Glucose Uptake in Muscle, Visceral Adipose Tissue, and Brain Predict Whole-Body Insulin Resistance and May Contribute to the Development of Type 2 Diabetes: A Combined PET/MR Study. *Hormone and Metabolic Research* 50:E10.

Bolinder, J., Ljunggren, Ö, Kullberg, J., Johansson, L., Wilding, J., Langkilde, A.M., Sugg, J. & Parikh, S. (2012) Effects of Dapagliflozin on Body Weight, Total Fat Mass, and Regional Adipose Tissue Distribution in Patients with Type 2 Diabetes Mellitus with Inadequate Glycemic Control on Metformin. *Journal of Clinical Endocrinology and Metabolism* 97:1020-1031.

Bonner, C., Kerr-Conte, J., Gmyr, V., Queniat, G., Moerman, E., Thévenet, J., Beaucamps, C., Delalleau, N., Popescu, I., Malaisse, W.J., Sener, A., Deprez, B., Abderrahmani, A., Staels, B. & Pattou, F. (2015) Inhibition of the Glucose Transporter SGLT2 with Dapagliflozin in Pancreatic Alpha Cells Triggers Glucagon Secretion. *Nature Medicine* 21:512-517.

Born, J., Fehm, H.L., Kern, W., Lange, T., Bickel, U. & Mcgregor, G.P. (2002) Sniffing Neuropeptides: A Transnasal Approach to the Human Brain. *Nature Neuroscience* 5:514-516.

Bøtker, H.E., Böttcher, M., Schmitz, O., Gee, A., Hansen, S.B., Cold, G.E., Nielsen, T.T. & Gjedde, A. (1997) Glucose Uptake and Lumped Constant Variability in Normal Human Hearts Determined with [18F]Fluorodeoxyglucose. *Journal of Nuclear Cardiology* 4:125-132.

Boucher, J., Kleinridders, A. & Kahn, C.R. (2014) Insulin Receptor Signaling in Normal and Insulin-Resistant States. *Cold Spring Harbor Perspectives in Biology* 6:A009191.

Bouzakri, K., Zachrisson, A., Al-Khalili, L., Zhang, B.B., Koistinen, H.A., Krook, A. & Zierath, J.R. (2006) Sirna-Based Gene Silencing Reveals Specialized Roles of IRS-1/Akt2 and IRS-2/Akt1 in Glucose and Lipid Metabolism in Human Skeletal Muscle. *Cell Metabolism* 4:89-96.

Brooks, G.A. (2018) The Science and Translation of Lactate Shuttle Theory. *Cell Metabolism* 27:757-785.

Brünner, Y.F., Benedict, C. & Freiherr, J. (2013) Intranasal Insulin Reduces Olfactory Sensitivity in Normosmic Humans. *Journal of Clinical Endocrinology and Metabolism* 98:E1626-E1630.

Burén, J., Lindmark, S., Renström, F. & Eriksson, J.W. (2003) In Vitro Reversal of Hyperglycemia Normalizes Insulin Action in Fat Cells from Type 2 Diabetes Patients: Is Cellular Insulin Resistance Caused by Glucotoxicity in Vivo? *Metabolism* 52:239-245.

Camici, P., Araujo, L.I., Spinks, T., Lammertsma, A.A., Kaski, J.C., Shea, M.J., Selwyn, A.P., Jones, T. & Maseri, A. (1986) Increased Uptake of 18F-Fluorodeoxyglucose in Postischemic Myocardium of Patients with Exercise-Induced Angina. *Circulation* 74:81-88.

Campfield, L.A., Smith, F.J., Guisez, Y., Devos, R. & Burn, P. (1995) Recombinant Mouse OB Protein: Evidence for a Peripheral Signal Linking Adiposity and Central Neural Networks. *Science* 269:546-549.

Cannon, B. & Nedergaard, J. (2004) Brown Adipose Tissue: Function and Physiological Significance. *Physiological Reviews* 84:277-359.

Caro, J.F., Ittoop, O., Pories, W.J., Meelheim, D., Flickinger, E.G., Thomas, F., Jenquin, M., Silverman, J.F., Khazanie, P.G. & Sinha, M.K. (1986) Studies on the Mechanism of Insulin Resistance in the Liver from Humans with Noninsulin-Dependent Diabetes. Insulin Action and Binding in Isolated Hepatocytes, Insulin Receptor Structure, and Kinase Activity. *Journal of Clinical Investigation* 78:249-258.

Carpentier, A.C., Blondin, D.P., Virtanen, K.A., Richard, D., Haman, F. & Turcotte, ÉE. (2018) Brown Adipose Tissue Energy Metabolism in Humans. *Frontiers in Endocrinology* 9:447.

Cartee, G. (2015) Roles of TBC1D1 and TBC1D4 in Insulin- and Exercise-Stimulated Glucose Transport of Skeletal Muscle. *Diabetologia* 58:19-30.

Chavez, A.O., Molina-Carrion, M., Abdul-Ghani, M.A., Folli, F., Defronzo, R.A. & Tripathy, D. (2009) Circulating Fibroblast Growth Factor-21 is Elevated in Impaired Glucose Tolerance and Type 2 Diabetes and Correlates with Muscle and Hepatic Insulin Resistance. *Diabetes Care* 32:1542-1546.

Cho, H., Mu, J., Kim, J.K., Thorvaldsen, J.L., Chu, Q., Crenshaw, E.B., III, Kaestner, K.H., Bartolomei, M.S., Shulman, G.I. & Birnbaum, M.J. (2001) Insulin Resistance and a Diabetes Mellitus-Like Syndrome in Mice Lacking the Protein Kinase Akt2 (PKB Beta). *Science* 292:1728-1731.

Choi, S.H. & Ginsberg, H.N. (2011) Increased Very Low Density Lipoprotein (VLDL) Secretion, Hepatic Steatosis, and Insulin Resistance. *Trends in Endocrinology and Metabolism* 22:353-363.

Clegg, D.J., Riedy, C.A., Smith, K.A., Benoit, S.C. & Woods, S.C. (2003) Differential Sensitivity to Central Leptin and Insulin in Male and Female Rats. *Diabetes* 52:682-687.

Cline, G.W., Petersen, K.F., Krssak, M., Shen, J., Hundal, R.S., Trajanoski, Z., Inzucchi, S., Dresner, A., Rothman, D.L. & Shulman, G.I. (1999) Impaired Glucose Transport as a Cause of Decreased Insulin-Stimulated Muscle Glycogen Synthesis in Type 2 Diabetes. *New England Journal of Medicine* 341:240-246.

Considine, R.V., Sinha, M.K., Heiman, M.L., Kriauciunas, A., Stephens, T.W., Nyce, M.R., Ohannesian, J.P., Marco, C.C., Mckee, L.J., Bauer, T.L. & Caro, J.F. (1996) Serum Immunoreactive-Leptin Concentrations in Normal-Weight and Obese Humans. *New England Journal of Medicine* 334:292-295.

Coomans, C.P., Geerling, J.J., Guigas, B., Van Den Hoek, Anita M, Parlevliet, E.T., Ouwens, D.M., Pijl, H., Voshol, P.J., Rensen, P.C.N., Havekes, L.M. & Romijn, J.A. (2011a) Circulating Insulin Stimulates Fatty Acid Retention in White Adipose Tissue via KATP Channel Activation in the Central Nervous System Only in Insulin-Sensitive Mice. *Journal of Lipid Research* 52:1712-1722.

Coomans, C.P., Biermasz, N.R., Geerling, J.J., Guigas, B., Rensen, P.C.N., Havekes, L.M. & Romijn, J.A. (2011b) Stimulatory Effect of Insulin on Glucose Uptake by Muscle Involves the Central Nervous System in Insulin-Sensitive Mice. *Diabetes* 60:3132-3140.

Czech, M., Tencerova, M., Pedersen, D. & Aouadi, M. (2013) Insulin Signalling Mechanisms for Triacylglycerol Storage. *Diabetologia* 56:949-964.

Czech, M.P. (2017) Insulin Action and Resistance in Obesity and Type 2 Diabetes. *Nature Medicine* 23:804-814.

Daniele, G., Xiong, J., Solis-Herrera, C., Merovci, A., Eldor, R., Tripathy, D., Defronzo, R.A., Norton, L. & Abdul-Ghani, M. (2016) Dapagliflozin Enhances Fat Oxidation and Ketone Production in Patients with Type 2 Diabetes. *Diabetes Care* 39:2036-2041.

Dash, S., Xiao, C., Morgantini, C., Koulajian, K. & Lewis, G.F. (2015) Intranasal Insulin Suppresses Endogenous Glucose Production in Humans Compared with Placebo in the Presence of Similar Venous Insulin Concentrations. *Diabetes* 64:766-774.

Debons, A.F., Krimsky, I. & From, A. (1970) A Direct Action of Insulin on the Hypothalamic Satiety Center. *American Journal of Physiology* 219:938-943.

Defronzo, R.A., Tobin, J.D. & Andres, R. (1979) Glucose Clamp Technique: A Method for Quantifying Insulin Secretion and Resistance. *American Journal of Physiology - Endocrinology and Metabolism* 237:214.

Defronzo, R.A. & Tripathy, D. (2009) Skeletal Muscle Insulin Resistance is the Primary Defect in Type 2 Diabetes. *Diabetes Care* 32:S157-S163.

Defronzo, R.A. (2010) Insulin Resistance, Lipotoxicity, Type 2 Diabetes and Atherosclerosis: The Missing Links. The Claude Bernard Lecture 2009. *Diabetologia* 53:1270-1287.

Defronzo, R.A. (2017) Combination Therapy with GLP-1 Receptor Agonist and SGLT2 Inhibitor. *Diabetes, Obesity and Metabolism* 19:1353-1362.

Del Prato, S., Leonetti, F., Simonson, D., Sheehan, P., Matsuda, M. & Defronzo, R. (1994) Effect of Sustained Physiologic Hyperinsulinaemia and Hyperglycaemia on Insulin Secretion and Insulin Sensitivity in Man. *Diabetologia* 37:1025-1035.

Dienel, G.A., Behar, K.L. & Rothman, D.L. (2018) Cellular Origin of [^{18}F]FDG-PET Imaging Signals during Ceftriaxone-Stimulated Glutamate Uptake: Astrocytes and Neurons. *Neuroscientist* 24:316-328.

Dixon, W.T. (1984) Simple Proton Spectroscopic Imaging. *Radiology* 153:189-194.

Donnelly, K.L., Smith, C.I., Schwarzenberg, S.J., Jessurun, J., Boldt, M.D. & Parks, E.J. (2005) Sources of Fatty Acids Stored in Liver and Secreted via Lipoproteins in Patients with Nonalcoholic Fatty Liver Disease. *Journal of Clinical Investigation* 115:1343-1351.

Dresner, A., Laurent, D., Marcucci, M., Griffin, M.E., Dufour, S., Cline, G.W., Slezak, L.A., Andersen, D.K., Hundal, R.S., Rothman, D.L., Petersen, K.F. & Shulman, G.I. (1999) Effects of Free Fatty Acids on Glucose Transport and IRS-1–Associated Phosphatidylinositol 3-Kinase Activity. *Journal of Clinical Investigation* 103:253-259.

Dube, S., Errazuriz, I., Cobelli, C., Basu, R. & Basu, A. (2013) Assessment of Insulin Action on Carbohydrate Metabolism: Physiological and Non-Physiological Methods. *Diabetic Medicine* 30:664-670.

Edgerton, D.S., Lautz, M., Scott, M., Everett, C.A., Stettler, K.M., Neal, D.W., Chu, C.A. & Cherrington, A.D. (2006) Insulin's Direct Effects on the Liver Dominate the Control of Hepatic Glucose Production. *Journal of Clinical Investigation* 116:521-527.

Edgerton, D.S. & Cherrington, A.D. (2015) Is Brain Insulin Action Relevant to the Control of Plasma Glucose in Humans? *Diabetes* 64:696-699.

Elias, C.F., Lee, C., Kelly, J., Aschkenasi, C., Ahima, R.S., Couceyro, P.R., Kuhar, M.J., Saper, C.B. & Elmquist, J.K. (1998) Leptin Activates Hypothalamic CART Neurons Projecting to the Spinal Cord. *Neuron* 21:1375-1385.

Eriksson, J., Lundkvist, P., Jansson, P., Johansson, L., Kvarnström, M., Moris, L., Miliotis, T., Forsberg, G., Risérus, U., Lind, L. & Oscarsson, J. (2018) Effects of Dapagliflozin and N-3 Carboxylic Acids on Non-Alcoholic Fatty Liver Disease in People with Type 2 Diabetes: A Double-Blind Randomised Placebo-Controlled Study. *Diabetologia* 61:1923-1934.

Ermetici, F., Ermetici, F., Briganti, S., Briganti, S., Delnevo, A., Delnevo, A., Cannaò, P., Cannaò, P., Leo, G., Leo, G., Benedini, S., Benedini, S., Terruzzi, I., Terruzzi, I., Sardanelli, F., Sardanelli, F., Luzi, L. & Luzi, L. (2018) Bone Marrow Fat Contributes to Insulin Sensitivity and Adiponectin Secretion in Premenopausal Women. *Endocrine* 59:410-418.

Esterline, R.L., Vaag, A., Oscarsson, J. & Vora, J. (2018) Mechanisms in Endocrinology: SGLT2 Inhibitors: Clinical Benefits by Restoration of Normal Diurnal Metabolism? *European Journal of Endocrinology* 178:R113-R125.

Esterson, Y.B., Carey, M., Boucai, L., Goyal, A., Raghavan, P., Zhang, K., Mehta, D., Feng, D., Wu, L., Kehlenbrink, S., Koppaka, S., Kishore, P. & Hawkins, M. (2016) Central Regulation of Glucose Production May Be Impaired in Type 2 Diabetes. *Diabetes* 65:2569-2579.

Farese, R.V. & Sajan, M.P. (2010) Metabolic Functions of Atypical Protein Kinase C: "Good" and "Bad" as Defined by Nutritional Status. *American Journal of Physiology - Endocrinology and Metabolism* 298:385-394.

Ferrannini, E., Barrett, E.J., Bevilacqua, S. & Defronzo, R.A. (1983) Effect of Fatty Acids on Glucose Production and Utilization in Man. *Journal of Clinical Investigation* 72:1737-1747.

Ferrannini, E., Gastaldelli, A., Matsuda, M., Miyazaki, Y., Pettiti, M., Glass, L. & Defronzo, R.A. (2003) Influence of Ethnicity and Familial Diabetes on Glucose Tolerance and Insulin Action: A Physiological Analysis. *Journal of Clinical Endocrinology and Metabolism* 88:3251-3257.

Ferrannini, E., Seman, L., Seewaldt-Becker, E., Hantel, S., Pinnetti, S. & Woerle, H.J. (2013) A Phase IIb, Randomized, Placebo-Controlled Study of the SGLT2 Inhibitor Empagliflozin in Patients with Type 2 Diabetes. *Diabetes, Obesity and Metabolism* 15:721-728.

Ferrannini, E., Muscelli, E., Frascerra, S., Baldi, S., Mari, A., Heise, T., Broedl, U.C. & Woerle, H.J. (2014) Metabolic Response to Sodium-Glucose Cotransporter 2 Inhibition in Type 2 Diabetic Patients. *Journal of Clinical Investigation* 124:1868.

Ferrannini, E., Baldi, S., Frascerra, S., Astiarraga, B., Heise, T., Bizzotto, R., Mari, A., Pieber, T.R. & Muscelli, E. (2016a) Shift to Fatty Substrate Utilization in Response to Sodium–Glucose Cotransporter 2 Inhibition in Subjects Without Diabetes and Patients with Type 2 Diabetes. *Diabetes* 65:1190-1195.

Ferrannini, E., Mark, M. & Mayoux, E. (2016) CV Protection in the EMPA-REG OUTCOME Trial: A "Thrifty Substrate" Hypothesis. *Diabetes Care* 39:1108-1114.

Filippi, B., Yang, C., Tang, C. & Lam, T.T. (2012) Insulin Activates Erk1/2 Signaling in the Dorsal Vagal Complex to Inhibit Glucose Production. *Cell Metabolism* 16:500-510.

Foretz, M., Colette Guichard, Pascal Ferré & Fabienne Foufelle (1999) Sterol Regulatory Element Binding Protein-1c is a Major Mediator of Insulin Action on the Hepatic Expression of Glucokinase and Lipogenesis-Related Genes. *Proceedings of the National Academy of Sciences of the United States of America* 96:12737-12742.

Fuchsberger, C., Flannick, J., Teslovich, T.M., Mahajan, A., Agarwala, V., Gaulton, K.J., Ma, C., Fontanillas, P., Moutsianas, L., Mccarthy, D.J., Rivas, M.A., Perry, J.R.B., Sim, X., Blackwell, T.W., Robertson, N.R., Rayner, N.W., Cingolani, P., Locke, A.E., Fernandez Tajes, J., ... Mccarthy, M.I. (2016) The Genetic Architecture of Type 2 Diabetes. *Nature* 536:41-47.

Gabbouj, S., Ryhänen, S., Marttinen, M., Wittrahm, R., Takalo, M., Kemppainen, S., Martiskainen, H., Tanila, H., Haapasalo, A., Hiltunen, M. & Natunen, T. (2019a) Altered Insulin Signaling in Alzheimer's Disease Brain - Special Emphasis on PI3K-Akt Pathway. *Frontiers in Neuroscience* 13:629.

Gabbouj, S., Natunen, T., Koivisto, H., Jokivarsi, K., Takalo, M., Marttinen, M., Wittrahm, R., Kemppainen, S., Naderi, R., Posado-Fernández, A., Ryhänen, S., Mäkinen, P., Paldanius, K.M.A., Doria, G., Poutiainen, P., Flores, O., Haapasalo, A., Tanila, H. & Hiltunen, M. (2019b) Intranasal Insulin Activates Akt2 Signaling Pathway in the Hippocampus of Wild-Type but Not in APP/PS1 Alzheimer Model Mice. *Neurobiology of Aging* 75:98-108.

Gancheva, S., Koliaki, C., Bierwagen, A., Nowotny, P., Heni, M., Fritsche, A., Häring, H., Szendroedi, J. & Roden, M. (2015) Effects of Intranasal Insulin on Hepatic Fat Accumulation and Energy Metabolism in Humans. *Diabetes* 64:1966-1975.

Garofalo, R.S., Orena, S.J., Rafidi, K., Torchia, A.J., Stock, J.L., Hildebrandt, A.L., Coskran, T., Black, S.C., Brees, D.J., Wicks, J.R., Mcneish, J.D. & Coleman, K.G. (2003) Severe Diabetes, Age-Dependent Loss of Adipose Tissue, and Mild Growth Deficiency in Mice Lacking Akt2/Pkbβ. *Journal of Clinical Investigation* 112:197-208.

George, S., Rochford, J.J., Wolfrum, C., Gray, S.L., Schinner, S., Wilson, J.C., Soos, M.A., Murgatroyd, P.R., Williams, R.M., Acerini, C.L., Dunger, D.B., Barford, D., Umpleby, A.M., Wareham, N.J., Davies, H.A., Schafer, A.J., Stoffel, M., O'Rahilly, S. & Barroso, I. (2004) A Family with Severe Insulin Resistance and Diabetes Due to a Mutation in AKT2. *Science* 304:1325-1328.

Giannini, C., Feldstein, A.E., Santoro, N., Kim, G., Kursawe, R., Pierpont, B. & Caprio, S. (2013) Circulating Levels of FGF-21 in Obese Youth: Associations with Liver Fat Content and Markers of Liver Damage. *Journal of Clinical Endocrinology and Metabolism* 98:2993-3000.

Gil-Lozano, M., Pérez-Tilve, D., Alvarez-Crespo, M., Martís, A., Fernandez, A.M., Catalina, P.A.F., Gonzalez-Matias, L.C. & Mallo, F. (2010) GLP-1(7-36)-Amide and Exendin-4 Stimulate the HPA Axis in Rodents and Humans. *Endocrinology* 151:2629-2640.

Gjedde, A. (1982) Calculation of Cerebral Glucose Phosphorylation from Brain Uptake of Glucose Analogs in Vivo: A Re-examination. *Brain Research* 257:237.

Glick, Z. (1982) Inverse Relationship Between Brown Fat Thermogenesis and Meal Size: The Thermostatic Control of Food Intake Revisited. *Physiology and Behavior* 29:1137-1140.

Gonzalez, E., Flier, E., Molle, D., Accili, D. & Mcgraw, T.E. (2011) Hyperinsulinemia Leads to Uncoupled Insulin Regulation of the GLUT4 Glucose Transporter and the Foxo1 Transcription Factor. *Proceedings of the National Academy of Sciences of the United States of America* 108:10162-10167.

Gonzalez, E. & Mcgraw, T.E. (2009) The Akt Kinases: Isoform Specificity in Metabolism and Cancer. *Cell Cycle* 8:2502-2508.

Goodpaster, B.H. & Sparks, L.M. (2017) Metabolic Flexibility in Health and Disease. *Cell Metabolism* 25:1027-1036.

Grams, J. & Garvey, W.T. (2015) Weight Loss and the Prevention and Treatment of Type 2 Diabetes Using Lifestyle Therapy, Pharmacotherapy, and Bariatric Surgery: Mechanisms of Action. *Current Obesity Reports* 4:287-302.

Grayson, B.E., Seeley, R.J. & Sandoval, D.A. (2013) Wired on Sugar: The Role of the CNS in the Regulation of Glucose Homeostasis. *Nature Reviews Neuroscience* 14:24-37.

Griffin, M.E., M J Marcucci, G W Cline, K Bell, N Barucci, D Lee, L J Goodyear, E W Kraegen, M F White & G I Shulman (1999) Free Fatty Acid-Induced Insulin Resistance is Associated with Activation of Protein Kinase C Theta and Alterations in the Insulin Signaling Cascade. *Diabetes* 48:1270-1274.

Guilherme, A., Henriques, F., Bedard, A.H. & Czech, M.P. (2019) Molecular Pathways Linking Adipose Innervation to Insulin Action in Obesity and Diabetes Mellitus. *Nature Reviews Endocrinology* 15:207-225.

Guthoff, M., Grichisch, Y., Canova, C., Tschritter, O., Veit, R., Hallschmid, M., HäRing, H., Preissl, H., Hennige, A.M. & Fritsche, A. (2010) Insulin Modulates Food-Related Activity in the Central Nervous System. *Journal of Clinical Endocrinology and Metabolism* 95:748-755.

Gutt, M., Davis, C.L., Spitzer, S.B., Llabre, M.M., Kumar, M., Czarnecki, E.M., Schneiderman, N., Skyler, J.S. & Marks, J.B. (2000) Validation of the Insulin Sensitivity Index (ISI 0,120): Comparison with Other Measures. *Diabetes Research and Clinical Practice* 47:177-184.

Hahn, T.M., Breininger, J.F., Baskin, D.G. & Schwartz, M.W. (1998) Coexpression of Agrp and NPY in Fasting-Activated Hypothalamic Neurons. *Nature Neuroscience* 1:271-272.

Halaas, J.L., Gajiwala, K.S., Maffei, M., Cohen, S.L., Chait, B.T., Rabinowitz, D., Lallone, R.L., Burley, S.K. & Friedman, J.M. (1995) Weight-Reducing Effects of the Plasma Protein Encoded by the Obese Gene. *Science* 269:543-546.

Hallschmid, M., Benedict, C., Schultes, B., Fehm, H., Born, J. & Kern, W. (2004) Intranasal Insulin Reduces Body Fat in Men but Not in Women. *Diabetes* 53:3024-3029.

Hamacher, K., Coenen, H.H. & Stocklin, G. (1986) Efficient Stereospecific Synthesis of No-Carrier-Added 2-[18F]-Fluoro-2-Deoxy-D-Glucose Using Aminopolyether Supported Nucleophilic Substitution. *Journal of Nuclear Medicine* 27:235.

Havrankova, J., Roth, J. & Brownstein, M. (1978) Insulin Receptors are Widely Distributed in the Central Nervous System of the Rat. *Nature* 272:827-829.

Hawley, J.A. & Lessard, S.J. (2008) Exercise Training-Induced Improvements in Insulin Action. *Acta Physiologica* 192:127-135.

Heni, M., Hennige, A.M., Peter, A., Siegel-Axel, D., Ordelheide, A., Krebs, N., Machicao, F., Fritsche, A., Häring, H. & Staiger, H. (2011) Insulin Promotes Glycogen Storage and Cell Proliferation in Primary Human Astrocytes. *Plos One* 6:E21594.

Heni, M., Kullmann, S., Ketterer, C., Guthoff, M., Linder, K., Wagner, R., Stingl, K.T., Veit, R., Staiger, H., Häring, H., Preissl, H. & Fritsche, A. (2012) Nasal Insulin Changes Peripheral Insulin Sensitivity Simultaneously with Altered Activity in Homeostatic and Reward-Related Human Brain Regions. *Diabetologia* 55:1773-1782.

Heni, M., Wagner, R., Kullmann, S., Veit, R., Mat Husin, H., Linder, K., Benkendorff, C., Peter, A., Stefan, N., Häring, H., Preissl, H. & Fritsche, A. (2014) Central Insulin Administration Improves Whole-Body Insulin Sensitivity via Hypothalamus and Parasympathetic Outputs in Men. *Diabetes* 63:4083-4088.

Heni, M., Kullmann, S., Preissl, H., Fritsche, A. & Häring, H. (2015a) Impaired Insulin Action in the Human Brain: Causes and Metabolic Consequences. *Nature Reviews Endocrinology* 11:701-711.

Heni, M., Wagner, R., Kullmann, S., Preissl, H. & Fritsche, A. (2015b) Response to Comment on Heni Et Al. Central Insulin Administration Improves Whole-Body Insulin Sensitivity via Hypothalamus and Parasympathetic Outputs in Men. Diabetes 2014;63:4083–4088. *Diabetes* 64:E8-E9.

Heni, M., Wagner, R., Kullmann, S., Gancheva, S., Roden, M., Peter, A., Stefan, N., Preissl, H., Häring, H. & Fritsche, A. (2017) Hypothalamic and Striatal Insulin Action Suppresses Endogenous Glucose Production and May Stimulate Glucose Uptake during Hyperinsulinemia in Lean but Not in Overweight Men. *Diabetes* 66:1797-1806.

Himsworth, H.P. (1936) Diabetes Mellitus: Its Differentiation into Insulin-Sensitive and Insulin-Insensitive Types. *Lancet* 227:127-130.

Hirvonen, J., Virtanen, K.A., Nummenmaa, L., Hannukainen, J.C., Honka, M., Bucci, M., Nesterov, S.V., Parkkola, R., Rinne, J., Iozzo, P. & Nuutila, P. (2011) Effects of Insulin on Brain Glucose Metabolism in Impaired Glucose Tolerance. *Diabetes* 60:443-447.

Honka, H., Mäkinen, J., Hannukainen, J., Tarkia, M., Oikonen, V., Teräs, M., Fagerholm, V., Ishizu, T., Saraste, A., Stark, C., Vähäsilta, T., Salminen, P., Kirjavainen, A., Soinio, M., Gastaldelli, A., Knuuti, J., Iozzo, P. & Nuutila, P. (2013) Validation of [18F]Fluorodeoxyglucose and Positron Emission Tomography (PET) for the Measurement of Intestinal Metabolism in Pigs, and Evidence of Intestinal Insulin Resistance in Patients with Morbid Obesity. *Diabetologia* 56:893-900.

Horton, R.W., Meldrum, B.S. & Bachelard, H.S. (1973) Enzymic and Cerebral Metabolic Effects of 2-Deoxy-D-Glucose. *Journal of Neurochemistry* 21:507-520.

Hou, J.C., Min, L. & Pessin, J.E. (2009) Insulin Granule Biogenesis, Trafficking and Exocytosis. *Vitamins and Hormones* 80:473-506.

Htike, Z.Z., Zaccardi, F., Papamargaritis, D., Webb, D.R., Khunti, K. & Davies, M.J. (2017) Efficacy and Safety of Glucagon-Like Peptide-1 Receptor Agonists in Type 2 Diabetes: A Systematic Review and Mixed-Treatment Comparison Analysis. *Diabetes, Obesity and Metabolism* 19:524-536.

Huang, S.C., Phelps, M.E., Hoffman, E.J., Sideris, K., Selin, C.J. & Kuhl, D.E. (1980) Noninvasive Determination of Local Cerebral Metabolic Rate of Glucose in Man. *American Journal of Physiology - Endocrinology and Metabolism* 238:69-82.

Hundal, R.S., M Krssak, S Dufour, D Laurent, V Lebon, V Chandramouli, S E Inzucchi, W C Schumann, K F Petersen, B R Landau & G I Shulman (2000) Mechanism by Which Metformin Reduces Glucose Production in Type 2 Diabetes. *Diabetes* 49:2063-2069.

Huovinen, V., Bucci, M., Lipponen, H., Kiviranta, R., Sandboge, S., Raiko, J., Koskinen, S., Koskensalo, K., Eriksson, J.G., Parkkola, R., Iozzo, P. & Nuutila, P. (2016) Femoral Bone Marrow Insulin Sensitivity is Increased by Resistance Training in Elderly Female Offspring of Overweight and Obese Mothers. *Plos One* 11:E0163723.

Hällsten, K., Virtanen, K.A., Lönnqvist, F., Sipilä, H., Oksanen, A., Viljanen, T., Rönnemaa, T., Viikari, J., Knuuti, J. & Nuutila, P. (2002) Rosiglitazone but Not Metformin Enhances Insulin- and Exercise-Stimulated Skeletal Muscle Glucose Uptake in Patients with Newly Diagnosed Type 2 Diabetes. *Diabetes* 51:3479-3485.

ICRP (1975) The International Commission on Radiotogical Protection. Report of the Task Group on Reference Man. A Report Prepared by a Task Group of Committee 2 of the International Commission on Radiological Protection. *Annals of the ICRP/ICRP Publication* 23.

Inoue, H., Ogawa, W., Asakawa, A., Okamoto, Y., Nishizawa, A., Matsumoto, M., Teshigawara, K., Matsuki, Y., Watanabe, E., Hiramatsu, R., Notohara, K., Katayose, K., Okamura, H., Kahn, C.R., Noda, T., Takeda, K., Akira, S., Inui, A. & Kasuga, M. (2006) Role of Hepatic STAT3 in Brain-Insulin Action on Hepatic Glucose Production. *Cell Metabolism* 3:267-275.

International Diabetes Federation. (2019) IDF Diabetes Atlas, Ninth Edition. Brussels, Belgium. <Http://Www.Diabetesatlas.Org> Cited 28.2.2020.

Iozzo, P., Pratipanawatr, T., Pijl, H., Vogt, C., Kumar, V., Pipek, R., Matsuda, M., Mandarino, L.J., Cusi, K.J. & Defronzo, R.A. (2001) Physiological Hyperinsulinemia Impairs Insulin-Stimulated Glycogen Synthase Activity and Glycogen Synthesis. *American Journal of Physiology - Endocrinology and Metabolism* 280:712-719.

Iozzo, P., Gastaldelli, A., Jarvisalo, M.J., Kiss, J., Borra, R., Buzzigoli, E., Viljanen, A., Naum, G., Viljanen, T., Oikonen, V., Knuuti, J., Savunen, T., Salvadori, P.A., Ferrannini, E. & Nuutila, P. (2006) 18F-FDG Assessment of Glucose Disposal and Production Rates during Fasting and Insulin Stimulation: A Validation Study. *Journal of Nuclear Medicine* 47:1016.

Iozzo, P., Jarvisalo, M.J., Kiss, J., Borra, R., Naum, G.A., Viljanen, A., Viljanen, T., Gastaldelli, A., Buzzigoli, E., Guiducci, L., Barsotti, E., Savunen, T., Knuuti, J., Haaparanta–Solin, M., Ferrannini, E. & Nuutila, P. (2007) Quantification of Liver Glucose Metabolism by Positron Emission Tomography: Validation Study in Pigs. *Gastroenterology* 132:531-542.

Iozzo, P. & Guzzardi, M.A. (2019) Imaging of Brain Glucose Uptake by PET in Obesity and Cognitive Dysfunction: Life-Course Perspective. *Endocrine Connections* 8:R169-R183.

Ito, D., Shimizu, S., Inoue, K., Saito, D., Yanagisawa, M., Inukai, K., Akiyama, Y., Morimoto, Y., Noda, M. & Shimada, A. (2017) Comparison of Ipragliflozin and Pioglitazone Effects on Nonalcoholic Fatty Liver Disease in Patients with Type 2 Diabetes: A Randomized, 24-Week, Open-Label, Active-Controlled Trial. *Diabetes Care* 40:1364-1372.

Iwen, K.A., Scherer, T., Heni, M., Sayk, F., Wellnitz, T., Machleidt, F., Preissl, H., Häring, H., Fritsche, A., Lehnert, H., Buettner, C. & Hallschmid, M. (2014) Intranasal Insulin Suppresses Systemic but Not Subcutaneous Lipolysis in Healthy Humans. *Journal of Clinical Endocrinology and Metabolism* 99:E246-E251.

Janssen, B., Vugts, D.J., Funke, U., Molenaar, G.T., Kruijer, P.S., Van Berckel, B.N.M., Lammertsma, A.A. & Windhorst, A.D. (2016) Imaging of Neuroinflammation in Alzheimer's Disease, Multiple Sclerosis and Stroke: Recent Developments in Positron Emission Tomography. *BBA - Molecular Basis of Disease* 1862:425-441.

Jansson, P.A., Larsson, A., Smith, U. & Lönnroth, P. (1992) Glycerol Production in Subcutaneous Adipose Tissue in Lean and Obese Humans. *Journal of Clinical Investigation* 89:1610-1617.

Jauch-Chara, K., Friedrich, A., Rezmer, M., Melchert, U.H., G Scholand-Engler, H., Hallschmid, M. & Oltmanns, K.M. (2012) Intranasal Insulin Suppresses Food Intake via Enhancement of Brain Energy Levels in Humans. *Diabetes* 61:2261-2268.

Jeong, J.Y., Jeoung, N.H., Park, K. & Lee, I. (2012) Transcriptional Regulation of Pyruvate Dehydrogenase Kinase. *Diabetes and Metabolism* 36:328-335.

Jiang, S., Yan, C., Fang, Q., Shao, M., Zhang, Y., Liu, Y., Deng, Y., Shan, B., Liu, J., Li, H., Yang, L., Zhou, J., Dai, Z., Liu, Y. & Jia, W. (2014) Fibroblast Growth Factor 21 is Regulated by the IRE1α-XBP1 Branch of the Unfolded Protein Response and Counteracts Endoplasmic Reticulum Stress-Induced Hepatic Steatosis. *Journal of Biological Chemistry* 289:29751-29765.

Jiang, Y., Wang, Z., Ma, B., Fan, L., Yi, N., Lu, B., Wang, Q. & Liu, R. (2018) GLP-1 Improves Adipocyte Insulin Sensitivity Following Induction of Endoplasmic Reticulum Stress. *Frontiers in Pharmacology* 9:1168.

Kashyap, S.R., Belfort, R., Berria, R., Suraamornkul, S., Pratipranawatr, T., Finlayson, J., Barrentine, A., Bajaj, M., Mandarino, L., Defronzo, R.A. & Cusi, K. (2004) Discordant Effects of a Chronic Physiological Increase in Plasma FFA on Insulin Signaling in Healthy Subjects with or Without a Family History of Type 2 Diabetes. *American Journal of Physiology - Endocrinology and Metabolism* 287:537-546.

Katz, A., Nambi, S.S., Mather, K., Baron, A.D., Follmann, D.A., Sullivan, G. & Quon, M.J. (2000) Quantitative Insulin Sensitivity Check Index: A Simple, Accurate Method for Assessing Insulin Sensitivity in Humans. *Journal of Clinical Endocrinology and Metabolism* 85:2402-2410.

Kelley, D.E., Mokan, M., Simoneau, J.A. & Mandarino, L.J. (1993) Interaction between Glucose and Free Fatty Acid Metabolism in Human Skeletal Muscle. *Journal of Clinical Investigation* 92:91-98.

Ketterer, C., Heni, M., Thamer, C., Herzberg-Schäfer, S.A., Häring, H. & Fritsche, A. (2011) Acute, Short-Term Hyperinsulinemia Increases Olfactory Threshold in Healthy Subjects. *International Journal of Obesity* 35:1135-1138.

Kieffer, T.J., Heller, R.S., Leech, C.A., Holz, G.G. & Habener, J.F. (1997) Leptin Suppression of Insulin Secretion by the Activation of ATP-Sensitive K+ Channels in Pancreatic Beta-Cells. *Diabetes* 46:1087-1093.

Kim, K., Seeley, R.J. & Sandoval, D.A. (2018) Signalling from the Periphery to the Brain That Regulates Energy Homeostasis. *Nature Reviews Neuroscience* 19:185-196.

King, G.L. & Johnson, S.M. (1985) Receptor-Mediated Transport of Insulin across Endothelial Cells. *Science* 227:1583-1586.

Kishore, P., Boucai, L., Zhang, K., Li, W., Koppaka, S., Kehlenbrink, S., Schiwek, A., Esterson, Y.B., Mehta, D., Bursheh, S., Su, Y., Gutierrez-Juarez, R., Muzumdar, R., Schwartz, G.J. & Hawkins, M. (2012) Activation of KATP Channels Suppresses Glucose Production in Humans. *Journal of Clinical Investigation* 122:2326.

Kleinridders, A., Ferris, H.A., Cai, W. & Kahn, C.R. (2014) Insulin Action in Brain Regulates Systemic Metabolism and Brain Function. *Diabetes* 63:2232-2243.

Knowler, W.C., Barrett-Connor, E., Fowler, S.E., Hamman, R.F., Lachin, J.M., Walker, E.A., Nathan, D.M. & Diabetes Prevention Program Research Group. (2002) Reduction in the Incidence of Type 2 Diabetes with Lifestyle Intervention or Metformin. *New England Journal of Medicine* 346:393-403.

Koch, L., Wunderlich, F.T., Seibler, J., Könner, A.C., Hampel, B., Irlenbusch, S., Brabant, G., Kahn, C.R., Schwenk, F. & Brüning, J.C. (2008) Central Insulin Action Regulates Peripheral Glucose and Fat Metabolism in Mice. *Journal of Clinical Investigation* 118:2132-2147.

Koliaki, C., Szendroedi, J., Kaul, K., Jelenik, T., Nowotny, P., Jankowiak, F., Herder, C., Carstensen, M., Krausch, M., Knoefel, W., Schlensak, M. & Roden, M. (2015) Adaptation of Hepatic Mitochondrial Function in Humans with Non-Alcoholic Fatty Liver is Lost in Steatohepatitis. *Cell Metabolism* 21:739-746.

Könner, A.C., Janoschek, R., Plum, L., Jordan, S.D., Rother, E., Ma, X., Xu, C., Enriori, P., Hampel, B., Barsh, G.S., Kahn, C.R., Cowley, M.A., Ashcroft, F.M. & Brüning, J.C. (2007) Insulin Action in Agrp-Expressing Neurons is Required for Suppression of Hepatic Glucose Production. *Cell Metabolism* 5:438-449.

Koopmans, S.J., Kushwaha, R.S. & Defronzo, R.A. (1999) Chronic Physiologic Hyperinsulinemia Impairs Suppression of Plasma Free Fatty Acids and Increases De Novo Lipogenesis but Does Not Cause Dyslipidemia in Conscious Normal Rats. *Metabolism* 48:330-337.

Koren, S., Dipilato, L., Emmett, M., Shearin, A., Chu, Q., Monks, B. & Birnbaum, M. (2015) The Role of Mouse Akt2 in Insulin-Dependent Suppression of Adipocyte Lipolysis in Vivo. *Diabetologia* 58:1063-1070.

Krings, A., Rahman, S., Huang, S., Lu, Y., Czernik, P.J. & Lecka-Czernik, B. (2012) Bone Marrow Fat Has Brown Adipose Tissue Characteristics, Which are Attenuated with Aging and Diabetes. *Bone* 50:546-552.

Krssak, M., Brehm, A., Bernroider, E., Anderwald, C., Nowotny, P., Dalla Man, C., Cobelli, C., Cline, G.W., Shulman, G.I., Waldhäusl, W. & Roden, M. (2004) Alterations in Postprandial Hepatic Glycogen Metabolism in Type 2 Diabetes. *Diabetes* 53:3048-3056.

Kuchay, M.S., Krishan, S., Mishra, S.K., Farooqui, K.J., Singh, M.K., Wasir, J.S., Bansal, B., Kaur, P., Jevalikar, G., Gill, H.K., Choudhary, N.S. & Mithal, A. (2018) Effect of Empagliflozin on Liver Fat in Patients with Type 2 Diabetes and Nonalcoholic Fatty Liver Disease: A Randomized Controlled Trial (E-LIFT Trial). *Diabetes Care* 41:1801-1808.

Kullberg, J., Johansson, L., Ahlström, H., Courivaud, F., Koken, P., Eggers, H. & Börnert, P. (2009) Automated Assessment of Whole-Body Adipose Tissue Depots from Continuously Moving Bed MRI: A Feasibility Study. *Journal of Magnetic Resonance Imaging* 30:185-193.

Kullmann, S., Heni, M., Veit, R., Scheffler, K., Machann, J., Häring, H., Fritsche, A., & Preissl, H. (2015). Selective Insulin Resistance in Homeostatic and Cognitive Control Brain Areas in Overweight and Obese Adults. *Diabetes Care* 38(6):1044-1050.

Kullmann, S., Fritsche, A., Wagner, R., Schwab, S., Häring, H., Preissl, H., & Heni, M. (2017). Hypothalamic Insulin Responsiveness is Associated with Pancreatic Insulin Secretion in Humans. *Physiology and Behavior* 176:134-138.

Laakso, M., Kuusisto, J., Stančáková, A., Kuulasmaa, T., Pajukanta, P., Lusis, A.J., Collins, F.S., Mohlke, K.L. & Boehnke, M. (2017) The Metabolic Syndrome in Men Study: A Resource for Studies of Metabolic and Cardiovascular Diseases. *Journal of Lipid Research* 58:481-493.

Lacroix, M., Badonnel, K., Meunier, N., Tan, F., Poupon, C.S., Durieux, D., Monnerie, R., Baly, C., Congar, P., Salesse, R. & Caillol, M. (2008) Expression of Insulin System in the Olfactory Epithelium: First Approaches to Its Role and Regulation. *Journal of Neuroendocrinology* 20:1176-1190.

Lanz, B., Gruetter, R. & Duarte, J.M.N. (2013) Metabolic Flux and Compartmentation Analysis in the Brain in Vivo. *Frontiers in Endocrinology* 4:1.

Leavens, K.F., Easton, R.M., Shulman, G.I., Previs, S.F. & Birnbaum, M.J. (2009) Akt2 is Required for Hepatic Lipid Accumulation in Models of Insulin Resistance. *Cell Metabolism* 10:405-418.

Lee, Y.S., Kim, J., Osborne, O., Oh, D.Y., Sasik, R., Schenk, S., Chen, A., Chung, H., Murphy, A., Watkins, S.M., Quehenberger, O., Johnson, R.S. & Olefsky, J.M. (2014) Increased Adipocyte O2 Consumption Triggers HIF-1α, Causing Inflammation and Insulin Resistance in Obesity. *Cell* 157:1339-1352.

Leto, D. & Saltiel, A.R. (2012) Regulation of Glucose Transport by Insulin: Traffic Control of GLUT4. *Nature Reviews Molecular Cell Biology* 13:383-396.

Li, X., Monks, B., Ge, Q. & Birnbaum, M.J. (2007) Akt/PKB Regulates Hepatic Metabolism by Directly Inhibiting PGC-1α Transcription Coactivator. *Nature* 447:1012-1016.

Li, Y., Schnabl, K., Gabler, S., Willershäuser, M., Reber, J., Karlas, A., Laurila, S., Lahesmaa, M., U Din, M., Bast-Habersbrunner, A., Virtanen, K.A., Fromme, T., Bolze, F., O'Farrell, L.S., Alsina-Fernandez, J., Coskun, T., Ntziachristos, V., Nuutila, P. & Klingenspor, M. (2018) Secretin-Activated Brown Fat Mediates Prandial Thermogenesis to Induce Satiation. *Cell* 175:1561-1574.E12.

List, J.F., Woo, V., Morales, E., Tang, W. & Fiedorek, F.T. (2009) Sodium-Glucose Cotransport Inhibition with Dapagliflozin in Type 2 Diabetes. *Diabetes Care* 32:650-657.

Lopaschuk, G.D., Ussher, J.R., Folmes, C.D.L., Jaswal, J.S. & Stanley, W.C. (2010) Myocardial Fatty Acid Metabolism in Health and Disease. *Physiological Reviews* 90:207-258.

Lorenzo, C., Haffner, S. M., Stančáková, A., Kuusisto, J., & Laakso, M. (2015). Fasting and OGTT-Derived Measures of Insulin Resistance as Compared with the Euglycemic-Hyperinsulinemic Clamp in Nondiabetic Finnish Offspring of Type 2 Diabetic Individuals. *Journal of Clinical Endocrinology and Metabolism,* 100(2), 544-550.

Lundkvist, P., Pereira, M.J., Kamble, P.G., Katsogiannos, P., Langkilde, A.M., Esterline, R., Johnsson, E. & Eriksson, J.W. (2019) Glucagon Levels during Short-Term SGLT2 Inhibition are Largely Regulated by Glucose Changes in Patients with Type 2 Diabetes. *Journal of Clinical Endocrinology and Metabolism* 104:193-201.

Lundqvist, M.H., Almby, K., Abrahamsson, N. & Eriksson, J.W. (2019) Is the Brain a Key Player in Glucose Regulation and Development of Type 2 Diabetes? *Frontiers in Physiology* 10:457.

Lönnroth, P., Jansson, P.A. & Smith, U. (1987) A Microdialysis Method Allowing Characterization of Intercellular Water Space in Humans. *American Journal of Physiology - Endocrinology and Metabolism* 253:228-231.

Mahajan, A., Taliun, D., Thurner, M., Robertson, N. R., Torres, J. M., Rayner, N. W., Payne, A. J., Steinthorsdottir, V., Scott, R. A., Grarup, N., Cook, J. P., Schmidt, E. M., Wuttke, M., Sarnowski, C., Mägi, R., Nano, J., Gieger, C., Trompet, S., Lecoeur, C., . . ., Mccarthy M., I. (2018). Fine-

Mapping Type 2 Diabetes Loci to Single-Variant Resolution Using High-Density Imputation and Islet-Specific Epigenome Maps. *Nature Genetics* 50(11), 1505-1513.

Malmberg, F., Nordenskjöld, R., Strand, R. & Kullberg, J. (2017) Smartpaint: A Tool for Interactive Segmentation of Medical Volume Images. *Computer Methods in Biomechanics and Biomedical Engineering: Imaging and Visualization* 5:36-44.

Manning, A., Highland, H.M., Gasser, J., Sim, X., Tukiainen, T., Fontanillas, P., Grarup, N., Rivas, M.A., Mahajan, A., Locke, A.E., Cingolani, P., Pers, T.H., Viñuela, A., Brown, A.A., Wu, Y., Flannick, J., Fuchsberger, C., Gamazon, E.R., Gaulton, K.J., ... Lindgren, C.M. (2017) A Low-Frequency Inactivating AKT2 Variant Enriched in the Finnish Population is Associated with Fasting Insulin Levels and Type 2 Diabetes Risk. *Diabetes* 66:2019-2032.

Marcus, C., Mena, E. & Subramaniam, R.M. (2014) Brain PET in the Diagnosis of Alzheimer's Disease. *Clinical Nuclear Medicine* 39:E413-6.

Margolis, R.U. & Altszuler, N. (1967) Insulin in the Cerebrospinal Fluid. *Nature* 215:1375-1376.

Mari, A., Pacini, G., Murphy, E., Ludvik, B. & Nolan, J.J. (2001) A Model-Based Method for Assessing Insulin Sensitivity from the Oral Glucose Tolerance Test. *Diabetes Care* 24:539-548.

Mason, S. (2017) Lactate Shuttles in Neuroenergetics—Homeostasis, Allostasis and Beyond. *Frontiers in Neuroscience* 11:43.

Matsuba, R., Matsuba, I., Shimokawa, M., Nagai, Y. & Tanaka, Y. (2018) Tofogliflozin Decreases Body Fat Mass and Improves Peripheral Insulin Resistance. *Diabetes, Obesity and Metabolism* 20:1311-1315.

Matsuda, M. & Defronzo, R.A. (1999) Insulin Sensitivity Indices Obtained from Oral Glucose Tolerance Testing: Comparison with the Euglycemic Insulin Clamp. *Diabetes Care* 22:1462-1470.

Matthews, D., Hosker, J., Rudenski, A., Naylor, B., Treacher, D. & Turner, R. (1985) Homeostasis Model Assessment: Insulin Resistance and B-Cell Function from Fasting Plasma Glucose and Insulin Concentrations in Man. *Diabetologia* 28:412-419.

Mayerson, A.B., Hundal, R.S., Dufour, S., Lebon, V., Befroy, D., Cline, G.W., Enocksson, S., Inzucchi, S.E., Shulman, G.I. & Petersen, K.F. (2002) The Effects of Rosiglitazone on Insulin Sensitivity, Lipolysis, and Hepatic and Skeletal Muscle Triglyceride Content in Patients with Type 2 Diabetes. *Diabetes* 51:797-802.

Mazucanti, C.H., Liu, Q., Lang, D., Huang, N., O'Connell, J.F., Camandola, S. & Egan, J.M. (2019) Release of Insulin Produced by the Choroid Plexus is Regulated by Serotonergic Signaling. *JCI Insight* 4.

Merovci, A., Solis-Herrera, C., Daniele, G., Eldor, R., Fiorentino, T.V., Tripathy, D., Xiong, J., Perez, Z., Norton, L., Abdul-Ghani, M.A. & Defronzo, R.A. (2014) Dapagliflozin Improves Muscle Insulin Sensitivity but Enhances Endogenous Glucose Production. *Journal of Clinical Investigation* 124:509-514.

Merovci, A., Abdul-Ghani, M., Mari, A., Solis-Herrera, C., Xiong, J., Daniele, G., Tripathy, D. & Defronzo, R.A. (2016) Effect of Dapagliflozin with and Without Acipimox on Insulin Sensitivity and Insulin Secretion in T2DM Males. *Journal of Clinical Endocrinology and Metabolism* 101:1249-1256.

Mohamed-Ali, V., Goodrick, S., Rawesh, A., Katz, D.R., Miles, J.M., Yudkin, J.S., Klein, S. & Coppack, S.W. (1997) Subcutaneous Adipose Tissue Releases Interleukin-6, but Not Tumor Necrosis Factor-Alpha, in Vivo. *Journal of Clinical Endocrinology and Metabolism* 82:4196.

Mudaliar, S., Henry, R.R., Boden, G., Smith, S., Chalamandaris, A., Duchesne, D., Iqbal, N. & List, J. (2014) Changes in Insulin Sensitivity and Insulin Secretion with the Sodium Glucose Cotransporter 2 Inhibitor Dapagliflozin. *Diabetes Technology and Therapeutics* 16:137-144.

Mueller, W.M., Gregoire, F.M., Stanhope, K.L., Mobbs, C.V., Mizuno, T.M., Warden, C.H., Stern, J.S. & Havel, P.J. (1998) Evidence That Glucose Metabolism Regulates Leptin Secretion from Cultured Rat Adipocytes. *Endocrinology* 139:551.

Musso, G., Cassader, M., Rosina, F. & Gambino, R. (2012) Impact of Current Treatments on Liver Disease, Glucose Metabolism and Cardiovascular Risk in Non-Alcoholic Fatty Liver Disease (NAFLD): A Systematic Review and Meta-Analysis of Randomised Trials. *Diabetologia* 55:885-904.

Mäki, M.T., Haaparanta, M., Nuutila, P., Oikonen, V., Luolahti, M., Eskola, O. & Knuuti, J.M. (1998) Free Fatty Acid Uptake in the Myocardium and Skeletal Muscle Using Fluorine-18-Fluoro-6-Thia-Heptadecanoic Acid. *Journal of Nuclear Medicine* 39:1320.

Nguyen, N.C., Vercher-Conejero, J.L., Sattar, A., Miller, M.A., Maniawski, P.J., Jordan, D.W., Muzic, J., Raymond F, Su, K., O'Donnell, J.K. & Faulhaber, P.F. (2015) Image Quality and Diagnostic Performance of a Digital PET Prototype in Patients with Oncologic Diseases: Initial Experience and Comparison with Analog PET. *Journal of Nuclear Medicine* 56:1378-1385.

Nuutila, P., Koivisto, V.A., Knuuti, J., Ruotsalainen, U., Teräs, M., Haaparanta, M., Bergman, J., Solin, O., Voipio-Pulkki, L.M. & Wegelius, U. (1992) Glucose-Free Fatty Acid Cycle Operates in Human Heart and Skeletal Muscle in Vivo. *Journal of Clinical Investigation* 89:1767-1774.

Obici, S., Zhang, B.B., Karkanias, G. & Rossetti, L. (2002) Hypothalamic Insulin Signaling is Required for Inhibition of Glucose Production. *Nature Medicine* 8:1376-1382.

Ohn, J.H., MD, Kwak, S.H., MD, Cho, Y.M., MD, Lim, S., MD, Jang, H.C., Prof, Park, K.S., Prof & Cho, N.H., Prof (2016) 10-Year Trajectory of B-Cell Function and Insulin Sensitivity in the Development of Type 2 Diabetes: A Community-Based Prospective Cohort Study. *Lancet Diabetes and Endocrinology* 4:27-34.

Oikonen, V. (2018) Fractional Uptake Rate (FUR). Retrieved from <Http://Www.Turkupetcentre.Net/Petanalysis/Model_Fur.Html> Cited 15.11.2019.

Oikonen, V. (2019) Multiple Time Graphical Analysis (MTGA). Retrieved from <Http://Www.Turkupetcentre.Net/Petanalysis/Model_Mtga.Html> Cited 27.4.2020.

Orava, J., Nuutila, P., Lidell, M., Oikonen, V., Noponen, T., Viljanen, T., Scheinin, M., Taittonen, M., Niemi, T., Enerbäck, S. & Virtanen, K. (2011) Different Metabolic Responses of Human Brown Adipose Tissue to Activation by Cold and Insulin. *Cell Metabolism* 14:272-279.

Orava, J., Nuutila, P., Noponen, T., Parkkola, R., Viljanen, T., Enerbäck, S., Rissanen, A., Pietiläinen, K.H. & Virtanen, K.A. (2013) Blunted Metabolic Responses to Cold and Insulin Stimulation in Brown Adipose Tissue of Obese Humans. *Obesity* 21:2279-2287.

Otten, J., Ahrén, B. & Olsson, T. (2014) Surrogate Measures of Insulin Sensitivity vs the Hyperinsulinaemic–Euglycaemic Clamp: A Meta-Analysis. *Diabetologia* 57:1781-1788.

Pan, X.R., Li, G.W., Hu, Y.H., Wang, J.X., Yang, W.Y., An, Z.X., Hu, Z.X., Lin, J., Xiao, J.Z., Cao, H.B., Liu, P.A., Jiang, X.G., Jiang, Y.Y., Wang, J.P., Zheng, H., Zhang, H., Bennett, P.H. & Howard, B.V. (1997) Effects of Diet and Exercise in Preventing NIDDM in People with Impaired Glucose Tolerance. The Da Qing IGT and Diabetes Study. *Diabetes Care* 20:537-544.

Pardridge, W.M., R J Boado & C R Farrell (1990) Brain-Type Glucose Transporter (GLUT-1) is Selectively Localized to the Blood-Brain Barrier. Studies with Quantitative Western Blotting and in Situ Hybridization. *Journal of Biological Chemistry* 265:18035.

Pasarica, M., Sereda, O.R., Redman, L.M., Albarado, D.C., Hymel, D.T., Roan, L.E., Rood, J.C., Burk, D.H. & Smith, S.R. (2009) Reduced Adipose Tissue Oxygenation in Human Obesity: Evidence for Rarefaction, Macrophage Chemotaxis, and Inflammation Without an Angiogenic Response. *Diabetes* 58:718-725.

Paternostro, G., Camici, P.G., Lammerstma, A.A., Marinho, N., Baliga, R.R., Kooner, J.S., Radda, G.K. & Ferrannini, E. (1996) Cardiac and Skeletal Muscle Insulin Resistance in Patients with Coronary Heart Disease. a Study with Positron Emission Tomography. *Journal of Clinical Investigation* 98:2094-2099.

Patlak, C.S., Blasberg, R.G. & Fenstermacher, J.D. (1983) Graphical Evaluation of Blood-To-Brain Transfer Constants from Multiple-Time Uptake Data. *Journal of Cerebral Blood Flow and Metabolism* 3:1-7.

Patlak, C.S. & Blasberg, R.G. (1985) Graphical Evaluation of Blood-To-Brain Transfer Constants from Multiple-Time Uptake Data. Generalizations. *Journal of Cerebral Blood Flow and Metabolism* 5:584-590.

Pellerin, L. & Magistretti, P.J. (1994) Glutamate Uptake into Astrocytes Stimulates Aerobic Glycolysis: A Mechanism Coupling Neuronal Activity to Glucose Utilization. *Proceedings of the National Academy of Sciences of the United States of America* 91:10625-10629.

Peltoniemi, P., Lönnroth, P., Laine, H., Oikonen, V., Tolvanen, T., Grönroos, T., Strindberg, L., Knuuti, J. & Nuutila, P. (2000) Lumped Constant for [18F]Fluorodeoxyglucose in Skeletal Muscles of

Obese and Nonobese Humans. *American Journal of Physiology - Endocrinology and Metabolism* 279:1122-1130.

Perrin, C., Knauf, C. & Burcelin, R. (2004) Intracerebroventricular Infusion of Glucose, Insulin, and the Adenosine Monophosphate-Activated Kinase Activator, 5-Aminoimidazole-4-Carboxamide-1-B-D-Ribofuranoside, Controls Muscle Glycogen Synthesis. *Endocrinology* 145:4025-4033.

Perry, R., Camporez, J., Kursawe, R., Titchenell, P., Zhang, D., Perry, C., Jurczak, M., Abudukadier, A., Han, M., Zhang, X., Ruan, H., Yang, X., Caprio, S., Kaech, S., Sul, H., Birnbaum, M., Davis, R., Cline, G., Petersen, K. & Shulman, G. (2015) Hepatic Acetyl Coa Links Adipose Tissue Inflammation to Hepatic Insulin Resistance and Type 2 Diabetes. *Cell* 160:745-758.

Perseghin, G., Regalia, E., Battezzati, A., Vergani, S., Pulvirenti, A., Terruzzi, I., Baratti, D., Bozzetti, F., Mazzaferro, V. & Luzi, L. (1997a) Regulation of Glucose Homeostasis in Humans with Denervated Livers. *Journal of Clinical Investigation* 100:931-941.

Perseghin, G., Caumo, A., Caloni, M., Testolin, G. & Luzi, L. (2001) Incorporation of the Fasting Plasma FFA Concentration into QUICKI Improves Its Association with Insulin Sensitivity in Nonobese Individuals. *Journal of Clinical Endocrinology and Metabolism* 86:4776-4781.

Perseghin, G., Ghosh, S., Gerow, K. & Shulman, G.I. (1997b) Metabolic Defects in Lean Nondiabetic Offspring of NIDDM Parents: A Cross-Sectional Study. *Diabetes* 46:1001-1009.

Phelps, M.E., Huang, S.C., Hoffman, E.J., Selin, C., Sokoloff, L. & Kuhl, D.E. (1979) Tomographic Measurement of Local Cerebral Glucose Metabolic Rate in Humans with (F-18)2-Fluoro-2-Deoxy-D-Glucose: Validation of Method. *Annals of Neurology* 6:371-388.

Plomgaard, P., Hansen, J.S., Ingerslev, B., Clemmesen, J.O., Secher, N.H., Van Hall, G., Fritsche, A., Weigert, C., Lehmann, R., Häring, H. & Heni, M. (2019) Nasal Insulin Administration Does Not Affect Hepatic Glucose Production at Systemic Fasting Insulin Levels. *Diabetes, Obesity and Metabolism* 21:993-1000.

Pocai, A., Lam, T.K.T., Gutierrez-Juarez, R., Obici, S., Schwartz, G.J., Bryan, J., Aguilar-Bryan, L. & Rossetti, L. (2005) Hypothalamic KATP Channels Control Hepatic Glucose Production. *Nature* 434:1026-1031.

Van Der Poorten, D., Milner, K., Hui, J., Hodge, A., Trenell, M.I., Kench, J.G., London, R., Peduto, T., Chisholm, D.J. & George, J. (2008) Visceral Fat: A Key Mediator of Steatohepatitis in Metabolic Liver Disease. *Hepatology* 48:449-457.

Porte, D., Baskin, D.G. & Schwartz, M.W. (2002) Leptin and Insulin Action in the Central Nervous System. *Nutrition Reviews* 60:S20-S29.

Puigserver, P., Rhee, J., Donovan, J., Walkey, C.J., Yoon, J.C., Oriente, F., Kitamura, Y., Altomonte, J., Dong, H., Accili, D. & Spiegelman, B.M. (2003) Insulin-Regulated Hepatic Gluconeogenesis through FOXO1-PGC-1alpha Interaction. *Nature* 423:550.

Qiang, G., Whang Kong, H., Xu, S., Pham, H.A., Parlee, S.D., Burr, A.A., Gil, V., Pang, J., Hughes, A., Gu, X., Fantuzzi, G., Macdougald, O.A. & Liew, C.W. (2016) Lipodystrophy and Severe Metabolic Dysfunction in Mice with Adipose Tissue-Specific Insulin Receptor Ablation. *Molecular Metabolism* 5:480-490.

Qiu, J., Zhang, C., Borgquist, A., Nestor, C., Smith, A., Bosch, M., Ku, S., Wagner, E., Rønnekleiv, O. & Kelly, M. (2014) Insulin Excites Anorexigenic Proopiomelanocortin Neurons via Activation of Canonical Transient Receptor Potential Channels. *Cell Metabolism* 19:682-693.

Radziuk, J. (2000) Insulin Sensitivity and Its Measurement: Structural Commonalities among the Methods. *Journal of Clinical Endocrinology and Metabolism* 85:4426-4433.

Rahmouni, K., Morgan, D.A., Morgan, G.M., Liu, X., Sigmund, C.D., Mark, A.L. & Haynes, W.G. (2004) Hypothalamic PI3K and MAPK Differentially Mediate Regional Sympathetic Activation to Insulin. *Journal of Clinical Investigation* 114:652-658.

Ramnanan, C.J., Saraswathi, V., Smith, M.S., Donahue, E.P., Farmer, B., Farmer, T.D., Neal, D., Williams, P.E., Lautz, M., Mari, A., Cherrington, A.D. & Edgerton, D.S. (2011) Brain Insulin Action Augments Hepatic Glycogen Synthesis Without Suppressing Glucose Production or Gluconeogenesis in Dogs. *Journal of Clinical Investigation* 121:3713-3723.

Ramnanan, C., Edgerton, D. & Cherrington, A. (2012) Evidence Against a Physiologic Role for Acute Changes in CNS Insulin Action in the Rapid Regulation of Hepatic Glucose Production. *Cell Metabolism* 15:656-664.

Ramnanan, C.J., Kraft, G., Smith, M.S., Farmer, B., Neal, D., Williams, P.E., Lautz, M., Farmer, T., Donahue, E.P., Cherrington, A.D. & Edgerton, D.S. (2013) Interaction Between the Central and Peripheral Effects of Insulin in Controlling Hepatic Glucose Metabolism in the Conscious Dog. *Diabetes* 62:74-84.

Ratib, O., Phelps, M.E., Huang, S., Henze, E., Selin, C.E. & Schelbert, H.R. (1982) Positron Tomography with Deoxyglucose for Estimating Local Myocardial Glucose Metabolism. *Journal of Nuclear Medicine* 23:577.

Rebelos, E., Immonen, H., Bucci, M., Hannukainen, J.C., Nummenmaa, L., Honka, M., Soinio, M., Salminen, P., Ferrannini, E., Iozzo, P. & Nuutila, P. (2019) Brain Glucose Uptake is Associated with Endogenous Glucose Production in Obese Patients Before and After Bariatric Surgery and Predicts Metabolic Outcome at Follow-Up. *Diabetes, Obesity and Metabolism* 21:218-226.

Reeder, S.B., Hu, H.H. & Sirlin, C.B. (2012) Proton Density Fat-Fraction: A Standardized MR-Based Biomarker of Tissue Fat Concentration. *Journal of Magnetic Resonance Imaging* 36:1011-1014.

Renner, D.B., Svitak, A.L., Gallus, N.J., Ericson, M.E., Frey, W.H. & Hanson, L.R. (2012) Intranasal Delivery of Insulin via the Olfactory Nerve Pathway. *Journal of Pharmacy and Pharmacology* 64:1709-1714.

Reno, C.M., Puente, E.C., Sheng, Z., Daphna-Iken, D., Bree, A.J., Routh, V.H., Kahn, B.B. & Fisher, S.J. (2017) Brain GLUT4 Knockout Mice Have Impaired Glucose Tolerance, Decreased Insulin Sensitivity, and Impaired Hypoglycemic Counterregulation. *Diabetes* 66:587-597.

Rizza, R.A., Mandarino, L.J. & Gerich, J.E. (1981) Dose-Response Characteristics for Effects of Insulin Onproduction and Utilization of Glucose in Man. *American Journal of Physiology* 240:630.

Roach, P.J., Depaoli-Roach, A.A., Hurley, T.D. & Tagliabracci, V.S. (2012) Glycogen and Its Metabolism: Some New Developments and Old Themes. *Biochemical Journal* 441:763-787.

Roberts, C.K., Hevener, A.L. & Barnard, R.J. (2013) Metabolic Syndrome and Insulin Resistance: Underlying Causes and Modification by Exercise Training. *Comprehensive Physiology* 3:1-58.

Roden, M. & Shulman, G.I. (2019) The Integrative Biology of Type 2 Diabetes. *Nature* 576:51-60.

Romijn, J.A., Coyle, E.F., Sidossis, L.S., Gastaldelli, A., Horowitz, J.F., Endert, E. & Wolfe, R.R. (1993) Regulation of Endogenous Fat and Carbohydrate Metabolism in Relation to Exercise Intensity and Duration. *American Journal of Physiology - Endocrinology and Metabolism* 265:380.

Rossetti, L., Giaccari, A. & Defronzo, R.A. (1990) Glucose Toxicity. *Diabetes Care* 13:610-630.

Rui, L. (2014) Energy Metabolism in the Liver. *Comprehensive Physiology* 4:177-197.

Rutter, G.A., Pullen, T.J., Hodson, D.J. & Martinez-Sanchez, A. (2015) Pancreatic B-Cell Identity, Glucose Sensing and the Control of Insulin Secretion. *Biochemical Journal* 466:203-218.

Ryu, V., Garretson, J.T., Liu, Y., Vaughan, C.H. & Bartness, T.J. (2015) Brown Adipose Tissue Has Sympathetic-Sensory Feedback Circuits. *Journal of Neuroscience* 35:2181-2190.

Saad, M.F., R L Anderson, a Laws, R M Watanabe, W W Kades, Y D Chen, R E Sands, D Pei, P J Savage & R N Bergman (1994) A Comparison Between the Minimal Model and the Glucose Clamp in the Assessment of Insulin Sensitivity across the Spectrum of Glucose Tolerance. Insulin Resistance Atherosclerosis Study. *Diabetes* 43:1114-1121.

Saad, M.F., Steil, G.M., Kades, W.W., Ayad, M.F., Elsewafy, W.A., Boyadjian, R., Jinagouda, S.D. & Bergman, R.N. (1997) Differences Between the Tolbutamide-Boosted and the Insulin-Modified Minimal Model Protocols. *Diabetes* 46:1167-1171.

Saltiel, A.R. & Kahn, C.R. (2001) Insulin Signalling and the Regulation of Glucose and Lipid Metabolism. *Nature* 414:799-806.

Samuel, V.T. & Shulman, G.I. (2016) The Pathogenesis of Insulin Resistance: Integrating Signaling Pathways and Substrate Flux. *Journal of Clinical Investigation* 126:12-22.

Sanguinetti, E., Guzzardi, M.A., Panetta, D., Tripodi, M., De Sena, V., Quaglierini, M., Burchielli, S., Salvadori, P.A. & Iozzo, P. (2019) Combined Effect of Fatty Diet and Cognitive Decline on Brain Metabolism, Food Intake, Body Weight, and Counteraction by Intranasal Insulin Therapy in 3×Tg Mice. *Frontiers in Cellular Neuroscience* 13:188.

Sarbassov, D.D., Guertin, D.A., Ali, S.M. & Sabatini, D.M. (2005) Phosphorylation and Regulation of Akt/PKB by the Rictor-Mtor Complex. *Science* 307:1098-1101.

Scherer, T., O'Hare, J., Diggs-Andrews, K., Schweiger, M., Cheng, B., Lindtner, C., Zielinski, E., Vempati, P., Su, K., Dighe, S., Milsom, T., Puchowicz, M., Scheja, L., Zechner, R., Fisher, S.J.,

Previs, S.F. & Buettner, C. (2011) Brain Insulin Controls Adipose Tissue Lipolysis and Lipogenesis. *Cell Metabolism* 13:183-194.

Scherer, T. & Buettner, C. (2011) Yin and Yang of Hypothalamic Insulin and Leptin Signaling in Regulating White Adipose Tissue Metabolism. *Reviews in Endocrine and Metabolic Disorders* 12:235-243.

Scherer, T., Lindtner, C., O'Hare, J., Hackl, M., Zielinski, E., Freudenthaler, A., Baumgartner-Parzer, S., Tödter, K., Heeren, J., Krššák, M., Scheja, L., Fürnsinn, C. & Buettner, C. (2016) Insulin Regulates Hepatic Triglyceride Secretion and Lipid Content via Signaling in the Brain. *Diabetes* 65:1511-1520.

Scherer, T., Wolf, P., Smajis, S., Gaggini, M., Hackl, M., Gastaldelli, A., Klimek, P., Einwallner, E., Marculescu, R., Luger, A., Fürnsinn, C., Trattnig, S., Buettner, C., Krššák, M. & Krebs, M. (2017) Chronic Intranasal Insulin Does Not Affect Hepatic Lipids but Lowers Circulating Bcaas in Healthy Male Subjects. *Journal of Clinical Endocrinology and Metabolism* 102:1325-1332.

Schwartz, M.W., Prigeon, R.L., Kahn, S.E., Nicolson, M., Moore, J., Morawiecki, A., Boyko, E.J. & Porte, D. (1997) Evidence That Plasma Leptin and Insulin Levels are Associated with Body Adiposity via Different Mechanisms. *Diabetes Care* 20:1476-1481.

Schwartz, M.W., Woods, S.C., Porte, D., Seeley, R.J. & Baskin, D.G. (2000) Central Nervous System Control of Food Intake. *Nature* 404:661-671.

Shearin, A.L., Monks, B.R., Seale, P. & Birnbaum, M.J. (2016) Lack of AKT in Adipocytes Causes Severe Lipodystrophy. *Molecular Metabolism* 5:472-479.

Shen, S., Reaven, G.M. & Farquhar, J.W. (1970) Comparison of Impedance to Insulin-Mediated Glucose Uptake in Normal Subjects and in Subjects with Latent Diabetes. *Journal of Clinical Investigation* 49:2151-2160.

Shibuya, T., Fushimi, N., Kawai, M., Yoshida, Y., Hachiya, H., Ito, S., Kawai, H., Ohashi, N. & Mori, A. (2018) Luseogliflozin Improves Liver Fat Deposition Compared to Metformin in Type 2 Diabetes Patients with Non-Alcoholic Fatty Liver Disease: A Prospective Randomized Controlled Pilot Study. *Diabetes, Obesity and Metabolism* 20:438-442.

Shulman, G.I. (2014) Ectopic Fat in Insulin Resistance, Dyslipidemia, and Cardiometabolic Disease. *New England Journal of Medicine* 371:1131-1141.

Shungin, D., Winkler, T.W., Croteau-Chonka, D.C., Ferreira, T., Locke, A.E., Mägi, R., Strawbridge, R.J., Pers, T.H., Fischer, K., Justice, A.E., Workalemahu, T., Wu, J.M.W., Buchkovich, M.L., Heard-Costa, N.L., Roman, T.S., Ng, A.W., Song, C., Gustafsson, S., Day, F.R., Esko, T., Fall, T., Kutalik, Z., Luan, J., Randall, J.C., Scherag, A., Vedantam, S., Wood, A.R., Chen, J., Fehrmann, R., Karjalainen, J., Kahali, B., Liu, C., Schmidt, E.M., Absher, D., Amin, N., Anderson, D., Beekman, M., Bragg-Gresham, J.L., Buyske, S., Demirkan, A., Ehret, G.B., Feitosa, M.F., Goel, A., Jackson, A.U., Johnson, T., Kleber, M.E., Henneman, P., Hovingh, G.K., Kastelein, J.J.P. & Chen, W. (2015) New Genetic Loci Link Adipose and Insulin Biology to Body Fat Distribution. *Nature* 518:187-U378.

Sitruk-Ware, R. & Nath, A. (2011) Metabolic Effects of Contraceptive Steroids. *Reviews in Endocrine and Metabolic Disorders* 12:63-75.

Soga, F., Tanaka, H., Tatsumi, K., Mochizuki, Y., Sano, H., Toki, H., Matsumoto, K., Shite, J., Takaoka, H., Doi, T. & Hirata, K. (2018) Impact of Dapagliflozin on Left Ventricular Diastolic Function of Patients with Type 2 Diabetic Mellitus with Chronic Heart Failure. *Cardiovascular Diabetology* 17:132.

Sokoloff, L., Reivich, M., Kennedy, C., Des Rosiers, M.H., Patlak, C.S., Pettigrew, K.D., Sakurada, O. & Shinohara, M. (1977) The [14C]Deoxyglucose Method for the Measurement of Local Cerebral Glucose Utilization: Theory, Procedure, and Normal Values in the Conscious and Anesthetized Albino Rat. *Journal of Neurochemistry* 28:897-916.

Spanswick, D., Smith, M.A., Mirshamsi, S., Routh, V.H. & Ashford, M.L.J. (2000) Insulin Activates ATP-Sensitive K + Channels in Hypothalamic Neurons of Lean, but Not Obese Rats. *Nature Neuroscience* 3:757-758.

Sparks, J., Sparks, C. & Adeli, K. (2012) Selective Hepatic Insulin Resistance, VLDL Overproduction, and Hypertriglyceridemia. *Arteriosclerosis, Thrombosis, and Vascular Biology* 32:2104-2112.

Stafford, J.M., Yu, F., Printz, R., Hasty, A.H., Swift, L.L. & Niswender, K.D. (2008) Central Nervous System Neuropeptide Y Signaling Modulates VLDL Triglyceride Secretion. *Diabetes* 57:1482-1490.

Stančáková, A., Javorský, M., Kuulasmaa, T., Haffner, S.M., Kuusisto, J. & Laakso, M. (2009) Changes in Insulin Sensitivity and Insulin Release in Relation to Glycemia and Glucose Tolerance in 6,414 Finnish Men. *Diabetes* 58:1212-1221.

Steele, R., Wall, J.S., De Bodo, R.C. & Altszuler, N. (1956) Measurement of Size and Turnover Rate of Body Glucose Pool by the Isotope Dilution Method. *American Journal of Physiology - Legacy* 187:15-24.

Steinert, R.E., Feinle-Bisset, C., Asarian, L., Horowitz, M., Beglinger, C. & Geary, N. (2017) Ghrelin, CCK, GLP-1, and PYY(3–36): Secretory Controls and Physiological Roles in Eating and Glycemia in Health, Obesity, and After RYGB. *Physiological Reviews* 97:411-463.

Stern, S.E., Williams, K., Ferrannini, E., Defronzo, R.A., Bogardus, C. & Stern, M.P. (2005). Identification of Individuals with Insulin Resistance Using Routine Clinical Measurements. *Diabetes* 54(2), 333-339.

Stumvoll, M., Mitrakou, A., Pimenta, W., Jenssen, T., Yki-Järvinen, H., Van Haeften, T., Renn, W. & Gerich, J. (2000) Use of the Oral Glucose Tolerance Test to Assess Insulin Release and Insulin Sensitivity. *Diabetes Care* 23:295-301.

Sutherland, C., Leighton, I.A. & Cohen, P. (1993) Inactivation of Glycogen Synthase Kinase-3βby Phosphorylation: New Kinase Connections in Insulin and Growth-Factor Signalling. *Biochemical Journal* 296 (Pt 1):15-19.

Swinnen, S. G. H. A, Holleman, F. & Devries, J.H. (2008) The Interpretation of Glucose Clamp Studies of Long-Acting Insulin Analogues: From Physiology to Marketing and Back. *Diabetologia* 51:1790-1795.

Tabák, A.G., Jokela, M., Akbaraly, T., Brunner, E.J., Kivimäki, M. & Witte, D.R. (2009) Trajectories of Glycaemia, Insulin Sensitivity, and Insulin Secretion Before Diagnosis of Type 2 Diabetes: an Analysis from the Whitehall II Study. *Lancet* 373:2215-2221.

Tencerova, M., Okla, M. & Kassem, M. (2019) Insulin Signaling in Bone Marrow Adipocytes. *Current Osteoporosis Reports* 17:446-454.

Thaler, J.P., Yi, C., Schur, E.A., Guyenet, S.J., Hwang, B.H., Dietrich, M.O., Zhao, X., Sarruf, D.A., Izgur, V., Maravilla, K.R., Nguyen, H.T., Fischer, J.D., Matsen, M.E., Wisse, B.E., Morton, G.J., Horvath, T.L., Baskin, D.G., Tschöp, M.H. & Schwartz, M.W. (2012) Obesity is Associated with Hypothalamic Injury in Rodents and Humans. *Journal of Clinical Investigation* 122:778.

Thie, J.A. (1995) Clarification of a Fractional Uptake Concept. *Journal of Nuclear Medicine* 36:711.

Thomas, D. & Apovian, C. (2017) Macrophage Functions in Lean and Obese Adipose Tissue. *Metabolism* 72:120-143.

Titchenell, P.M., Chu, Q., Monks, B.R. & Birnbaum, M.J. (2015) Hepatic Insulin Signalling is Dispensable for Suppression of Glucose Output by Insulin in Vivo. *Nature Communications* 6:7078.

Tuomilehto, J., Lindstrom, J., Eriksson, J.G., Valle, T.T., Hamalainen, H., Ilanne-Parikka, P., Keinänen-Kiukaanniemi, S., Laakso, M., Louheranta, A., Rastas, M., Salminen, V., Aunola, S., Cepaitis, Z., Moltchanov, V., Hakumaki, M., Mannelin, M., Martikkala, V., Sundvall, J., Uusitupa, M. & Finnish Diabetes Prevention Study Group (2001) Prevention of Type 2 Diabetes Mellitus by Changes in Lifestyle Among Subjects with Impaired Glucose Tolerance. *New England Journal of Medicine* 344:1343-1350.

Turkington, T.G. (2001) Introduction to PET Instrumentation. *Journal of Nuclear Medicine Technology* 29:4.

Tuulari, J.J., Karlsson, H.K., Hirvonen, J., Hannukainen, J.C., Bucci, M., Helmiö, M., Ovaska, J., Soinio, M., Salminen, P., Savisto, N., Nummenmaa, L. & Nuutila, P. (2013) Weight Loss After Bariatric Surgery Reverses Insulin-Induced Increases in Brain Glucose Metabolism of the Morbidly Obese. *Diabetes* 62:2747-2751.

U Din, M., Raiko, J., Saari, T., Saunavaara, V., Kudomi, N., Solin, O., Parkkola, R., Nuutila, P. & Virtanen, K.A. (2017) Human Brown Fat Radiodensity Indicates Underlying Tissue Composition

and Systemic Metabolic Health. *Journal of Clinical Endocrinology and Metabolism* 102:2258-2267.

Utriainen, T., Takala, T., Luotolahti, M., Rönnemaa, T., Laine, H., Ruotsalainen, U., Haaparanta, M., Nuutila, P. & Yki-Järvinen, H. (1998) Insulin Resistance Characterizes Glucose Uptake in Skeletal Muscle but Not in the Heart in NIDDM. *Diabetologia* 41:555-559.

Vaag, A., Henriksen, J.E. & Beck-Nielsen, H. (1992) Decreased Insulin Activation of Glycogen Synthase in Skeletal Muscles in Young Nonobese Caucasian First-Degree Relatives of Patients with Non-Insulin-Dependent Diabetes Mellitus. *Journal of Clinical Investigation* 89:782-788.

Verel, I., Visser, G. W. M., & Van Dongen, G. A. (2005). The Promise of Immuno-PET in Radioimmunotherapy. *Journal of Nuclear Medicine, 46*(1 Suppl), 164S.

Verma, S., Mazer, C., Yan, A., Mason, T., Garg, V., Teoh, H., Zuo, F., Quan, A., Farkouh, M., Fitchett, D., Goodman, S., Goldenberg, R., Al-Omran, M., Gilbert, R., Bhatt, D., Leiter, L., Jüni, P., Zinman, B. & Connelly, K. (2019) Effect of Empagliflozin on Left Ventricular Mass in Patients with Type 2 Diabetes Mellitus and Coronary Artery Disease: The EMPA-HEART Cardiolink-6 Randomized Clinical Trial. *Circulation* 140:1693-1702.

Viljanen, A.P.M., Virtanen, K.A., JäRvisalo, M.J., HäLlsten, K., Parkkola, R., RöNnemaa, T., LöNnqvist, F., Iozzo, P., Ferrannini, E. & Nuutila, P. (2005) Rosiglitazone Treatment Increases Subcutaneous Adipose Tissue Glucose Uptake in Parallel with Perfusion in Patients with Type 2 Diabetes: A Double-Blind, Randomized Study with Metformin. *Journal of Clinical Endocrinology and Metabolism* 90:6523-6528.

Virtanen, K.A., Peltoniemi, P., Marjamäki, P., Asola, M., Strindberg, L., Parkkola, R., Huupponen, R., Knuuti, J., Lönnroth, P. & Nuutila, P. (2001) Human Adipose Tissue Glucose Uptake Determined Using [18F]-Fluoro-Deoxy-Glucose ([18F]FDG) and PET in Combination with Microdialysis. *Diabetologia* 44:2171-2179.

Virtanen, K.A., LöNnroth, P., Parkkola, R., Peltoniemi, P., Asola, M., Viljanen, T., Tolvanen, T., Knuuti, J., RöNnemaa, T., Huupponen, R. & Nuutila, P. (2002) Glucose Uptake and Perfusion in Subcutaneous and Visceral Adipose Tissue during Insulin Stimulation in Nonobese and Obese Humans. *Journal of Clinical Endocrinology and Metabolism* 87:3902-3910.

Vogt, C., Ardehali, H., Iozzo, P., Yki-Järvinen, H., Koval, J., Maezono, K., Pendergrass, M., Printz, R., Granner, D., Defronzo, R. & Mandarino, L. (2000) Regulation of Hexokinase II Expression in Human Skeletal Muscle in Vivo. *Metabolism* 49:814-818.

Wan, M., Leavens, K., Hunter, R., Koren, S., Von Wilamowitz-Moellendorff, A., Lu, M., Satapati, S., Chu, Q., Sakamoto, K., Burgess, S. & Birnbaum, M. (2013) A Noncanonical, GSK3-Independent Pathway Controls Postprandial Hepatic Glycogen Deposition. *Cell Metabolism* 18:99-105.

Wang, X., Bao, W., Liu, J., Ouyang, Y., Wang, D., Rong, S., Xiao, X., Shan, Z., Zhang, Y., Yao, P. & Liu, L. (2013) Inflammatory Markers and Risk of Type 2 Diabetes: A Systematic Review and Meta-Analysis. *Diabetes Care* 36:166-175.

Welle, S., Lilavivat, U. & Campbell, R.G. (1981) Thermic Effect of Feeding in Man: Increased Plasma Norepinephrine Levels Following Glucose but Not Protein or Fat Consumption. *Metabolism* 30:953-958.

Whitesell, R.R., Ward, M., Mccall, A.L., Granner, D.K. & May, J.M. (1995) Coupled Glucose Transport and Metabolism in Cultured Neuronal Cells: Determination of the Rate-Limiting Step. *Journal of Cerebral Blood Flow and Metabolism* 15:814-826.

Winzeler, B., Da Conceição, I., Refardt, J., Sailer, C.O., Dutilh, G. & Christ-Crain, M. (2019) Effects of Glucagon-Like Peptide-1 Receptor Agonists on Hypothalamic-Pituitary-Adrenal Axis in Healthy Volunteers. *Journal of Clinical Endocrinology and Metabolism* 104:202-208.

Woods, S.C., Lotter, E.C., Mckay, L.D. & Porte, D. (1979) Chronic Intracerebroventricular Infusion of Insulin Reduces Food Intake and Body Weight of Baboons. *Nature* 282:503-505.

Wright, E.M., Loo, D.D.F. & Hirayama, B.A. (2011) Biology of Human Sodium Glucose Transporters. *Physiological Reviews* 91:733-794.

Wu, H., Bergsneider, M., Glenn, T.C., Yeh, E., Hovda, D.A., Phelps, M.E. & Huang, S. (2003) Measurement of the Global Lumped Constant for 2-Deoxy-2-[18F]Fluoro-D-Glucose in Normal Human Brain Using [15O]Water and 2-Deoxy-2-[18F]Fluoro-D-Glucose Positron Emission

Tomography Imaging: A Method with Validation Based on Multiple Methodologies. *Molecular Imaging and Biology* 5:32-41.

Xiao, C., Dash, S., Stahel, P. & Lewis, G. (2017) Effects of Intranasal Insulin on Triglyceride-Rich Lipoprotein Particle Production in Healthy Men. *Arteriosclerosis, Thrombosis, and Vascular Biology* 37:1776-1781.

Xiao, C., Dash, S., Stahel, P. & Lewis, G.F. (2018) Effects of Intranasal Insulin on Endogenous Glucose Production in Insulin-Resistant Men. *Diabetes, Obesity and Metabolism* 20:1751-1754.

Yecies, J., Zhang, H., Menon, S., Liu, S., Yecies, D., Lipovsky, A., Gorgun, C., Kwiatkowski, D., Hotamisligil, G., Lee, C. & Manning, B. (2011) Akt Stimulates Hepatic SREBP1c and Lipogenesis Through Parallel Mtorc1-Dependent and Independent Pathways. *Cell Metabolism* 14:280.

Yeung, E.H., Zhang, C., Mumford, S.L., Ye, A., Trevisan, M., Chen, L., Browne, R.W., Wactawski-Wende, J. & Schisterman, E.F. (2010) Longitudinal Study of Insulin Resistance and Sex Hormones Over the Menstrual Cycle: The Biocycle Study. *Journal of Clinical Endocrinology and Metabolism* 95:5435-5442.

Yki-Järvinen, H., Puhakainen, I. & Koivisto, V.A. (1991) Effect of Free Fatty Acids on Glucose Uptake and Nonoxidative Glycolysis across Human Forearm Tissues in the Basal State and during Insulin Stimulation. *Journal of Clinical Endocrinology and Metabolism* 72:1268-1277.

Yu, C., Chen, Y., Cline, G.W., Zhang, D., Zong, H., Wang, Y., Bergeron, R., Kim, J.K., Cushman, S.W., Cooney, G.J., Atcheson, B., White, M.F., Kraegen, E.W. & Shulman, G.I. (2002) Mechanism by Which Fatty Acids Inhibit Insulin Activation of Insulin Receptor Substrate-1 (IRS-1)-Associated Phosphatidylinositol 3-Kinase Activity in Muscle. *Journal of Biological Chemistry* 277:50230-50236.

Yu, E.W., Greenblatt, L., Eajazi, A., Torriani, M. & Bredella, M.A. (2016) Marrow Adipose Tissue Composition in Adults with Morbid Obesity. *Bone* 97:38-42.

Zander, M., Madsbad, S., Madsen, J.L. & Holst, J.J. (2002) Effect of 6-Week Course of Glucagon-Like Peptide 1 on Glycaemic Control, Insulin Sensitivity, and B-Cell Function in Type 2 Diabetes: A Parallel-Group Study. *Lancet* 359:824-830.

Zierler, K.L. (1961) Theory of the Use of Arteriovenous Concentration Differences for Measuring Metabolism in Steady and Non-Steady States. *Journal of Clinical Investigation* 40:2111-2125.

Zimmer, E.R., Parent, M.J., Souza, D.G., Leuzy, A., Lecrux, C., Kim, H., Gauthier, S., Pellerin, L., Hamel, E. & Rosa-Neto, P. (2017) [18F]FDG PET Signal is Driven by Astroglial Glutamate Transport. *Nature Neuroscience* 20:393-395.

Åkerblom, A., Oldgren, J., Latva-Rasku, A., Johansson, L., Lisovskaja, V., Karlsson, C., Oscarsson, J. & Nuutila, P. (2019) Effects of Dapagliflozin on Cardiac Substrate Uptake, Myocardial Efficiency, and Myocardial Contractile Work in Type 2 Diabetes Patients-A Description of the DAPACARD Study. *Upsala Journal of Medical Sciences* 124:59-64.

UNIVERSITY OF TURKU

Painosalama Oy, Turku, Finland 2020

ISBN 978-951-29-8111-3 (PRINT)
ISBN 978-951-29-8112-0 (PDF)
ISSN 0355-9483 (Print)
ISSN 2343-3213 (Online)